

CO₂ Capture With MEA: Integrating the Absorption Process and Steam Cycle of an Existing Coal-Fired Power Plant

by

Colin F. Alie

A thesis
presented to the University of Waterloo
in fulfillment of the
thesis requirement for the degree of
Master of Applied Science
in
Chemical Engineering

Waterloo, Ontario, Canada, 2004

© Colin F. Alie 2004

I hereby declare that I am the sole author of this thesis. This is a true copy of the thesis, including any required final revisions, as accepted by my examiners.

I understand that my thesis may be made electronically available to the public.

Abstract

In Canada, coal-fired power plants are the largest anthropogenic point sources of atmospheric CO₂. The most promising near-term strategy for mitigating CO₂ emissions from these facilities is the post-combustion capture of CO₂ using MEA (monoethanolamine) with subsequent geologic sequestration.

While MEA absorption of CO₂ from coal-derived flue gases on the scale proposed above is technologically feasible, MEA absorption is an energy intensive process and especially requires large quantities of low-pressure steam. It is the magnitude of the cost of providing this supplemental energy that is currently inhibiting the deployment of CO₂ capture with MEA absorption as means of combatting global warming.

The steam cycle of a power plant ejects large quantities of low-quality heat to the surroundings. Traditionally, this waste has had no economic value. However, at different times and in different places, it has been recognized that the diversion of lower quality streams could be beneficial, for example, as an energy carrier for district heating systems. In a similar vein, using the waste heat from the power plant steam cycle to satisfy the heat requirements of a proposed CO₂ capture plant would reduce the required outlay for supplemental utilities; the economic barrier to MEA absorption could be removed.

In this thesis, state-of-the-art process simulation tools are used to model coal combustion, steam cycle, and MEA absorption processes. These disparate models are then combined to create a model of a coal-fired power plant with integrated CO₂ capture. A sensitivity analysis on the integrated model is performed to ascertain the process variables which most strongly influence the CO₂ energy penalty.

From the simulation results with this integrated model, it is clear that there is a substantial thermodynamic advantage to diverting low-pressure steam from the steam cycle for use in the CO₂ capture plant. During the course of the investigation, methodologies for using Aspen Plus[®] to predict column pressure profiles and for converging the MEA absorption process flowsheet were developed and are herein presented.

Acknowledgements

I would like extend my thanks and my appreciation to all those who have assisted me in preparing this thesis:

- Dr. Eric Croiset and Dr. Peter Douglas for the privilege of working with them and for their guidance and mentorship.
- Blair Seckington, personally, and Ontario Power Generation (OPG), as a whole, for their financial and technical support.
- Dr. Thomas Duever, Graeme Lamb, Dr. William Anderson, Dennis Herman, and Wendy Irving who, when called upon, provided their insight and assistance.

And, lastly, to my loving wife Amanda, who supported me through what will surely be the longest “two weeks” of our lives...

Contents

Acronyms and Abbreviations	xiv
Chemical Symbols and Formulae	xvii
Nomenclature	xix
1 Introduction	1
1.1 Objective	1
1.2 Motivation	1
1.2.1 Fossil fuels, carbon dioxide, and climate change	1
1.2.2 Fossil fuels and electric power generation	2
1.2.3 Generating electricity while mitigating CO ₂ emissions	4
1.2.4 Capturing CO ₂ with MEA	8
1.3 Implementation	10
1.3.1 Selection of study basis	10
1.3.2 Selection of simulation software	10
1.3.3 Outline of thesis	11
2 Flue Gas Synthesis	13
2.1 Objective	13
2.2 Rationale	13
2.2.1 Model flexibility	13

2.2.2	Model accuracy	14
2.3	Implementation	15
2.3.1	Specifying properties	15
2.3.2	Specifying streams	18
2.3.3	Specifying blocks	18
2.4	Model Validation	19
2.4.1	Coal heat of combustion	19
2.4.2	Flue gas flow rate	19
2.5	Conclusions and Recommendations	21
3	Simulation of Steam Cycle	22
3.1	Objective	22
3.2	Motivation	22
3.3	Points of emphasis	23
3.4	Implementation	24
3.4.1	Specifying properties	24
3.4.2	Specifying streams	26
3.4.3	Specifying blocks	26
3.5	Model validation	33
3.5.1	Property method	33
3.5.2	Steam temperature, pressure, and flow potential	34
3.5.3	Part-load power output and heat input	34
3.5.4	Turbine and unit heat rate	34
3.6	Conclusions and recommendations	39
4	Simulation of MEA Absorption Process	42
4.1	Objective	42
4.2	Motivation	42
4.2.1	Process flowsheet evaluation	42

4.2.2	Equipment design	45
4.2.3	Solvent selection	46
4.2.4	Optimizing process operating conditions	47
4.2.5	Process integration exploration	48
4.3	Points of emphasis	48
4.4	Implementation	49
4.4.1	Specifying properties	49
4.4.2	Specifying streams	52
4.4.3	Specifying blocks	53
4.5	Model Parameter elucidation	58
4.5.1	Property method selection	58
4.5.2	<i>Absorber</i> and <i>Stripper</i> internal configuration	62
4.6	Conclusions and recommendations	71
5	Integration of Power Plant and MEA Absorption	73
5.1	Introduction	73
5.2	Implementation	76
5.2.1	Location of steam extraction and condensate re-injection	76
5.2.2	Maximum available steam for <i>Stripper</i> reboiler heating	82
5.2.3	Flue gas pre-conditioning	83
5.2.4	<i>Stripper</i> reboiler	84
5.2.5	<i>Blower</i> and <i>CO₂ Compressor</i>	84
5.3	Process Simulation	84
5.3.1	Sensitivity of CO ₂ capture to recycle CO ₂ loading	84
5.3.2	Sensitivity of CO ₂ capture to <i>Absorber</i> height	87
5.3.3	Sensitivity of CO ₂ capture to <i>Stripper</i> height	89
5.4	Model validation	91
5.5	Conclusions and recommendations	94

6	Conclusion and Future Work	95
6.1	Conclusion	95
6.2	Future work	97
A	Conditions of steam at potential extraction locations	99
B	Sieve Tray Column Hydrodynamic Design Recipe	101
B.1	Tower diameter	101
B.2	Downcomer flooding	103
B.3	Tray pressure drop	106
B.4	Downcomer seal	107
B.5	Weeping	107
C	Steam Energy Calculations	108
D	Comparison of Calculated CO₂ Solubility With Experimental Values	111
E	Aspen Plus Input file for Power Plant With Integrated MEA Absorption	116
	Glossary	149
	List of References	150

List of Tables

1.1	Canadian emissions of greenhouse gases, 2000	2
1.2	Electricity generation in Canada, 2000	3
1.3	Electricity generation from thermal power plants, 2000	3
1.4	Coal use across Canada, 2000	7
1.5	Age distribution of Canadian coal power plants: 2000 and 2010	8
2.1	Coal characteristics	16
2.2	Comparison of $(\Delta_c h)^\circ$ with observed <i>GCV</i>	19
2.3	Flue gas flow rate simulation input data	20
2.4	Comparison of calculated flue gas flow rate with observed values	20
2.5	Flue gas composition	21
3.1	Design inlet volumetric flow rates into turbine sections	27
3.2	Ratio of discharge pressure to inlet pressure for turbine groups	28
3.3	Fractional isentropic efficiency of turbine groups	29
3.4	Comparison of calculated internal power with design values	33
3.5	Comparison of calculated heat input with design values	34
4.1	Hydrodynamic performance neglect matrix	49
4.2	Property methods and model available for CO ₂ -MEA-H ₂ O system	51
4.3	UOM's in MEA absorption process model	53
4.4	Design parameters for sizing and hydrodynamic evaluation of columns	56
4.5	Survey of CO ₂ delivery pressures used in MEA absorption studies	57

4.6	Summary of results from <i>Absorber</i> study	66
4.7	MEA absorption process model initialization parameters	71
5.1	Scope of MEA absorption sensitivity analysis	84
5.2	MEA absorption process energy duties	92
5.3	<i>Stripper</i> reboiler specific heat duty	93
5.4	Summary of best cases from sensitivity studies	94
A.1	Base and part-load conditions in Nanticoke steam cycle	99
B.1	Required input for sizing and hydrodynamic evaluation of tray columns	102
C.1	Changes in steam internal energy in steam cycle	110

List of Figures

1.1	Utilization of natural resources for electricity generation	4
1.2	Process flow diagram for CO ₂ removal via chemical absorption	9
2.1	Coal combustion simulation flowsheet	15
3.1	Steam cycle simulation flowsheet	25
3.2	High-pressure section pressure ratio at part-load	27
3.3	<i>LP3</i> and <i>LP4</i> stage groups' isentropic efficiency at part-load	30
3.4	Turbine 'bleed' steam flow rates at part-load	31
3.5	Boiler feed water temperature at part-load	32
3.6	Potential steam extraction locations in steam cycle	35
3.7	Steam temperature at part-load	35
3.8	Steam pressure at part-load	36
3.9	Steam flow rate at part-load	37
3.10	Turbine power output at part-load	37
3.11	Turbine heat duty at part-load	38
3.12	Main turbine Sankey diagram	38
3.13	Main turbine work and energy flows	40
3.14	Boiler feed water pump turbine mechanical power losses	40
3.15	Turbine and unit heat rate at part-load	41
4.1	Base MEA absorption process flowsheet	43
4.2	Amine Guard FS TM process flowsheet	43

4.3	Kerr-McGee/Lummus Crest Global MEA absorption process flowsheet	44
4.4	'Split feed' MEA absorption process flowsheet	45
4.5	MEA absorption simulation flowsheet	50
4.6	Solubility of CO ₂ in 30 wt% MEA solution	59
4.7	Comparison of calculated VLE with experimental values at 40°C	60
4.8	Comparison of calculated VLE with experimental values at 120°C	60
4.9	Residual analysis of VLE data — ΔP_{CO_2} vs α_{lean} at 40°C	61
4.10	Residual analysis of VLE data — ΔP_{CO_2} vs α_{lean} at 120°C	62
4.11	Sensitivity of F_{lean} to <i>Absorber</i> height	64
4.12	Sensitivity of <i>Absorber</i> downcomer flooding to <i>Absorber</i> tray spacing	67
4.13	Sensitivity of Q_{reb} to <i>Stripper</i> height	69
4.14	Sensitivity of <i>Stripper</i> downcomer flooding to <i>Stripper</i> tray spacing	70
5.1	Enthalpy-entropy curve for power plant	74
5.2	Implication of steam extraction on steam cycle work and heat flows	75
5.3	Power plant with integrated MEA absorption simulation flowsheet	77
5.4	Base-load steam conditions in steam cycle	79
5.5	High-pressure section of Nanticoke turbine	80
5.6	Intermediate-pressure section of Nanticoke turbine	80
5.7	Low-pressure section of Nanticoke turbine	81
5.8	Lengthwise view of Nanticoke turbine	81
5.9	Sensitivity of power plant electricity output to steam extraction	82
5.10	Sensitivity of $(\Delta P)_{\text{Absorber}}$ and Q_{reb} to CO ₂ loading	85
5.11	Sensitivity of capture plant's electricity demand to CO ₂ loading	85
5.12	Sensitivity of power plant electricity output to CO ₂ loading	86
5.13	Sensitivity of $(\Delta P)_{\text{Absorber}}$ and Q_{reb} to <i>Absorber</i> height	87
5.14	Sensitivity of capture plant's electricity demand to <i>Absorber</i> height	88
5.15	Sensitivity of power plant electricity output to <i>Absorber</i> height	88
5.16	Sensitivity of $(\Delta P)_{\text{Absorber}}$ and Q_{reb} to <i>Stripper</i> height	89

5.17	Sensitivity of capture plant's electricity demand to <i>Stripper</i> height	90
5.18	Sensitivity of power plant electricity output to <i>Stripper</i> height	90
6.1	Influence of CO ₂ loading on plant thermal efficiency	96
6.2	Influence of <i>Absorber</i> height on plant thermal efficiency	96
6.3	Influence of <i>Stripper</i> height on plant thermal efficiency	97
D.1	Comparison of calculated VLE with experimental values at 0°C	111
D.2	Comparison of calculated VLE with experimental values at 25°C	112
D.3	Comparison of calculated VLE with experimental values at 40°C	112
D.4	Comparison of calculated VLE with experimental values at 60°C	113
D.5	Comparison of calculated VLE with experimental values at 80°C	113
D.6	Comparison of calculated VLE with experimental values at 100°C . . .	114
D.7	Comparison of calculated VLE with experimental values at 120°C . . .	114
D.8	Comparison of calculated VLE with experimental values at 150°C . . .	115

Acronyms and Abbreviations

ABB	Asea Brown Boveri Ltd.
AMP	2-amino-2-methyl-1-propanol
ASME.....	American Society of Mechanical Engineers
CFC's	chlorofluorocarbons
CORAL	CO ₂ -removal absorption liquid
DEA	diethanolamine
DGA	diglycolamine
DIPA	diisopropanolamine
DTD	drain temperture difference In a feed water preheater, the difference in temperature between the condensate outlet and the feed water outlet.
EOR.....	enhanced oil recovery
EOS	equation of state
FG	flue gas
GCV	gross calorific value
GHG	greenhouse gas
HFC's	hydrofluorocarbons
HP	high-pressure
IEA	International Energy Agency

IGCC	integrated gasification combined cycle
IP	intermediate-pressure
IPCC	Intergovernmental Panel on Climate Change
KEPCO	Kansai Electric Power Company Inc.
KP	Kansai packing
KS	Kansai solvent
LP	low-pressure
MCR	maximum continuous rating
MDEA	methyldiethanolamine
MEA	monoethanolamine
MHI	Mitsubishi Heavy Industries Ltd.
N/A	not available/not applicable
NBS	National Bureau of Standards
NCV	net calorific value
NGCC	natural gas combined cycle
NRC	National Research Council
OPG	Ontario Power Generation
PCC	pulverized coal combustion
PRB	Powder River Basin
SOFC	solid oxide fuel cell
TEA	triethanolamine
THR	turbine heat rate
TNO	Short-form of official dutch name Nederlandse Organisatie voor toegepast-natuurwetenschappelijk onderzoek TNO (<i>Netherlands Organisation for Applied Scientific Research TNO</i> , in english).

TTD terminal temperature difference In a feed water preheater, the difference between the saturation temperature of the steam and the temperature of the feed water or condensate outlet.

UHR unit heat rate

UOM unit operation model

UOP Universal Oil Products LLC

USLS U. S. low-sulphur

VLE vapour-liquid equilibrium

Chemical Symbols and Formulae

Ar	argon
C	carbon
CH ₄	methane
Cl	chlorine
CO	carbon monoxide
CO ₂	carbon dioxide
H	hydrogen
H ₂	molecular hydrogen
H ₂ O	water
HCl	hydrogen chloride
HF	hydrogen fluoride
N	nitrogen
N ₂	molecular nitrogen
N ₂ O	nitrous oxide
NaOH	sodium hydroxide
NO	nitrogen oxide
NO ₂	nitrogen dioxide
NO _x	nitrogen oxides

O₂..... molecular oxygen
S..... sulphur
SF₆..... sulphur hexafluoride
SO₂..... sulphur dioxide
SO_x..... sulphur oxides

Nomenclature

Variables

α	CO ₂ loading
A_a	active area of tray
A_h	area of tray covered by holes
a, b	regression parameters
EFA	approach to entrainment flooding
E	electrical power output
C_p	specific heat capacity
Δ	change in value
d_h	diameter of holes in tray
ΔE	electrical power loss
ϵ	roughness factor
F	liquid molar flow rate
f	length of weir specified as a fraction of tray diameter
G	vapour mass flow rate
$\Delta_c h$	specific heat of combustion
$\Delta_f h$	specific heat of formation
h_c	downcomer clearance; height of gap between tray and downcomer apron

h_w	weir height
H	weight percent hydrogen in coal, wet basis
h	specific enthalpy
k_{-1}	rate of reverse reaction
k_1	rate of forward reaction
k_y	vapour phase mass transfer coefficient
k	column tray spacing scale factor
ℓ	length
L	liquid mass flow rate
\dot{m}	mass flow rate
M	molecular mass
m	mass
η	efficiency
\mathcal{N}	molar flux
N	number of trays
n	number of moles
$\Delta\mathcal{P}$	power loss
ΔP	pressure drop
\mathcal{P}	power
P_x	partial pressure of component x
P	pressure
Q	heat flow rate
q	volumetric flow rate
ρ	density

R	gas constant
σ	surface tension
t_t	tray thickness
TS	tray spacing
T	temperature
U	internal energy
V	volume
w	weight fraction
x	mole fraction
y	vapour phase mole fraction

Subscripts

∞	conditions in bulk fluid
i	conditions at interface
abs	pertaining to the <i>Absorber</i>
$bfpt$	pertaining to boiler feed water pump turbine shaft
$bleed$	pertaining to bleed stream
$boil$	pertaining to block <i>BOIL</i> in steam cycle
b	pertaining to power plant boiler
col	pertaining to column
c	conditions at 'cold-side'
exc	pertaining to exciter
gen	pertaining to generator terminal
$gross$	before applicable losses have been accounted for
G	pertaining to gas phase

<i>in</i>	conditions at inlet
<i>lean</i>	pertaining to that part of the recycle loop of the MEA absorption process with a relatively low concentration of CO ₂
<i>L</i>	pertaining to liquid phase
<i>mech</i>	mechanical
<i>net</i>	after applicable losses have been accounted for
<i>out</i>	conditions at outlet
<i>plant</i>	pertaining to the power plant
<i>reb</i>	pertaining to the <i>Stripper</i> reboiler
<i>reht</i>	pertaining to block <i>REHT</i> in steam cycle
<i>sta</i>	pertaining to station service
<i>str</i>	pertaining to the <i>Stripper</i>
<i>s</i>	isentropic conditions
<i>th</i>	thermal
<i>trans</i>	pertaining to main transformer
<i>w</i>	pertaining to the tray weir

Superscripts

o	property at standard state
*	denotes set point or optimal value
<i>d</i>	dry basis
<i>i</i>	in reference to <i>i</i> 'th iteration
<i>min</i>	denotes minimum value
<i>m</i>	mineral matter-free basis
<i>sat</i>	property at saturated conditions
<i>d</i>	diameter

Chapter 1

Introduction

1.1 Objective

Capturing substantial amounts of CO₂ from the flue gas from a coal-fired power plant using amine absorption technology requires large amounts of energy, mostly in the form of heat. The objective of this thesis is to evaluate the feasibility of obtaining the heat required for amine absorption from the existing power plant.

1.2 Motivation

1.2.1 Fossil fuels, carbon dioxide, and climate change

The *greenhouse effect* refers to the phenomenon whereby gases in the upper atmosphere absorb a portion of the heat radiated by the earth. It is estimated that the Earth's temperature is 33°C warmer than it would be if this energy were instead transmitted to space [18]. Increasingly, the by-products of human activity are enhancing this 'natural' greenhouse effect stimulating a change in climate with potentially devastating effects for the planet's inhabitants.

The IPCC (Intergovernmental Panel on Climate Change) has identified six anthropogenic gases with climate change potential: CO₂, CH₄, N₂O, SF₆, CFC's (chlorofluorocarbons), and HFC's (hydrofluorocarbons). Table 1.1 shows Canadian emissions of these gases.

The first column of Table 1.1, *Global Warming Potential*, expresses each compound's ability to absorb heat radiation on a unit mass basis. While, of the six greenhouse gases,

Table 1.1: Canadian emissions of greenhouse gases, 2000 (Source: Environment Canada [47])

	Global Warming	1990		2000	
	Potential	[Mt]	[Mt CO ₂ eq.]	Mt	[Mt CO ₂ eq.]
CO ₂	1	472	472	571	571
CH ₄	21	3.5	73	4.4	91
N ₂ O	310	0.17	53	0.17	54
HFC's	40–1170				0.9
CFC's	6500–9200		6		6
SF ₆	23900		2.9		2.3

CO₂ has the lowest Global Warming Potential, it is has the largest global climate change impact because its total emissions are so much greater than the others. Thus, current efforts in preempting climate change focus on strategies for the reduction of CO₂ emissions.

1.2.2 Fossil fuels and electric power generation

Electricity is a means to an end and not an end in and of itself. We need energy that is chemical, thermal, mechanical, etc. and our societies have evolved or are evolving such that electrical energy is often an intermediate form.

Energy cannot be created or destroyed; it may be changed from one form to another. “Electric power generation” is actually “energy conversion”. The energy conversion process selected is often site specific — “you take what you can get”. In Canada — a large country with varied geography, topology, and geology — there are many different types of power plants. Table 1.2 presents the installed generating capacity and the actual generation of electric energy categorized loosely by type of power plant.

Most of Canada’s electricity is hydroelectric with significant contributions from ‘conventional’ steam, nuclear, and combustion turbine plants. The last four categories of power in Table 1.2 use non-renewable energy sources and the last three — ‘conventional’ steam, combustion turbine, and internal combustion — are the ones typically associated with CO₂ emissions (hydrocarbon fueled). Currently, most of this *thermal* electricity, 93.1%, is produced by utilities. Table 1.3 shows the amount of electric energy these utilities generated from the various non-renewable fuels.

Table 1.2: Electricity generation in Canada, 2000 (Source: Statistics Canada [22])

Source	Installed generating capacity		Generation of electric energy	
	[MW]	[%]	[MWh]	[%]
Hydro	67 407	60.6	354 548 767	60.5
Non-conventional	96	0.1	263 820	0.0
Nuclear	10 615	9.5	68 675 253	11.7
Conventional steam	27 721	24.9	143 262 501	24.5
Internal combustion	654	0.6	1 356 761	0.2
Combustion turbine	4 808	4.3	17 706 788	3.0
Total	111 301	100.0	585 813 890	100.0

Table 1.3: Electricity generation from thermal power plants, 2000 (Source: Statistics Canada [22])

Fuel	Generation of electric energy	
	[MWh]	[%]
Coal	106 429 553	49.5
Petroleum	10 600 250	4.9
Natural Gas	26 623 329	12.4
Wood	1 830 560	0.8
Uranium	68 675 251	31.9
Other	961 711	0.4
Total	215 120 654	100.0

1.2.3 Generating electricity while mitigating CO₂ emissions

A laudable goal is to reduce CO₂ emissions sufficiently to stabilize atmospheric CO₂ concentrations at a ‘comfortable’ level. Of the total GHG (greenhouse gas) emissions shown in Table 1.1, 128 Mt in 2000, 17.6% of the total for that year, resulted from the combustion of fossil fuels for the production of heat and electricity. In contrast, 95 Mt of GHG emissions were produced for the same reasons as in 1990 representing 15.7% of that year’s production. Apparently, doing nothing is not an option. So then, how can CO₂ production be mitigated during electricity generation? Figure 1.1 identifies five useful demarcation points in the discussion:

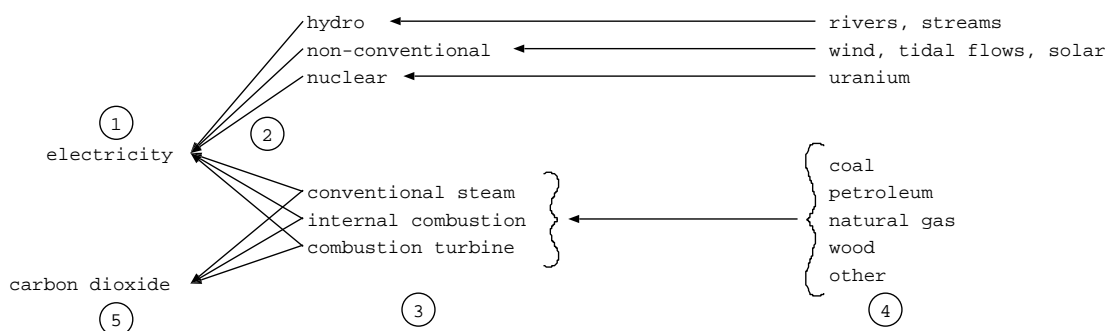


Figure 1.1: Utilization of natural resources for electricity generation

① Produce less electricity

In Canada, it is inconceivable that a shortfall exist between electricity supply and demand. Therefore, it is not possible for utilities to produce less power than is demanded and have brownouts, for example.

② Switch from CO₂ emitting to non-CO₂ emitting electricity sources

In cases where there is a mix of CO₂ emitting and non-CO₂ emitting electricity sources, it is probably already true that non-CO₂ emitting sources are used preferentially for economic reasons. For example, OPG (Ontario Power Generation), which owns 75% of the generating capacity in Ontario [21], uses its hydroelectric and nuclear capacity for base-load supply and its fossil fuel plants for peaking power [50].

There is potential for retiring CO₂ emitting plants and building new non-CO₂ emitting capacity.¹ However, the non-CO₂ emitting electricity options have other

¹For the record, even the ‘non-CO₂ emitting’ power plants will have associated, albeit secondary, GHG

challenges which detract from their appeal. Nuclear power plants have relatively lengthy construction schedules (on the order of a decade) so a decision today to switch to nuclear power would not realize CO₂ reductions in the short or near-medium term. Sources of electricity derived from the sun and/or wind are problematic principally because of their intermittency. So, a large installed capacity of non-conventional power plants would need to be accompanied by a large installed capacity of energy storage facilities or conventional power plants in order to keep the lights on when the sun isn't shining and/or the wind isn't blowing.

There are also issues that are neither of a technical or economic nature that need to be dealt with in taking this course of action. For example, in the case of more nuclear power, there are serious public concerns regarding the safety of nuclear power plants and the disposal of nuclear waste. In the case of wind power, there is some resistance to turbines "littering" the landscape. While these concerns may seem irrational or frivolous to some, they exist and along with the technical and economic concerns, would have to be addressed.

③ Improve energy efficiency of energy conversion processes

This occurs in three ways. One, upgrades are made to existing installations. For example, at OPG's Nanticoke Generating Station, new turbine blades installed in a couple of the units should improve the energy efficiency of these units by 1–2 percentage points [50].

Two, for existing process designs, technological advances allow new installations to operate more efficiently. For example, improvements in materials engineering has led to manufacture of steam boilers capable of working under higher pressures which has led to higher overall steam cycle efficiencies.

Three, altogether new processes have been developed which allow conventional fuels to be used more efficiently. For example, Canadian electric utility power plants using coal had an average thermal efficiency of 33.04% in 2000 [22]. In contrast, using coal in an IGCC (integrated gasification combined cycle), efficiencies of up to 51% are proposed.

④ Use lower carbon intensity fuels

This is commonly referred to as *fuel-switching* and almost always refers to substituting natural gas for coal. A 'back of the envelope' calculation shows that 2.5

emissions. Examples of secondary emissions include releases of methane gas caused by the decomposition of organic material in regions flooded by hydroelectric dams, CO₂ emissions associated with manufacturing cement used in construction and transportation of fuel and wastes to and from nuclear power plants.

times more CO₂ is released if coal is used rather than natural gas to produce a given amount of heat.²

A major disadvantage to this specific substitution is the price of natural gas. Firstly, natural gas, on a unit energy basis, is more expensive than coal. Secondly, its price is subject to much more fluctuation. Other disadvantages vis-à-vis this particular fuel-switch are that natural gas is more difficult to transport and store than coal and its proven reserves are also much less (according to the National Energy Board [6, p 75], as of 1991, there were 91 years of domestic coal reserves versus just nine years of natural gas reserves).

Bio-fuels could also represent a class of hydrocarbons with a lower carbon intensity than coal. The actual fuel combustion would be carbon-neutral; all associated carbon emissions would result from the ancillary collection, processing, and transportation activities. A full life cycle assessment would be necessary to determine if this type of fuel-switching is indeed beneficial.

⑤ Capture and storage of CO₂

The CO₂ produced as part of the energy conversion process is captured prior to being released to the atmosphere and subsequently stored. The capture can be performed either pre-combustion or post-combustion and there are a number of potential storage destinations: aquifers, porous geologic formations, depleted oil and gas reservoirs, coal seams, deep ocean floor. CO₂ capture and storage is a viable solution for CO₂ wherever fossil fuels are used as an energy source and opportunities for storage exist [35, p 249].

In Canada, 23 coal fired plants were used to create 106 TWh of the electricity generated in 2000. Table 1.4 shows the contribution that these coal plants made to the electrical generation capacity in each province.

Several technologies are available for capturing CO₂ from coal power plants:

- (a) Chemical absorption with amine solvents
- (b) O₂/CO₂ recycle combustion (oxy-fuel)
- (c) Cryogenics
- (d) Membrane separation either with or without absorption solvent

²Energy content of bituminous coal and natural gas used in Ontario during 2000; natural gas assumed to be pure methane with specific gravity of 0.585; coal assumed to contain only carbon and hydrogen in ratio of 80:20

Table 1.4: Coal use across Canada, 2000 (Source: Statistics Canada [21])

Province	Coal generating capacity [MW]	Percent of in- stalled capacity [%]
Nova Scotia	1 280	55.4
New Brunswick	570	13.6
Ontario	7 767	26.2
Manitoba	220	4.2
Saskatchewan	1 766	53.7
Alberta	5 900	60.1
Canada	17 503	15.7

Of the five CO₂-reduction ideas presented above, chemical absorption with amine solvents is the most promising near-term³ mitigation strategy for at least two reasons:

1. Table 1.5 shows the actual age distribution of Canadian coal-fired generating capacity in 1998 and forecasts the 2010 distribution assuming that all of these plants remain in service. There is a substantial investment in coal-fired capacity in Canada and, with a coal-fired power plant having a nominal useful-life of 40 years, this capital stock will be available in the near- to medium term. Amine absorption capitalizes on this investment as it does not require modification of the existing power plant.⁴ Converting these plants for oxy-fuel combustion or fuel-switching requires the plant boilers be replaced; switching to non-CO₂ emitting power plants or IGCC would imply moth-balling the existing equipment.
2. Technology to remove acid gases from relatively dilute, low pressure vapour streams is commercially available. The process is used for natural gas sweetening and to provide a source of CO₂ for various industrial processes: food processing, freezing, beverage carbonation, chilling, and enhanced oil recovery (EOR (enhanced

³In the more distant medium- and long-term, there is a particularly noteworthy technology which combines ideas ③, ④, and ⑤ presented above: SOFC (solid oxide fuel cell)'s. SOFC's, using synthesis gas generated from coal as a fuel source, would generate electricity more efficiently than either PCC (pulverized coal combustion) or IGCC and produce a high-purity CO₂ stream that is more or less ready for transportation and storage. Further CO₂ mitigation and higher efficiency could be achieved by using natural gas in lieu of coal. However, there are outstanding materials and systems issues that need to be resolved before this technology can be implemented on a utility scale.

⁴While it is true that amine absorption does not *require* modifications to the power plant, this thesis examines the benefits of extracting steam from the power plant for use in the CO₂ capture plant. So, in this work, it cannot be said that the power plant is entirely left alone.

Table 1.5: Age distribution of Canadian coal power plants: 1998 and 2010 (Source: Statistics Canada [21])⁶

Age of units years	1998 capacity		2010 capacity	
	[MW]	[%]	[MW]	[%]
1–24	8 989	46	2 728	16
25–29	3 404	16	2 632	15
30–34	4 503	25	3 629	21
35–39	212	3	3 404	19
≥ 40	394	10	5 110	29
Total	17 503	100	17 503	100

oil recovery)).⁷ Oxy-fuel is in the demonstration stage only, IGCC technology is commercially available but not with CO₂ capture (that part has yet to reach the demonstration stage), and membrane separation requires additional materials research and development before it becomes a possibility.

1.2.4 Capturing CO₂ with MEA

The general process flow diagram for amine absorption is shown in Figure 1.2. The fundamental underlying principle is the exothermic, reversible reaction between a weak acid (*e.g.*, CO₂) and a weak base (*e.g.*, MEA) to form a soluble salt. The inlet gas is contacted counter-currently with ‘lean’ solvent in the *Absorber*. The acid gases are preferentially absorbed by the solution. The solution, ‘enriched’ with CO₂, is pre-heated before entering the *Stripper* where, through the addition of heat, the reaction is reversed. From the bottom of the column, the ‘lean’ solvent exchanges heat with the ‘rich’ solvent entering the column and is recycled back to the *Absorber*. From the top, a high-purity (dry-basis) CO₂ is produced.

Large quantities of heat are required by the *Stripper* reboiler to regenerate the *rich* solvent; studies have shown that 0.37–1.90 kJ/kg CO₂ is needed⁸. For reference, a 500 *mathrmMW_e* unit burning sub-bituminous coal emits about 500 000 kg/hr of CO₂.

Deciding where this heat is to come from is a fundamental part of the design of an MEA absorption plant. One approach is to include auxiliary heat and, maybe, power generating equipment as part of the design [55, 54, 14, 40]. The other alternative is to

⁷That being said, it has never been used for the capture of CO₂ on a scale that the wholesale scrubbing of power plant flue gas entails.

⁸see 5.4 for the source of this range and a detailed analysis of the energy requirements.

1.3 Implementation

1.3.1 Selection of study basis

The basis for this work is a 500 MW unit from OPG's Nanticoke Generating Station. The Nanticoke Generating Station consists of eight Babcock and Wilcox units; each one is designed to generate about 3.3×10^6 lb/hr of steam at 2400 psig and 1000°F with re-heat also to 1000°F. Reasons for this site selection are as follows:

- the Nanticoke Generation Station is the largest point source of CO₂ emissions in the province of Ontario (1.7 Gt of CO₂ emitted in 1999 which represented more than half (53%) of the CO₂ emissions from power generation in that year [3]).
- OPG provided funding to support the work and access to operational data not available in the open literature.
- The unit size and coastal location — it is situated on the northern shore of Lake Erie — correspond with the basis for CO₂ capture studies chosen by the IEA (International Energy Agency) GHG R&D Programme Test Network for CO₂ Capture [32]. Therefore, it is expected that the results of this study will have immediate benefit for that group.
- In contrast to perceived conventional wisdom, it has recently been demonstrated that, within the proximity of Nanticoke, there exists a potential CO₂ sequestration reservoir capable of accepting many years worth of CO₂ from a 500 MW unit [52]. As noted above, CO₂ capture and sequestration as a CO₂ mitigation strategy is only worth considering where opportunities for CO₂ sequestration exist. Apparently, Nanticoke qualifies.

1.3.2 Selection of simulation software

The choice was made to use Aspen Plus[®] for all process simulation work. At the time that the study began, two generic process simulation software suites were readily available: HYSYS[®], marketed by Hyprotech, and Aspen Plus[®], developed by Aspen Technology, Inc. The initial decision to use Aspen Plus[®] over HYSYS[®] was based upon reported limitations of HYSYS[®] in modelling *Absorber* and *Stripper* columns with large numbers of trays [55, p 46]. As the work progressed, other advantages and disadvantages associated with using Aspen Plus[®] for this work became apparent:

- In May 2002, Aspen Technology, Inc. announced its acquisition of Hyprotech. Given that there was substantial overlap of the Aspen Plus[®] and HYSYS[®] product spaces, there was speculation, even among employees, that support for HYSYS[®] could be discontinued [19]. So, this seemed to reaffirm the decision to use Aspen Plus[®] as being correct.
- There are a number of reports of Aspen Plus[®] being used for modelling amine absorption processes [1, 54, 55, 27, 25, 26, 20] and, also a report of Aspen Plus[®] being used for modelling a power plant steam cycle [48]. This prior record suggests that Aspen Plus[®] is suited to the current endeavour.
- Aspen Plus[®] is updated often. Three major software revisions have been used during this study. This change can be both good and bad: good, in that every new revision brings the promise of improvements and bad, in the sense that many changes occur beneath the threshold sensitivity of the user which can unknowingly cause discontinuities in the results. However, in this work, the software changes did not appear to affect the outcomes of the simulations.
- Aspen Plus[®] allows the incorporation of almost any arbitrary Fortran code which makes it flexible and extensible.
- A major disadvantage, though, is that, being proprietary, there is no access to the underlying system design or source code which makes troubleshooting some behaviour particularly onerous (*i.e.*, requires building test cases to reverse engineer the software).

1.3.3 Outline of thesis

Assessing the feasibility of using steam from the power plant to ‘fuel’ CO₂ capture necessitated a number of discrete activities. Each task is presented in its own chapter:

- Chapter 2 describes the development of a simple coal combustion model that estimates the resultant heat and flue gas production from burning a given quantity and quality of coal.
- Chapter 3 describes the development of a steam cycle model that accurately predicts the power output and steam conditions of the power plant at part-load conditions.
- Chapter 4 discusses, in detail, the development of a model of CO₂ capture using amine absorption.

- Chapter 5 details the integration of the aforementioned three models to create a unified model of a coal-fired power plant with amine absorption of CO₂ where steam extraction from the power plant provides the heat required for capture.

The last section, Chapter 6, evaluates the integrated scheme shown in Chapter 5 with scenarios where the additional energy of CO₂ capture is provided by an auxiliary power plant.

Chapter 2

Flue Gas Synthesis

2.1 Objective

The objective is to develop a model that is able to predict the flow rate and composition of flue gas and heat output for a particular power plant given knowledge about the fuel used, boiler operating conditions, and plant power output.

2.2 Rationale

2.2.1 Model flexibility

Including coal combustion as part of the overall model increases its flexibility and, thereby, its usefulness. It allows the evaluation of the performance of MEA absorption for non-existent power plants or for fuels which are not currently in use.

- Nanticoke was originally designed to burn a high-sulphur, U.S. bituminous coal but now consumes a mixture of PRB (Powder River Basin) and USLS (U. S. low-sulphur) coals in order to mitigate SO_x emissions [4]. In evaluating CO_2 capture potential at Nanticoke, one scenario to consider is the return to high-sulphur, U.S. bituminous coal. Since this coal is not currently being used, the characteristics of its flue gas need to be estimated.
- The GHG R&D Programme Test Network for CO_2 Capture has agreed upon a basis for conducting studies in CO_2 capture [32]. The power plant is hypothetical so, indeed, a method for estimating the flue gas properties of this plant is required.

2.2.2 Model accuracy

The accuracy of the combustion model is important as its outputs — flue gas composition, flue gas flow rate, and specific heat output — affect the design, performance, and cost of MEA absorption.

- The mass flux of a component in the vapour phase can be expressed as the product of a driving force and the appropriate mass transfer coefficient:

$$\mathcal{N} = k_y (y_\infty - y_i)$$

The higher the concentration of CO₂ in the flue gas, the faster it is absorbed by the solvent. Different fossil fuels generate flue gases with very different CO₂ concentrations. For example, flue gas with 14 mol% CO₂ is typical for coal combustion; 8 mol% and 3 mol% CO₂ is normal for flue gas resulting from the use of natural gas in a natural gas boiler and an NGCC (natural gas combined cycle), respectively.

- There are a several compounds, typically present in flue gas, to which MEA absorption is particularly sensitive (*e.g.*, O₂, SO_x, NO_x). To a lesser or greater extent, the abundance of these molecules in the flue gas depends upon the composition of the fuel. The impacts on the design and operation of the capture process are many:
 - Additional pollution control equipment may be required to treat the flue gas upstream of MEA absorption.
 - The concentration of MEA may need to be restricted and/or additives may be required.
 - Additional make-up MEA may be required.
- The flue gas volumetric flow rate influences both the capital and operating costs of the MEA absorption process.
 - The volume of flue gas will determine the size of the ductwork and, more importantly, the size (and number) of *Absorber* required to capture the desired amount of CO₂.
 - A *Blower* is required to push the flue gas through any and all pollution control equipment upstream of the MEA absorption process and to overcome the pressure drop in the *Absorber*. The volume of flue gas will determine the work duty of this equipment.

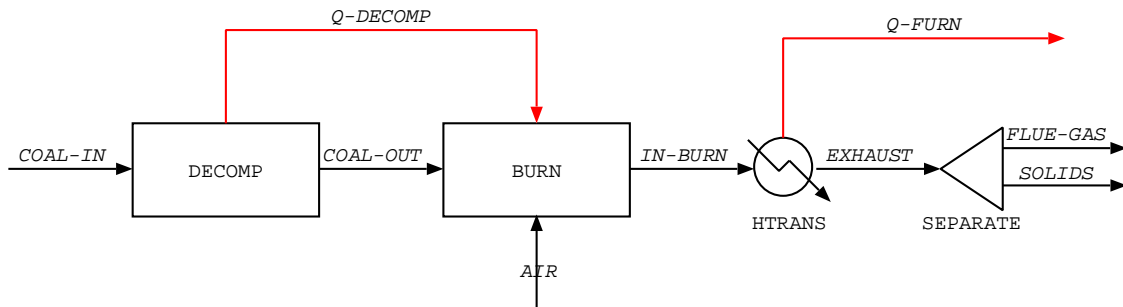


Figure 2.1: Coal combustion simulation flowsheet

2.3 Implementation

The synthesis of the Aspen Plus[®] input file draws heavily from the example *Modelling Coal Combustion* included in the systems documentation [9, pp 3-1–3-23]. The simulation flowsheet is given in Figure 2.1.

Below are discussed the areas where the Aspen Plus[®] model development differs from the example problem.

2.3.1 Specifying properties

Property Data

The ultimate, proximate, and sulphur analyses is provided for the three coals of immediate interest. Two of these coals are used at Nanticoke Power Generating Station [4] (*i.e.*, PRB and USLS) and the last is specified by the IEA for use in CO₂ mitigation studies [32]. The characteristics of these coals are given in Table 2.1.

In the case of PRB and USLS, with the absence of full analysis, component **ash** is specified as a ‘very poor coal’ (*i.e.*, coal with 100 wt% ash). The more rigorous approach is used for the IEA coal where the ash constituents are specified and the ENTHGEN and DNSTYGEN property methods are used to calculate its enthalpy and density.

Property Methods

The property method is changed from **IDEAL** to **PR-BM**. **PR-BM** is recommended for coal combustion applications [11].

Table 2.1: Coal characteristics

	Units	PRB	USLS	IEA
Proximate analysis (dry):				
Moisture	%	28.1	7.5	9.5
Volatiles	%	42.92	33.69	N/A
Ash	%	7.13	10.36	13.5
Fixed carbon	%	49.95	55.95	N/A
Ultimate analysis (dry):				
Carbon	%	69.4	77.2	71.4
Hydrogen	%	4.9	4.9	4.8
Nitrogen	%	1.0	1.5	1.6
Sulphur	%	0.4	1.0	1.0
Oxygen	%	17.2	5.0	7.8
Ash	%	7.1	10.4	13.5
High heating value:				
Dry	kJ/kg	27637	31768	
As fired	kJ/kg	19912	29385	
Calorific value:				
Gross	MJ/kg			27.06
Net	MJ/kg			25.87

Careful consideration is given to the manner in which enthalpy calculations for coal are handled in Aspen Plus[®]. Specific enthalpy of a coal is given by

$$h = \Delta_f h + \int_{298K}^T C_p dT$$

The Aspen Plus[®] coal enthalpy model is called HCOALGEN and its four option codes specify how enthalpy is calculated.

1. In HCOALGEN, heat of combustion is a GCV (gross calorific value), is expressed in Btu/lb of coal on a dry, mineral-matter-free basis, and is controlled by the first option code. There are five correlations in Aspen Plus[®] for the calculation of $(\Delta_c h)^{d,m}$ plus the ability for a user to specify $(\Delta_c h)^d$ directly.
2. The second option code selects one of two correlations for calculating the heat of formation, $\Delta_f h$; the first calculates heat of formation directly from the coal analyses and the other is based on the heat of combustion.

The heat of combustion correlation assumes that combustion results in complete oxidation of all of the elements except for sulphatic sulphur and ash. The numerical coefficients are combinations of stoichiometric coefficients and the heats of formation of CO₂, H₂O, NO₂, and HCl at 298.15 K.

$$\Delta_f h = (\Delta_c h)^d - (1.418 \times 10^6 w_H^d + 3.278 \times 10^5 w_C^d + 9.264 \times 10^4 w_S^d - 2.418 \times 10^6 w_N^d - 1.426 \times 10^4 w_{Cl}^d) 10^2$$

3. There are two correlations for calculating the heat capacity and these are selected via the third option code.
 - The Kirov correlation identifies five coal constituents — moisture, ash, fixed carbon, and primary and secondary volatile matter — and calculates the heat capacity as a weighted sum of cubic equations for each constituent.
 - The second correlation is a cubic temperature equation with parameters regressed from data for three lignite and one bituminous coal.
4. The remaining option code in HCOALGEN allows the user to specify the enthalpy basis. Aspen Plus[®] can be instructed to use either:

- elements in their standard states at 298.15 K and 1 atm or
- the component at 298.15 K.

The *Heat of Combustion* approach is used to calculate $\Delta_f h$ and values of $(\Delta_c h)^d$ are entered directly, The Kirov correlation is used to calculate the heat capacity because it takes into account the coal analyses whereas the cubic equation correlation does not, and, finally, the enthalpy basis used is that of the component at 298.15 K (*i.e.*, option code ‘6111’).

2.3.2 Specifying streams

The flowsheet has two inputs: **AIR** and **COAL-IN**.

- The composition of **AIR** is taken from literature [18, p 653] and is nominally 78% N₂, 21% O₂, and 1% Ar. **AIR** flow rate is calculated such that there is 21% excess O₂ “in the flame”.

AIR temperature is set to the outlet temperature of the air from the secondary air heater and atmospheric pressure is used.

- **COAL-IN** composition is given by specifying the relative abundance of each type of coal. **COAL-IN** flow rate is set such that the target heat duty, Q_{FURN}^* , is achieved. As an example, Q_{FURN}^* can be calculated from the plant power output and overall efficiency:

$$Q_{\text{FURN}}^* = \frac{E_{\text{trans}}}{\eta_{\text{th,plant}}}$$

COAL-IN temperature is set to the pulverizer outlet temperature and, again, atmospheric pressure is assumed.

2.3.3 Specifying blocks

HTRANS is modelled with the **HEATER** UOM (unit operation model) and is inserted between *BURN* and *SEPARATE*. This block removes from the combustion gases the useful heat transferred to the steam cycle. The temperature of the block is equivalent to the flue gas temperature at the economizer outlet.

2.4 Model Validation

2.4.1 Coal heat of combustion

The standard heat of combustion is determined for three different coals whose properties are given in Table 2.1 using the simulation flowsheet shown in Figure 2.1.

A coal's standard heat of combustion, $(\Delta_c h)^\circ$, should be approximately equal to its NCV (net calorific value). The NCV of the PRB and USLS coals is not available but can be calculated from the GCV by making an adjustment for pressure and the latent heat of vaporization of water [5]:

$$NCV = GCV - 215.5 [J/g] \cdot w_H$$

The NCV of IEA coal is reported on a dry basis. This converted to an "as fired" number via:

$$NCV = NCV^d \cdot (1 - w_{H_2O})$$

Table 2.2 compares the heat of combustion from the simulations with data obtained experimentally. Aspen Plus[®] calculates a heat of combustion which is slightly greater than the corresponding NCV.

Table 2.2: Comparison of calculated standard heat of combustion with observed NCV

	Units	USLS	PRB	IEA
NCV	kJ/kg	28149	18480	23412
$(\Delta_c h)^\circ$	kJ/kg	28710	19535	24112
Δ	%	2.0	5.7	3.0

2.4.2 Flue gas flow rate

The flue gas mass and volumetric flow rates at the economizer exit from a unit at Nanticoke Power Generating Station burning a 50/50 blend of PRB and USLS coals are estimated. The input data values and sources are shown in Table 2.3.

Table 2.4 compares the flue gas flow rate from the simulation with observed values. The estimated mass and volumetric flow rates are moderately higher and lower, respectively, than what is observed at the plant.

Table 2.3: Flue gas flow rate simulation input data

	Units	Value	Source
Overall plant:			
E_{gen}	kW	507611	[30]
$\eta_{th,plant}$	%	36	[51]
Q_{FURN}^*	10^6 Btu/hr	4816	
Streams:			
T_{AIR}	$^{\circ}$ F	519	[31]
$T_{COAL-IN}$	$^{\circ}$ F	160	[31]
Blocks:			
T_{HTRANS}	$^{\circ}$ C	320	[4]

Table 2.4: Comparison of calculated flue gas flow rate with observed values

	Mass [kg/hr]	Volumetric [m ³ /hr]
Actual	2424400	4182700
Simulated	2500291	4081180
Δ	3.0 %	-2.5 %

2.5 Conclusions and Recommendations

- The combustion model reasonably predicts the flue gas flow rate and heat output from a power plant boiler.
- For a 50/50 blend of PRB and USLS coals, Table 2.5 shows the flue gas composition.

Table 2.5: Flue gas composition

Component	mol %
N ₂	72.86
CO ₂	13.58
H ₂ O	8.18
O ₂	3.54
Ar	0.87
NO	0.50
CO	0.37
SO ₂	0.05
H ₂	0.04

Chapter 3

Simulation of Steam Cycle

3.1 Objective

The objective is to develop a model that simulates the part-load performance of the steam cycle of a 500 MW unit at OPG's Nanticoke Generating Station. That is, to create a model that predicts the required heat input to the boiler, power output from the turbine, and conditions (*i.e.*, temperature, pressure, flow rate) of steam and feed water throughout the steam cycle.

3.2 Motivation

Including the steam cycle as part of the overall model increases its flexibility and, thereby, its usefulness. It allows for the evaluation of the performance of MEA absorption when the power plant is operating at part-load and the exploration of different process integration configurations.

- For a number of reasons (*e.g.*, technical problems, desire to maintain reserve capacity, lack of demand), plants operate at loads other than their MCR (maximum continuous rating). The effect of plant load on CO₂ capture using MEA absorption can be studied.
- The heat and work duties of the MEA absorption process are considerable. It may be economically desirable for the large work and heat duties of the MEA absorption process to be reduced or paid for through process integration:

- use steam to provide heat for *Stripper* reboiler
 - use super-heat from steam destined for *Stripper* reboiler to pre-heat “rich” solvent
 - use steam to provide motive power for flue gas blower and CO₂ compressors
 - use boiler feed water for cooling in-between CO₂ compression stages
- Speaking strictly from the point of view of the steam cycle, process integration configurations differ from one another in terms of the location from which steam is extracted and, to a lesser extent, the position at which the condensate is re-injected. Each potential extraction location provides access to steam at a different temperature, pressure, and flow potential (*i.e.*, limit to the quantity of fluid that can be removed). Similarly, except for maybe the main and re-heat steam temperatures, changing plant load also changes the steam temperature and pressure throughout the process. The variations in steam quality affect the quantity of steam that needs to be diverted to the *Stripper* reboiler in order to satisfy a given heat duty which, in turn, increases or reduces the power output from the plant.

3.3 Points of emphasis

The accuracy of this steam cycle model is important as its outputs — heat input to the boiler, power output from the turbine, and conditions of steam and feed water — affect the performance and cost of MEA absorption.

- As the plant load decreases, so too does $\eta_{\text{th,plant}}$. More coal is required to produce each unit of power and, consequently, the quantity of flue gas emitted per unit of electricity produced increases. This will drive the specific cost of capture (*i.e.*, cost per unit mass of CO₂) upwards as the flue gas volumetric flow rate influences both the capital and operating costs of the MEA absorption process.
- Accurate plant power output estimation increases the confidence with which the following two questions can be answered:
 1. How much will MEA absorption de-rate the plant?
 2. How does MEA absorption compare with other mitigation options?

3.4 Implementation

OPG provided design heat balance of Nanticoke Generating Stations units 1–4 at 100%, 75%, and 50% load each of which displays the stream and equipment connectivity and provides the following information:

- for each stream, the mass flow rate and the temperature, pressure, and/or specific enthalpy.¹
- for each feed water pre-heater, the TTD (terminal temperature difference) and the DTD (drain temperature difference)
- the turbine and unit heat rate
- the main turbine Sankey diagram

The simulation flowsheet is shown in Figure 3.1. With the following notable exceptions, it reproduces the flow diagram in the design heat balance:

- streams with flow rates less than 10000 lb/hr, except for **ST-FPT1**, are ignored
- pressure drop across piping and feed water pre-heaters is ignored
- packing and valve stem leakages are ignored

The development of the Aspen Plus[®] input file is discussed below.

3.4.1 Specifying properties

There are two property methods within Aspen Plus[®] indicated for use for steam cycle simulation: **STEAM-TA** and **STEAMNBS**. **STEAM-TA** is based upon 1967 ASME steam table correlations. **STEAMNBS** is based upon 1984 NBS (National Bureau of Standards)/NRC (National Research Council) steam table correlations and is reportedly the more accurate of the two. In spite of its purported inferiority, **STEAM-TA** is used as it more closely matches the 1936 Keenan and Keyes steam tables upon which the original design is based.

¹In general, the specific enthalpy and only one of temperature and pressure are specified for any given stream in the heat design balance. Using a software implementation of the ASME (American Society of Mechanical Engineers) 1967 steam tables [41], temperature, pressure, specific enthalpy, specific entropy, and specific volume are calculated for each stream at each plant load, where missing. The conditions of important streams are given in Appendix A.

3.4.2 Specifying streams

Plant load is controlled by changing the flow rate of the boiler feed water, **H2O-BOIL**. This is the only stream specified in the input file and it is initialized using values for the design heat balance at 100% load:

	Units	Value
T	°F	488
P	psia	2700
\dot{m}	lb/hr	3358670

3.4.3 Specifying blocks

The steam cycle model has four sections:

1. main and boiler feed water turbines
2. condenser
3. boiler feed water pre-heaters
4. economizer, boiler, super-heater, and re-heater

The specification of each of these sections is discussed in turn.

Main and feed water pump turbines

The main turbine drives the generator producing electrical power for plant consumption and output to the grid. The other, smaller turbine drives the boiler feed water pumps. As is done elsewhere [23, 17, 48], each turbine is modelled as a series of single turbine stages interspersed with flow mixers and splitters as indicated by the flow path in the heat design balance [30].

Table 3.1 shows the volumetric flow rate of steam entering the HP (high-pressure), IP (intermediate-pressure), and LP (low-pressure) sections of the turbine. The steam pressure is throttled at part-load to maintain a constant flow rate into the HP and IP sections. This behaviour is emulated using *VALVE1* and *VALVE2*.

It is expected that, at part-load, the pressure ratios of stages between the governing stages and the last stage will be approximately constant [23]. This fact is borne out by

Table 3.1: Design inlet volumetric flow rates into turbine sections ($10^6 \text{ ft}^3/\text{hr}$)

Section	Plant Load			Mean	Std Dev	%RSD
	100%	75%	50%			
HP	1.157	1.155	1.154	1.155	0.001	0.13
IP	4.522	4.530	4.541	4.531	0.009	0.21
LP	20.724	20.784	20.828	20.779	0.052	0.25

the data in Table 3.2 which shows the ratio of outlet pressure to inlet pressure for each of the compressor stage groups in Figure 3.1. For turbine groups where constant pressure ratio is not observed, other criteria is used for specifying the outlet pressure:

- The pressure ratio of *HP* is calculated using a function of the form:

$$P_{out}/P_{in} = a\dot{m}_{in} + b$$

Figure 3.2 gives “least-squares” estimates of the parameters a and b and shows that the proposed model does a good job at explaining the variation in pressure ratio at part-load.

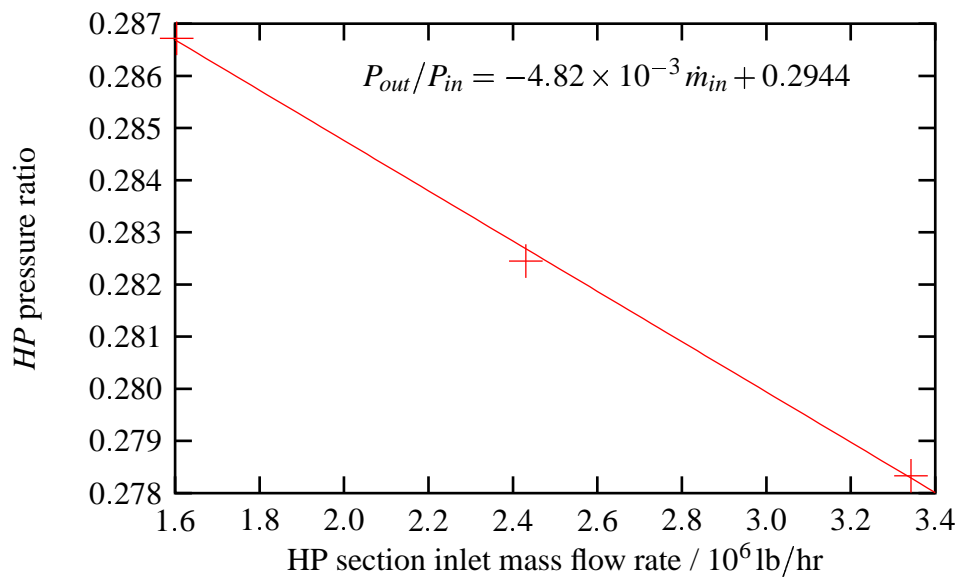


Figure 3.2: High-pressure section pressure ratio at part-load

Table 3.2: Ratio of discharge pressure to inlet pressure for turbine groups

Main turbine						
Block	Plant Load			Mean	Std Dev	%RSD
	100%	75%	50%			
HP	0.278	0.282	0.287	0.282	0.004	1.48
IP1	0.515	0.517	0.519	0.517	0.002	0.43
IP2	0.231	0.233	0.235	0.233	0.002	0.85
IP3	0.453	0.455	0.457	0.455	0.002	0.37
IP4	0.262	0.265	0.267	0.265	0.002	0.91
LP1	0.151	0.150	0.152	0.151	0.001	0.44
LP2	0.068	0.067	0.069	0.068	0.001	1.22
LP3	0.153	0.146	0.210	0.170	0.035	20.63
LP4	0.153	0.146	0.210	0.170	0.035	20.63
LP5	0.068	0.067	0.069	0.068	0.001	1.22
LP6	0.433	0.435	0.437	0.435	0.002	0.46

FP turbine						
Block	Plant Load			Mean	Std Dev	%RSD
	100%	75%	50%			
FPT1	0.107	0.080	0.054	0.080	0.027	33.34
FPT2	0.003	0.003	0.004	0.003	0.001	22.79

- The outlet pressure of *FPT1* is set equal to that of the **ST-FPT2**.
- The outlet pressure of *FPT2*, *LP3*, and *LP4* is set equal to that of the *Condenser*.

Given the constant volumetric flow rates and stage pressure ratios, it is expected that the isentropic efficiencies between the governing stage and the last stage stay about the same at part load [59]. Table 3.3 shows that this is indeed the case for all turbine groups except *LP3*, *LP4*, and *FPT1*. These blocks require special consideration.

Table 3.3: Fractional isentropic efficiency of turbine groups

Main turbine						
Block	Plant Load			Mean	Std Dev	%RSD
	100%	75%	50%			
HP	0.906	0.903	0.903	0.904	0.002	0.19
IP1	0.901	0.902	0.904	0.902	0.002	0.18
IP2	0.910	0.910	0.910	0.910	0.000	0.04
IP3	0.891	0.898	0.898	0.895	0.004	0.48
IP4	0.915	0.912	0.914	0.914	0.002	0.17
LP1	0.910	0.910	0.911	0.910	0.000	0.02
LP2	0.904	0.907	0.909	0.907	0.003	0.30
LP3	0.607	0.598	0.715	0.640	0.065	10.13
LP4	0.607	0.598	0.715	0.640	0.065	10.13
LP5	0.904	0.907	0.909	0.907	0.003	0.30
LP6	0.902	0.901	0.898	0.901	0.002	0.26

FP turbine						
Block	Plant Load			Mean	Std Dev	%RSD
	100%	75%	50%			
FPT1	0.182	0.153	0.126	0.153	0.028	18.22
FPT2	0.801	0.786	0.798	0.795	0.008	1.02

- The variation in the isentropic efficiency of *FPT1* is ignored as its low magnitude, even at base load, coupled with the low mass flow rate of steam through this part of the turbine makes its contribution to the overall feed water pump turbine output negligible. Therefore, the mean value is used in all cases.

- The efficiency of the last stage of a turbine is mostly dependent upon the annulus velocity [59]. Therefore, a model of the form

$$\eta_s = a q_{out} + b$$

is proposed to describe the part-load behaviour of *LP3* and *LP4*. Figure 3.3 gives “least-squares” estimates of the parameters *a* and *b* and compares the proposed model with the data from the design heat balance. The model does a fantastic job at explaining the variation in the isentropic efficiency of *LP3* and *LP4*.

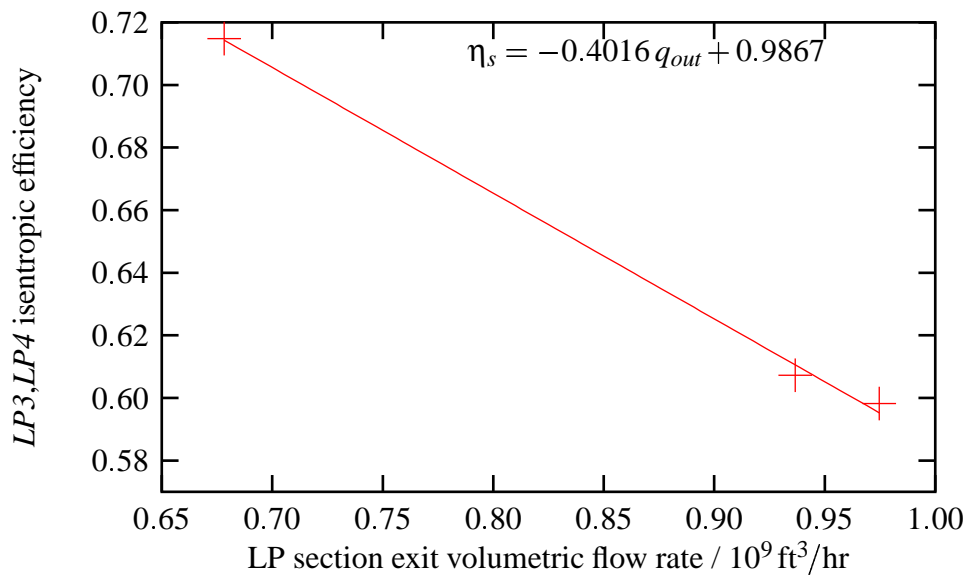


Figure 3.3: *LP3* and *LP4* stage groups’ isentropic efficiency at part-load

The final aspect of turbine behaviour that needs to be addressed is the bleed steam mass flow rates at part-load. Steam is extracted from the main turbine to drive the boiler feed water pump turbine and to pre-heat the boiler feed water. It is proposed that the bleed steam mass flow rates vary as a function of the steam mass flow rate at the inlet of the turbine section:

$$\dot{m}_{bleed} = a \dot{m}_{in} + b$$

“Least-squares” estimates of the parameters a and b are obtained for bleed stream and the proposed model is compared with data from the design heat balance in Figure 3.4. The proposed model explains essentially all of the variation in the bleed steam flow rates at part-load.

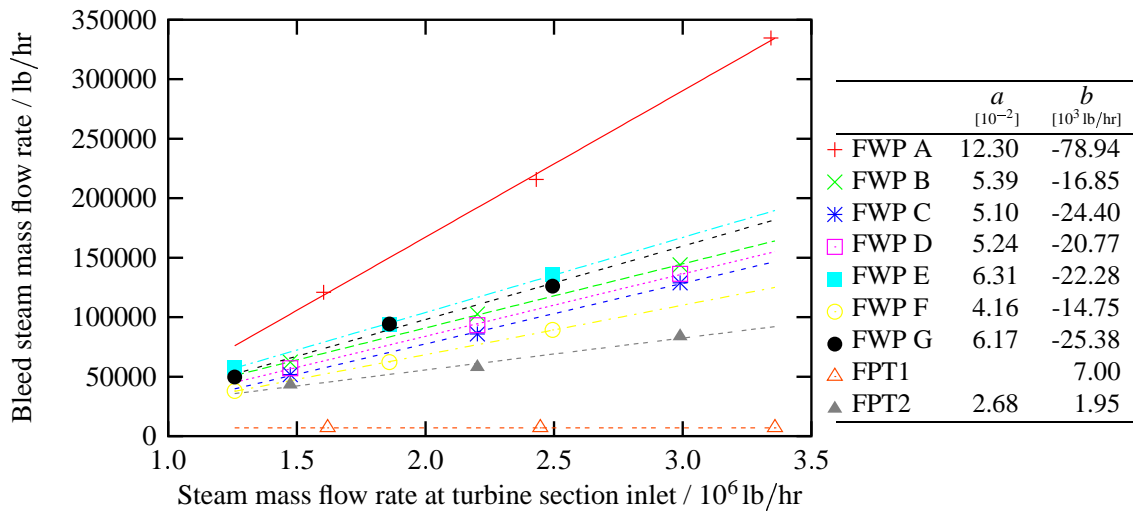


Figure 3.4: Turbine ‘bleed’ steam flow rates at part-load

Feed water pre-heaters

The feed water pre-heater section contains seven feed water pre-heaters, numbered A through G, and two pumps. Increasing the temperature of the boiler feed water increases the overall thermal efficiency of the power plant. Six of the feed water pre-heaters — A, B, D, E, F, G — are closed and the other, C, is open and also functions as a deaerator.

The closed feed water pre-heaters are shell and tube heat exchangers. These units are usually modelled in Aspen Plus[®] using **HEATX** UOM’s however, all attempts in this work to represent the feed water pre-heater section using **HEATX** UOM’s met with failure. It is believed that this difficulty could have been overcome if detailed heat exchanger design information or design heat balances at additional plant loads were available. That not being the case, the example of Ong’iro *et al.* [48], where each closed feed water pre-heater is modelled as a pair of *HEATER* blocks, is instead followed. The open feed water heater is modelled using the UOM *MIXER*.

For any regenerative cycle, the temperature to which the feed water is raised is a design variable that is ultimately fixed by economic considerations. This is also true of the temperature rise that is to be accomplished by each pre-heater [57, p 290]. The

‘cold-side’ exit temperatures are found to vary with plant load according to the following model:

$$T_{c,out} = a \ln \dot{m}_{c,in} + b$$

“Least-squares” estimates of the parameters a and b are calculated for each feed water pre-heater and the proposed model is compared with data from the design heat balance in Figure 3.5. All of the variation observed in the data is explained by the model.

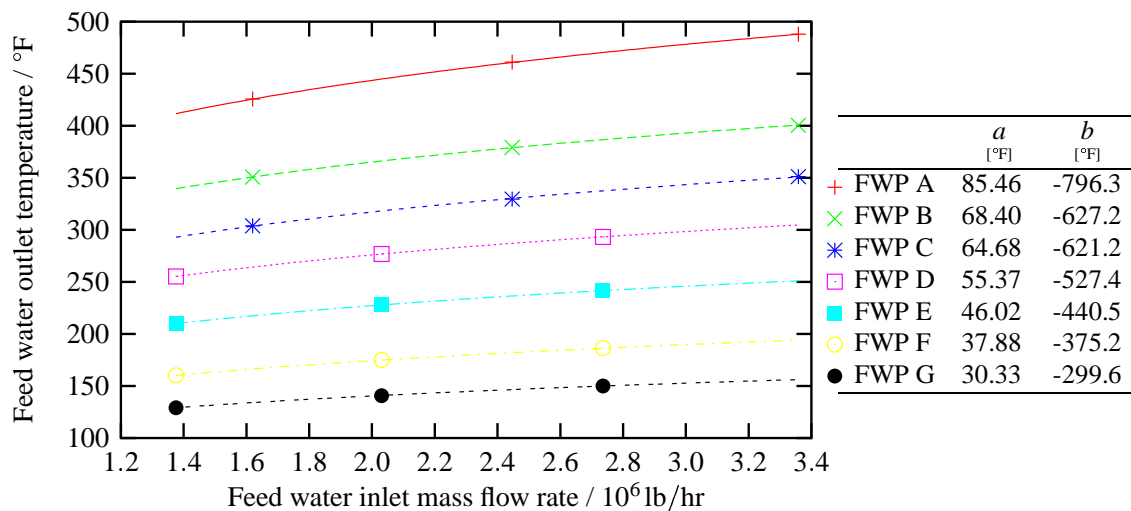


Figure 3.5: Boiler feed water temperature at part-load

The two feed water pumps are modelled using PUMP blocks. For *FWPUMP1*, in the absence of information in the design heat balance, the outlet pressure is selected such that it is marginally greater than that of the open feed water pre-heater, *FWP_C*. For *FWPUMP2*, the internal shaft power of the *Feed water pump turbine* is used as the power input to the pump. In both cases, efficiency is calculated using efficiency curves for water in a centrifugal pump [10].

Condenser

The condenser is modelled using a **HEATER** UOM. In the design heat balance, the condenser pressure is 1.4'' Hg at base load and 1.0'' Hg at both 75% and 50% load. It is not clear how condenser pressure changes with plant load. Therefore, the given value at base load is used at part-load.

Economizer, boiler, super-heater, and re-heater

The economizer, boiler, and super-heater are represented using a single **HEATER** block, *BOIL*, with outlet temperature and pressure of 1000°F and 2365 psia, respectively. The re-heater is represented by the **HEATER** block *REHT* with an outlet temperature of 1000°F and zero pressure drop.

3.5 Model validation

3.5.1 Property method

The basis for the Nanticoke Generating Station design heat balance is the 1936 Keenan and Keyes steam tables; note that the property methods in Aspen Plus[®] are based upon either the 1967 ASME or the 1984 NBS/NRC steam tables. It would be expected that changes in the underlying property data will cause changes in some of the calculated performance values. Tables 3.4 and 3.5 show the results of simulations performed with the two property methods alongside the data from the design heat balance. In these simulations, the **VALVE** and **COMPR** outlet pressures, **COMPR** isentropic efficiencies, and **FSPLIT** outlet flow rates are set using data directly from the design heat balance. That is, none of the correlations or assumptions presented above are used. As such, any differences observed between the simulation results and the design data result from differences in steam properties. Several conclusions can be drawn.

- The similarity between the observed and calculated values suggests that there were no gross errors in the transcription of the data.
- **STEAM-TA** is slightly better at reproducing internal power and **STEAMNBS** is slightly better at reproducing heat input. That being said, either property method is suitable for steam cycle modelling.

Table 3.4: Comparison of calculated internal power with design values (MW)

Plant Load	Design data theoretical	STEAM-TA		STEAMNBS	
		calculated	% diff	calculated	% diff
100%	516.97	517.73	0.15	518.37	0.27
75%	382.06	382.63	0.15	383.07	0.26
50%	255.04	256.31	0.50	256.57	0.60

Table 3.5: Comparison of calculated heat input with design values (MW)

Plant Load	Design data theoretical	STEAM-TA		STEAMNBS	
		calculated	% diff	calculated	% diff
100%	3919	3914	0.12	3917	0.03
75%	2938	2936	0.06	2939	0.02
50%	2016	2015	0.04	2016	0.02

3.5.2 Steam temperature, pressure, and flow potential

There are several locations along the turbine where it is feasible to extract steam for process use:

- at the inlet of the HP, IP, and LP sections
- at the turbine outlet
- at locations where steam is already extracted for feed water pre-heating

These locations are highlighted in the schematic of the turbine shown in Figure 3.6. Predicted steam conditions and flow rate at part-load at these key locations are compared to the design heat balance data in Figures 3.7, 3.8, and 3.9². In all cases, the model successfully describes the changes in steam conditions and flow rate at part-load.

3.5.3 Part-load power output and heat input

The internal power and heat input are estimated given boiler feed water flow rates from 1.6×10^6 to 3.4×10^6 lb/hr. This range covers plant performance from 50% to 100% of base-load. The simulation results are compared with the data from the design heat balance in Figures 3.10 and 3.11. Both in terms of power output and heat duty, the agreement between the model and the design data is very good.

3.5.4 Turbine and unit heat rate

The relationship between the turbine internal power, the electrical output to the grid, and the associated losses that occur along the way are illustrated in Figure 3.12.

²In the case of locations A through G, the flow rate shown is that which is available at the particular location and not necessarily the amount that is extracted for feed water pre-heating.

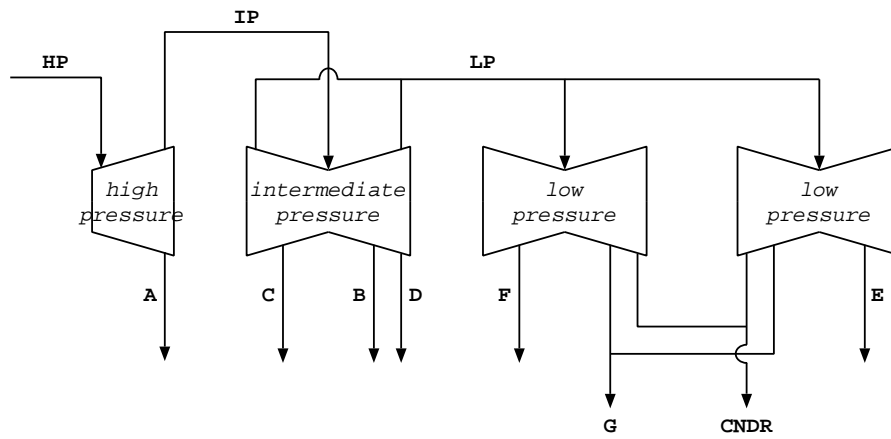


Figure 3.6: Potential steam extraction locations in steam cycle

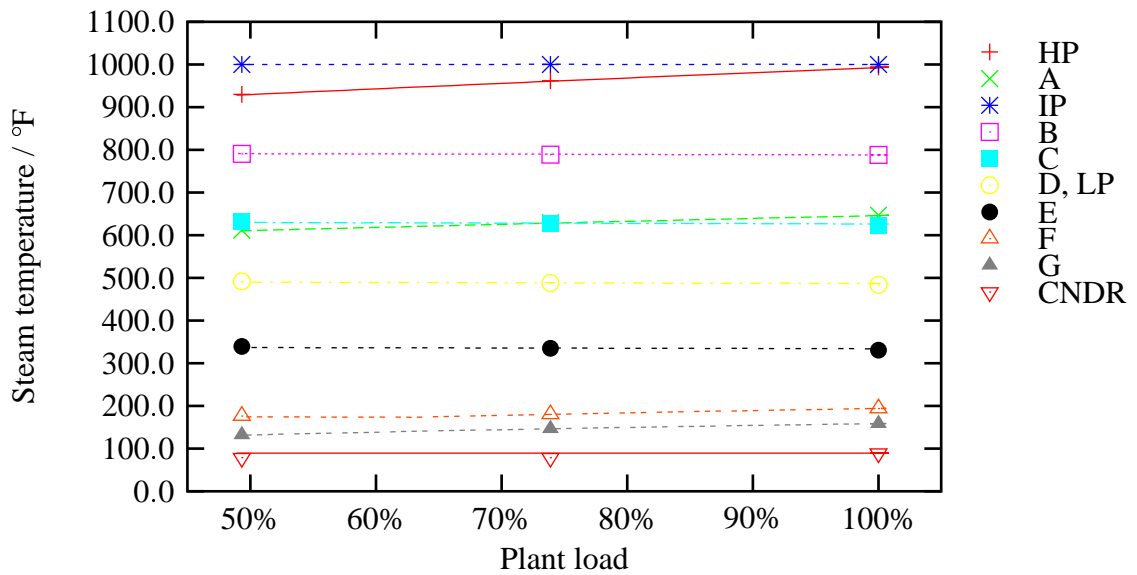


Figure 3.7: Steam temperature at part-load

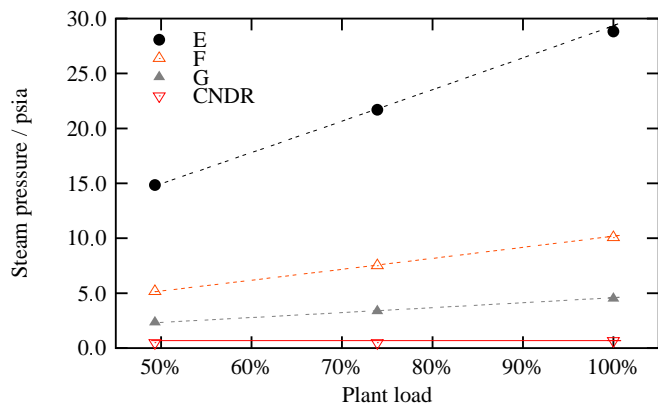
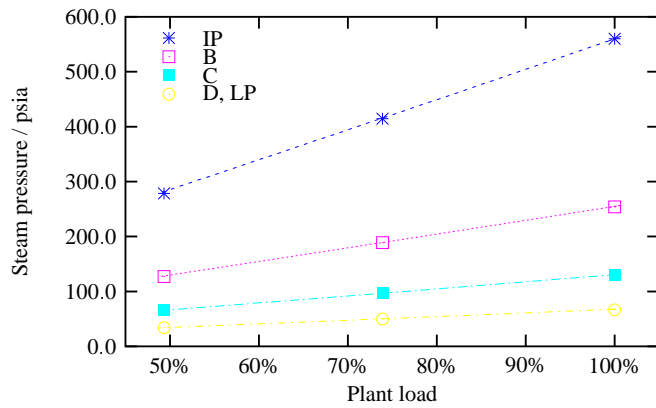
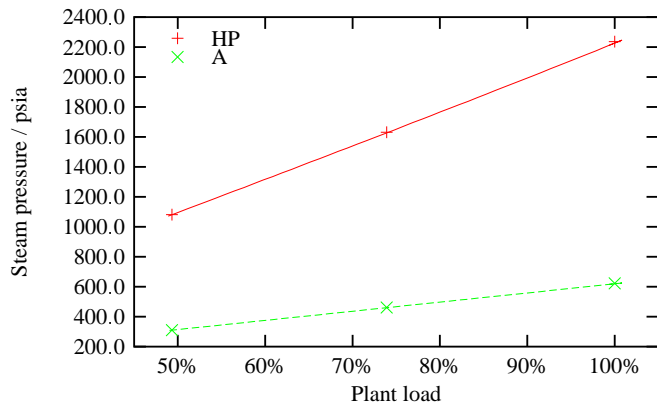


Figure 3.8: Steam pressure at part-load

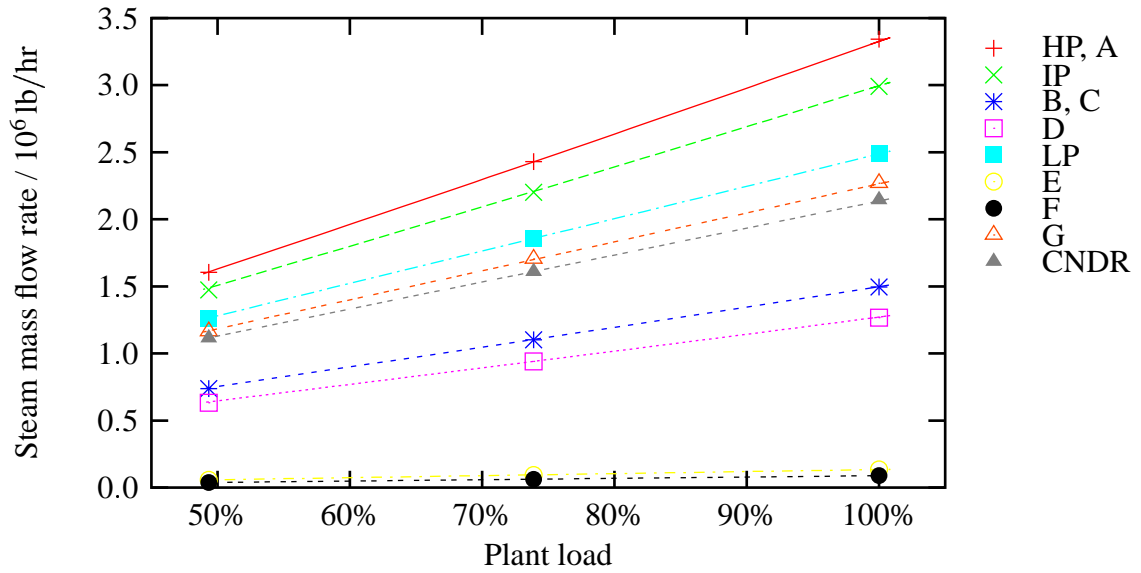


Figure 3.9: Steam flow rate at part-load

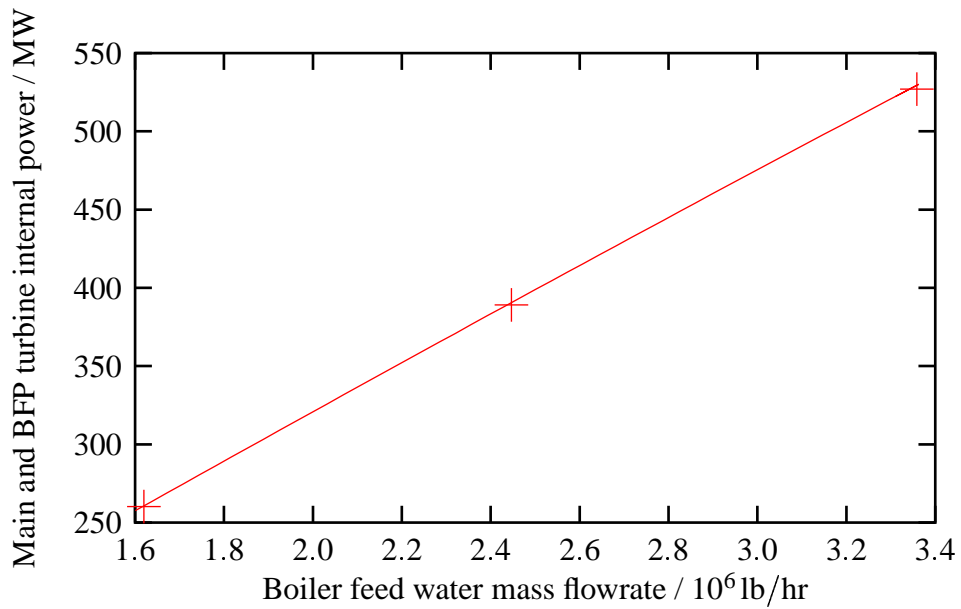


Figure 3.10: Turbine power output at part-load

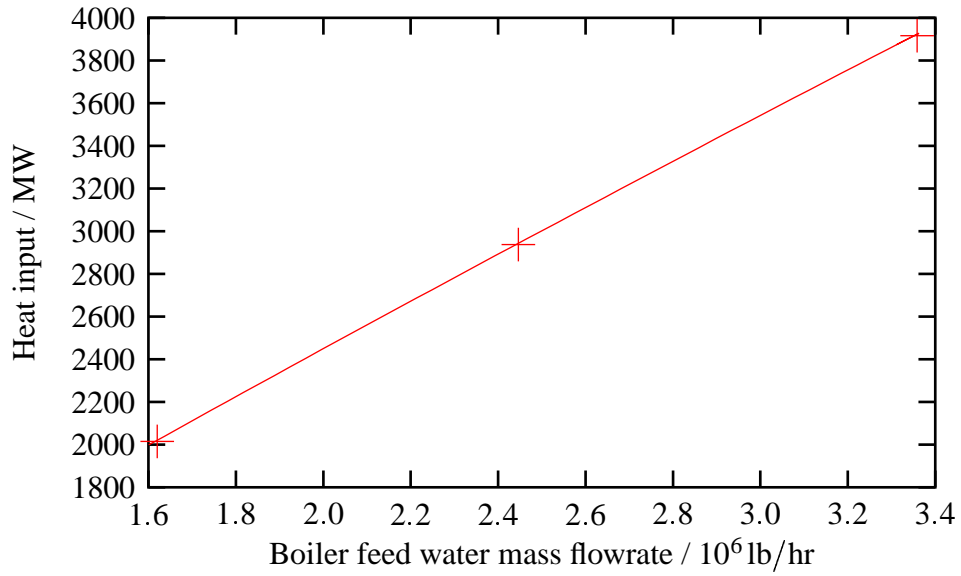


Figure 3.11: Turbine heat duty at part-load

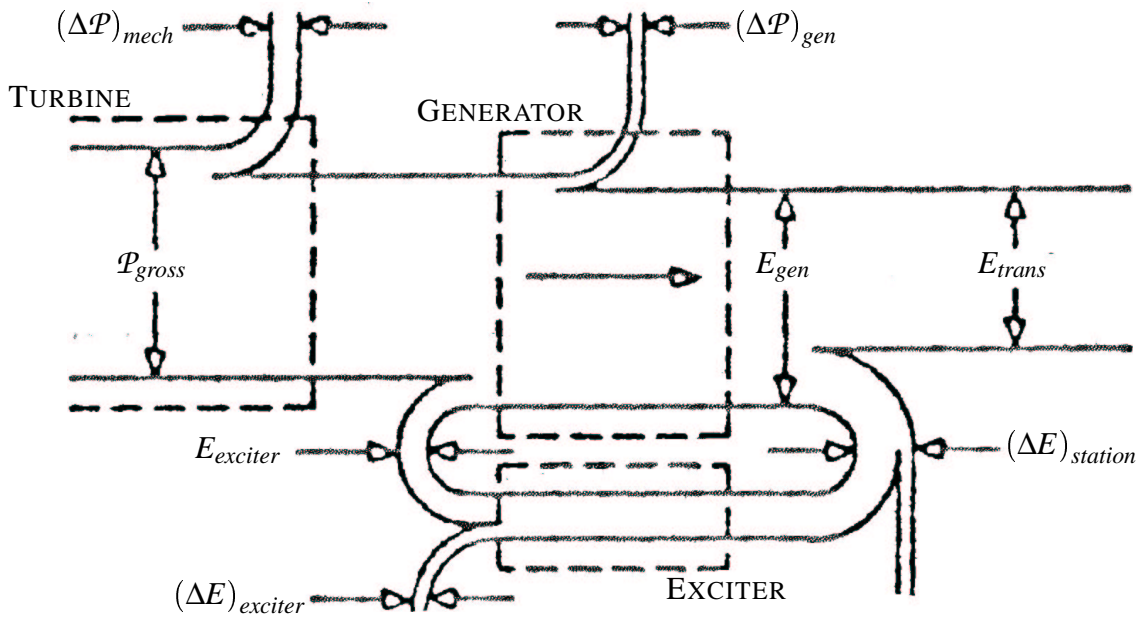


Figure 3.12: Main turbine Sankey diagram

Heat rate is an expression of the efficiency with which the internal power generated by the turbine is transformed into electrical energy. There are two “heat rates” given in the power plant design heat balances: THR (turbine heat rate) and UHR (unit heat rate). These can be calculated using the following expressions:

$$THR = \frac{\dot{m}_{BOIL} \times (h_{BOIL,out} - h_{BOIL,in}) + \dot{m}_{REHT} \times (h_{REHT,out} - h_{REHT,in})}{E_{gen} + P_{bfpt,net}}$$

$$UHR = \frac{\dot{m}_{BOIL} \times (h_{BOIL,out} - h_{BOIL,in}) + \dot{m}_{REHT} \times (h_{REHT,out} - h_{REHT,in})}{E_{trans} \times \eta_{b,th}}$$

Values for each of the aforementioned power ‘adjustments’ are available in the included Sankey diagram. These are plotted versus plant load in Figures 3.13 and 3.14.³ Models proposed for each factor, parameters regressed from the data, and the output from the models shown as straight lines in Figures 3.13 and 3.14. The agreement is very good except, perhaps, in the case of the *Boiler feed water pump turbine* mechanical losses. However, given the small magnitude of these losses, the effect on *THR* and *UHR* calculation is negligible.

Finally, using the above correlations, the turbine and unit heat rates, as a function of plant load, are calculated using the results from the Aspen Plus[®] steam cycle model. These results are compared to that offered in the design heat balances in Figure 3.15. As has come to be expected, the agreement between the design heat balance data and the results from the Aspen Plus[®] model is excellent.

3.6 Conclusions and recommendations

- The steam cycle model successfully predicts the part-load performance of the steam cycle of a 500 MW unit at OPG’s Nanticoke Generating Station.
- The performance of the model at part-loads below 50% needs to be validated.

³In Figures 3.13 through 3.15, the points represent data taken from the heat design balances and the lines represent simulation results.

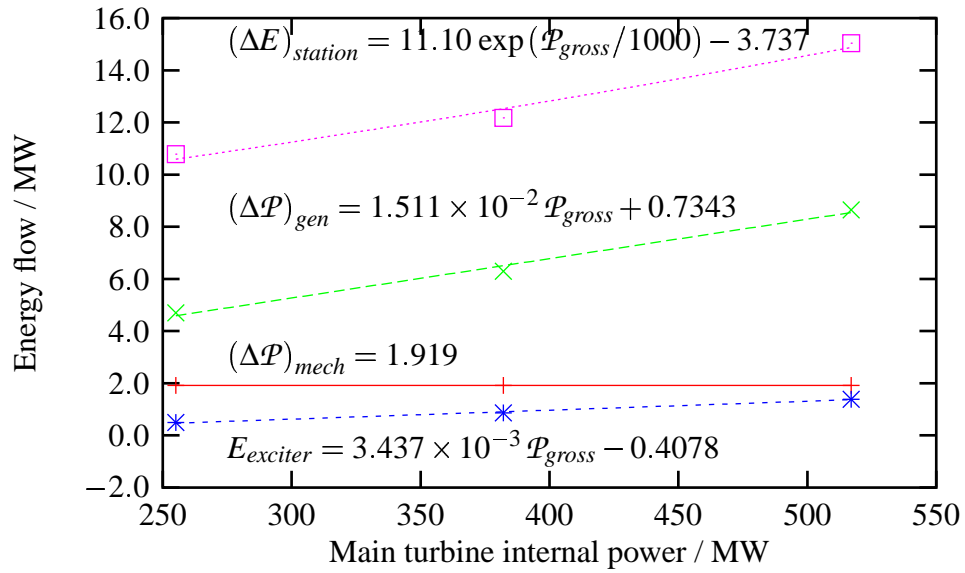


Figure 3.13: Main turbine work and energy flows

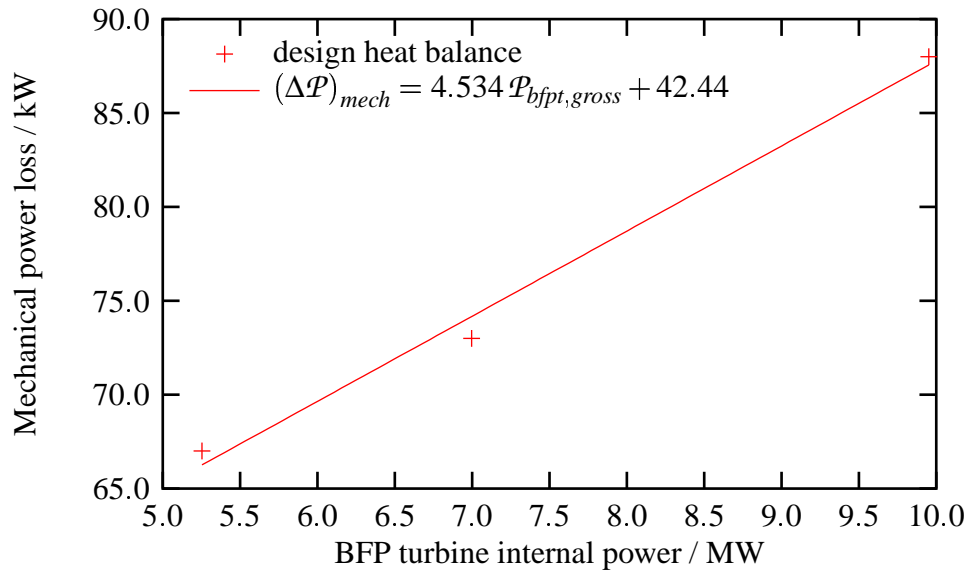


Figure 3.14: Boiler feed water pump turbine mechanical power losses

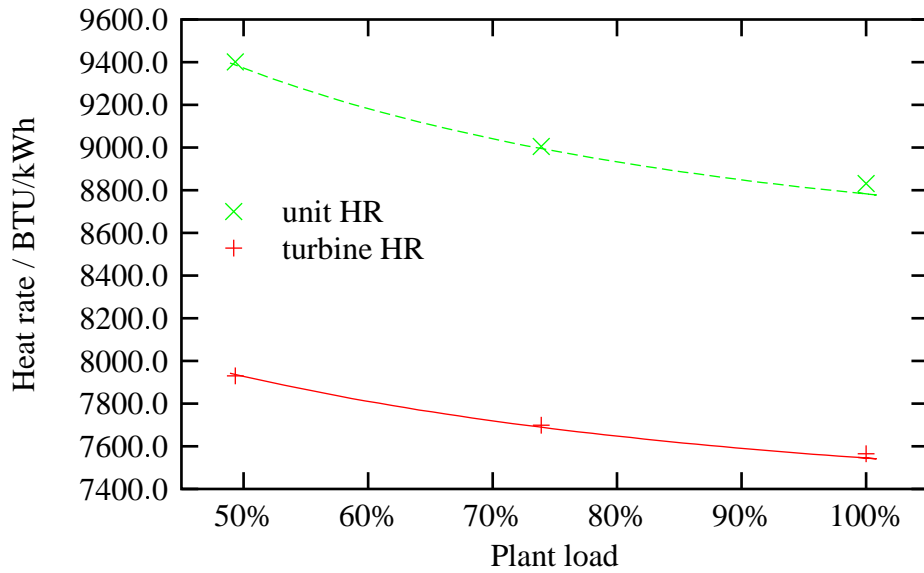


Figure 3.15: Turbine and unit heat rate at part-load

- The model should be extended such that it is able to predict off-spec performance of the steam cycle (*e.g.*, plant performance with one or more feed water pre-heaters off-line). This would allow the investigation of more complicated process integration configurations.

Chapter 4

Simulation of MEA Absorption Process

4.1 Objective

The objective of the work in this chapter is to develop an adaptable model that simulates the removal of CO₂ from power plant flue gas using MEA absorption. In particular, the model should report the work and heat duties required to achieve a particular recovery of CO₂ given a set of nominal equipment specifications and operating conditions.

4.2 Motivation

Having a detailed, adaptable model of MEA absorption increases the flexibility of the overall model and, thereby, its usefulness. It allows for the measurement of the sensitivity of the work and heat duties to changes in the process flowsheet, the design of key equipment, the choice of solvent, and the nominal operating conditions. A detailed model also increases the number of process integration scenarios that can be examined.

4.2.1 Process flowsheet evaluation

- For modelling CO₂ capture from flue gas, the MEA absorption flowsheet shown in Figure 4.1 is the one most frequently reported as being used [54, 55, 25, 26, 27, 20].¹

¹Singh *et al.* [54, 55] and Freguia *et al.* [25, 26, 27] do not close the recycle loop in their simulation flow sheets.

and the vapours are mixed with the *Stripper* overhead vapours.

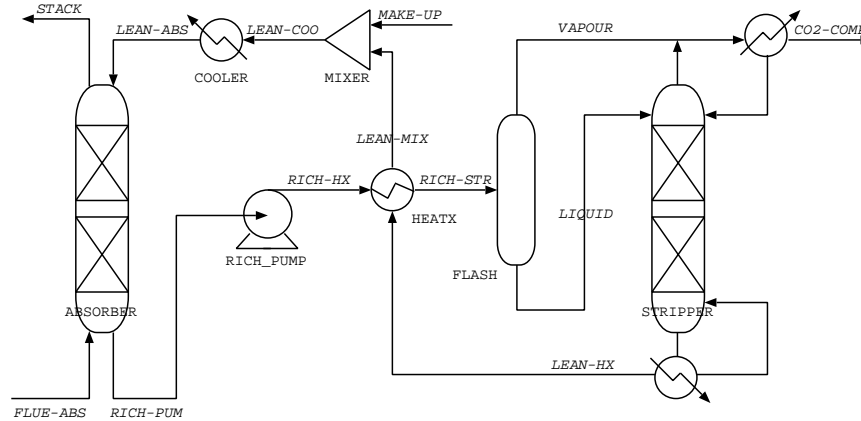


Figure 4.3: Kerr-McGee/Lummus Crest Global MEA absorption process flowsheet

In their examination of CO₂ capture cost sensitivity to solvent type, concentration, and flow rate and to the number of trays in each of the *Absorber* and *Stripper*, the simulation flowsheet description of Chakma *et al.* matches that shown in Figure 4.3 [14].²

- Soave and Feliu have demonstrated that, in a distillation tower, reboiler heat duty can be significantly lowered by only heating a fraction of the *Stripper* feed [58]. This implies that the flowsheet shown in Figure 4.4 may be preferred vis-à-vis those previously shown.
- The confluence of very large flue gas flow rates, a desire for a high recovery of CO₂, and the limits, in terms of diameter, with which separation columns can be constructed results in the necessity of multiple trains of *Absorbers* and/or *Strippers*.
 - Chapel *et al.*, in a review of Fluor Daniel’s Econamine FG (flue gas)TM process [15], state that CO₂ capture is limited by absorber size (taken to be a maximum of 12.8 metres for circular cross-section).
 - In an overview of CO₂ capture in Japan [65], Yokoyama mentions that the size of the *Absorber* dictates the required number of trains in the CO₂ capture plant. This is not necessarily a bad thing as multiple trains provide flexibility in the case of varying plant load.

²Curiously, in the process flow sheet shown and referenced by Chakma *et al.*, the aforementioned FLASH unit is not visible. Also, there would be two streams leaving this FLASH unit: one liquid and one vapour. The liquid stream presumably flows to the amine-amine heat exchanger but the vapour stream destination is not obvious and is not stated in the article.

- Freguia and Rochelle examine the relationship between *Absorber* and *Stripper* packing height and the reboiler heat duty [26, 27].³
- One of the three thrusts taken by MHI (Mitsubishi Heavy Industries Ltd.) and KEPCO (Kansai Electric Power Company Inc.) in improving their CO₂ recovery system is the development of packing materials with reduced pressure drop. This has led to the development of KP-1, a structured packing, which reduces the size of CO₂ absorbers and the horsepower requirements of flue gas blowers [46, 43, 42].
- Aroonwilas *et al.* examine the difference between selected random and structured packings on CO₂ absorption [7].

A flexible MEA absorption process model allows the performance of the different scenarios to be assessed.

4.2.3 Solvent selection

There are a variety of amine-based solvents that are used, or potentially could be used, to capture CO₂.

- Fluor Daniel's Econamine FG process uses an inhibited 30 wt% MEA solution. The inhibitor scavenges oxygen which has two benefits: allowing the use of carbon steel in construction and preventing oxygen from degrading MEA. The cost of inhibitor is 20% that of the make-up MEA [15].
- UOP licenses the Amine Guard FS™ process for acid gas removal. It makes use of Union Carbide's UCARSOL family of formulated amines. Corrosion inhibitors and quantitative removal of O₂ and NO_x allow amine concentrations in the range of 25–30 wt% to be used [15].
- Kerr-McGee/ABB Lummus Global licenses technology for CO₂ capture that uses an uninhibited MEA solution of either 15 or 20 wt% [15, 13].
- MHI and KEPCO have jointly developed a sterically-hindered amine, dubbed KS-1, which has several stated advantages over MEA: lower regeneration temperature, lower regeneration energy, non-corrosive to carbon steel in the presence of oxygen up to 130°C, and less prone to degradation [15, 46, 43, 34].

³The *Absorber* and *Stripper* diameters are kept constant.

As a follow-up, MHI and KEPCO efforts have yielded a second-generation solvent, dubbed KS-2, whose performance is marginally better than that of KS-1 [44].

As part of their research, some 80 different solvents were evaluated.

- Aroonwilas *et al.* compared the absorption performance of MEA, NaOH, and AMP [7].
- Chakma *et al.* evaluated the CO₂ absorption performance of aqueous solutions of MEA, DEA, DIPA, DGA, MDEA, and TEA [14].
- Marion *et al.* presented an ABB-designed MEA absorption process where an optimized mixture of MEA and MDEA is used to capture CO₂ [38].⁴
- Tontiwachwuthikul *et al.*, in a study of the economic feasibility of CO₂ capture for use in enhanced oil recovery, assessed the performance of both MEA and AMP [60].
- Paul Feron, on behalf of TNO, discusses the development of CORAL (CO₂-removal absorption liquid) which has the following stated advantages over MEA: stable operation with polyolefin membranes, better oxygen stability, less corrosive, and has no loss of active component (*i.e.*, does not degrade under operating conditions) [24].

The design of the MEA absorption model should not preclude the evaluation of different solvents for use in capturing CO₂.⁵

4.2.4 Optimizing process operating conditions

With large heat and work duties at stake, sub-optimal operation of the process is strongly undesirable.

- Freguia and Rochelle examine the relationship between *Absorber* (L/G) and reboiler heat duty [26, 27]. This is analogous to examining the relationship between lean solvent loading and reboiler heat duty.

They also examine the relationship between *Stripper* pressure and reboiler heat duty.

⁴The MEA/MDEA mixture could not be made O₂ tolerant. Therefore, oxygen is catalytically removed from the flue gas upstream of the *Absorber*.

⁵Note: There are two important solvent-related phenomena of particular interest to MEA absorption that a steady-state model cannot directly include: corrosion and solvent degradation.

- Aroonwilas *et al.* examined the effect of flue gas flow rate, flue gas CO₂ concentration, solvent flow rate, solvent concentration, and *Absorber* temperature on CO₂ absorption [7].

Effects of the recycle stream CO₂ loading, *Absorber* flue gas and *lean* solvent inlet temperature, *Absorber* vapour outlet pressure, *Stripper* reboiler pressure, amount of heat exchange between *rich* and *lean* solvent streams, *Stripper* condenser temperature, and CO₂ compressor inter-cooling temperature on work and energy duties can be assessed.

4.2.5 Process integration exploration

The principle contribution of this thesis is to begin to discern if the cost of CO₂ capture can be reduced by integrating the MEA absorption process with the adjacent steam cycle (*i.e.*, using power plant to provide MEA absorption process steam, power, and electricity). A prerequisite is a process simulation model which includes all of the stream conditions and the process heat and work duties.

4.3 Points of emphasis

- The recycle loop in the simulation flowsheet needs to be closed.
- The model should calculate the pressure profile of the *Absorber* and *Stripper*. Additionally, the model should assess the hydrodynamic performance of the columns. For whatever reason(s), column pressure profile and hydrodynamic performance has been overlooked in previous MEA absorption process simulation work. This neglect is manifest in three ways:
 - ① The *Absorber* and *Stripper* are specified with constant pressures throughout the columns.
 - ② The pressure drop across a column is obviously dependent upon process operating conditions, column type, and column configuration. However, the *Absorber* and *Stripper* pressures are never accordingly modified when of these aspects is changed.
 - ③ The reader is never informed that the column design is explicitly checked for stable and/or feasible operation (e.g. in the case of trayed columns: downcomer flooding, downcomer seal, weeping, *etc.*).

Table 4.1 lists references to MEA absorption simulation studies and indicates which of the above items apply.

Table 4.1: Hydrodynamic performance neglect matrix⁶

	①	②	③
Chakma <i>et al.</i> [14]	✓	✓	✓
Desideri and Paolucci [20]	✓	✓	✓
Freguia <i>et al.</i> [25]	×	✓	✓
Freguia <i>et al.</i> [26, 27]	N/A	✓	✓
Singh [55]	✓	✓	✓
Singh <i>et al.</i> [54]	✓	×	✓

This model needs to consider the hydrodynamic performance of the *Absorber* and *Stripper*. This feature enhances the model by allowing:

- assessment of sensitivity of work required by the *Blower*, *H₂O Pump*, *Rich Pump*, and *CO₂ Compressor* to process design and operation.
- more accurate representation of the *Absorber* and *Stripper* pressure profiles.
- provision of additional information regarding the feasibility of particular designs and process conditions.

4.4 Implementation

There is nothing ingenious in the synthesis of the simulation flowsheet. To the nominal MEA absorption process flowsheet from Figure 4.1 is prepended unit operations to precondition the flue gas prior to entering the *Absorber* and appended still more unit operations for the preparation of CO₂ for transport via pipeline. The final result is shown in Figure 4.5.

The development of the Aspen Plus[®] input file is discussed below.

4.4.1 Specifying properties

This section of the Aspen Plus[®] input file specifies the solution chemistry and the property method or model that is to be used to calculate fluid transport and thermodynamic properties.

⁶The checkmarks in the above table indicate that the particular group of authors is ‘guilty’ of the neglect referenced by the column heading.

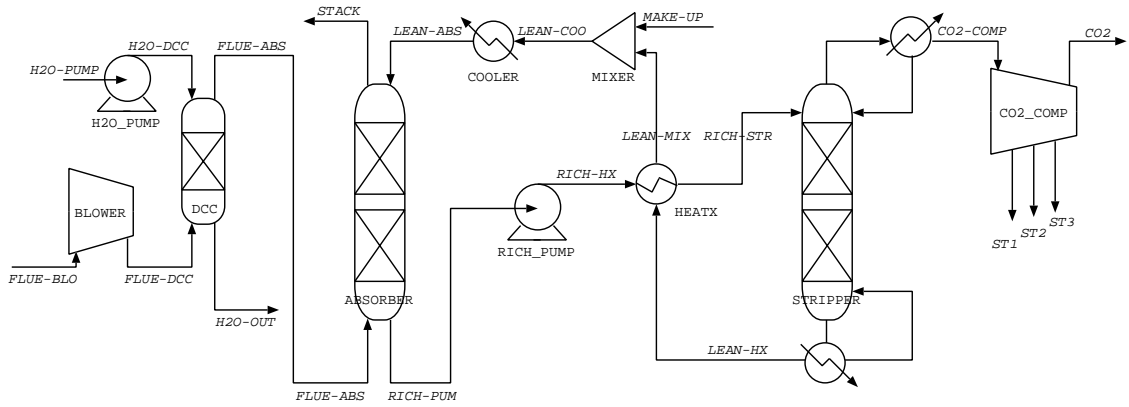
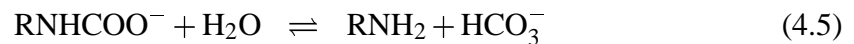
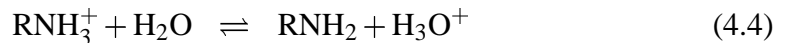
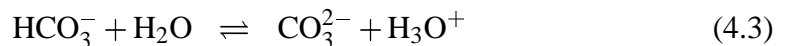
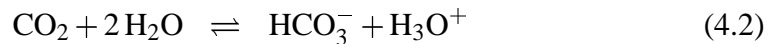
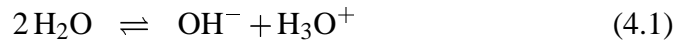


Figure 4.5: MEA absorption simulation flowsheet

The solution chemistry can be represented by equilibrium reactions 4.1 through 4.5. There is one class of property methods, one property model, and several property inserts that are indicated for use in modelling processes containing CO₂, MEA, and H₂O: the electrolyte NRTL methods, the **AMINES** property model, and the **emea**, **kemea**, **mea**, and **kmea** property inserts.⁷ These are listed and described in Table 4.2.⁸



⁷The Pitzer-based property methods **PITZER**, **PITZ-HG**, and **B-PITZER** are also indicated for use for aqueous electrolyte solutions. Unfortunately, the Aspen Physical Property System does not contain interaction parameters involving MEA, CO₂, or their derivatives.

⁸A complete description of these entities can be found in the software documentation [8].

Table 4.2: Property methods and model available for CO₂-MEA-H₂O system

Name	Description
ELECNRTL ENRTL-HG ENRTL-HF	<ul style="list-style-type: none"> • NRTL-RK method extended to accommodate interactions with ions in solution. Aspen Physical Property System contains binary and pair interaction parameters and chemical equilibrium constants for systems containing CO₂, H₂S, MEA, and H₂O with temperatures up to 120°C and amine concentrations up to 50 wt%.⁹ • ENRTL-HF uses the “HF” EOS (equation of state) to calculate vapour phase fugacity whereas ELECNRTL uses Redlich-Kwong. “HF” EOS is able to account for the association (principally hexamerization) that occurs between HF molecules at low pressure in the vapour phase. • The “HG” variant differs from ELECNRTL in that it uses the Helgeson model to very accurately and flexibly calculate standard enthalpy, entropy, Gibbs free energy, and volume for components in aqueous solutions. This adjustment improves the accuracy at high temperatures and pressures.
AMINES	<ul style="list-style-type: none"> • This property model is valid for systems with temperatures of 32–138°C, a maximum CO₂ loading of 0.5, and between 15–30 wt% MEA in solution. It uses the Kent-Eisenberg method for calculating K-values and enthalpy unless the amine concentration is outside of the recommended range in which case Chao-Seader correlation is used for K-value.¹⁰

⁹Parameter values are taken from D.M. Austgen, G.T. Rochelle, X. Peng, and C.C. Chen, “A Model of Vapor-Liquid Equilibria in the Aqueous Acid Gas-Alkanolamine System Using the Electrolyte-NRTL Equation,” Paper presented at the New Orleans AIChE Meeting, March 1988.

¹⁰Kent-Eisenberg and Chao-Seader correlations are only used to calculate fugacity of CO₂ and H₂S.

Property methods and model available for CO₂-MEA-H₂O system cont. . .

Name	Description
emea	<ul style="list-style-type: none"> • emea uses the ELECNRTL property method and is indicated for systems containing CO₂, H₂S, MEA, and H₂O with temperatures up to 120°C and amine concentrations up to 50 wt%. • kemea is identical to emea except that reaction 4.4 is replaced with a pair of kinetic reactions: $\begin{aligned} \text{CO}_2 + \text{OH}^- &\xrightarrow{k_1} \text{HCO}_3^- \\ \text{HCO}_3^- &\xrightarrow{k_{-1}} \text{CO}_2 + \text{OH}^- \end{aligned}$ <p>This substitution reportedly allows the system to be modelled more accurately when using RadFrac[®] or RateFrac[™] unit operation models.</p>
kemea	
mea	
kmea	
	<ul style="list-style-type: none"> • mea and kmea are analogous to emea and kemea except that they use the older SYSOP15M property method.

4.4.2 Specifying streams

As a minimum, the conditions and flow rates of all input streams must be specified. There are three such streams in Figure 4.5: **FLUE-GAS**, **H2O-PUMP**, and **MAKE-UP**.

- **FLUE-GAS** flow rate and composition is derived from the flue gas synthesis results shown previously in Tables 2.4 and 2.5 with one modification: the components O₂, Ar, NO, CO, SO₂, and H₂ are not included in the MEA absorption problem definition. As it turns out, the time required for convergence of the **RateFrac**[™] UOM is strongly dependent upon the number of components present in the feed and the *Stripper* rarely converges with all nine components included. The implication of the decision not to include these components, most notably O₂, NO, and SO₂, on the accuracy of the simulation results is discussed at the end of this chapter.
- **H2O-PUMP** consists solely of water and its flow rate is adjusted such that the flue gas is cooled to the desired *Absorber* inlet temperature. It is assumed that the water is available at atmospheric pressure and a temperature of 12°C.¹¹

¹¹The value of 12°C is taken from [32] and represents the average summer inlet temperature for a sea-

- **MAKE-UP** adds MEA and H₂O to the process to exactly offset the small amounts that are lost from the top of the *Absorber* and as part of the *Stripper* distillate. The molar flow rates of MEA and H₂O in this stream are calculated immediately prior to *Mixer* execution therefore any initial values suffice. It is assumed that this make-up solvent is available at atmospheric pressure and 25°C.

Additionally, to ease (*i.e.*, make possible?) flowsheet convergence, an initial specification is given to each of the two tear streams: **LEAN-ABS** and **LEAN-HX**.¹²

4.4.3 Specifying blocks

Table 4.3 lists the principal blocks in the MEA absorption process flowsheet and the Aspen Plus[®] UOM with which it is modelled. The specification of each block follows.

Table 4.3: UOM's in MEA absorption process model

Block	UOM
<i>Absorber</i>	RateFrac[™]
<i>Stripper</i>	RateFrac[™]
<i>Blower</i>	COMPR
<i>Compressor</i>	MCOMPR
<i>H₂O Pump</i>	PUMP
<i>Rich Pump</i>	PUMP
<i>Direct Contact Cooler</i>	RadFrac[®]
<i>Cooler</i>	HEATER

Absorber and Stripper

Selection of UOM Within Aspen Plus[®] there are two “general-purpose” UOM's indicated for simulating vapour-liquid absorption and stripping columns: **RateFrac[™]** and **RadFrac[®]**. **RateFrac[™]** takes as input the column type and some geometry information from which it computes the coefficients, flow velocities, and hold-up times needed to

water based cooling source in the Netherlands. Nanticoke obtains cooling water from Lake Erie and, maybe, similar average summer temperatures prevail.

¹²It should also be noted that, in this particular implementation, the flow rate of **LEAN-ABS** is the manipulated variable when a specific *lean* solvent CO₂ loading is desired.

calculate mass transfer. **RadFrac**[®] treats separation as an equilibrium problem. Where this assumption is invalid, the departure from equilibrium can be described by assigning a tray or Murphree efficiency to each stage.

Both **RadFrac**[®] and **RateFrac**[™] have been used in Aspen Plus[®] models of MEA absorption processes [55, 25, 26, 27, 20] but only **RateFrac**[™] is suitable for the development of this MEA absorption model. **RadFrac**[®] is fine in circumstances where tray and/or Murphree efficiencies are stable (*e.g.*, column *rating* mode under constant operating conditions). However, for the MEA absorption process model to be predictive under a wide variety of conditions, the more rigorous **RateFrac**[™] UOM is indicated.

The decision to use **RateFrac**[™] versus **RadFrac**[®] creates additional challenges:

1. **RateFrac**[™] UOM is more computationally complex which means that simulations will solve more slowly and with more difficulty (*i.e.*, increased probability of non-convergence). This disadvantage is mitigated by intelligent problem initialization.
2. As mentioned previously, one of the points of emphasis of the MEA absorption model is to precisely determine the pressure profile of the *Absorber* and *Stripper*. In achieving this end, there is an important difference to be considered in the manner with which **RadFrac**[®] and **RateFrac**[™] treat column pressure.

In **RadFrac**[®] the stage pressures can be included in the problem formulation as *variables*. Thus, in a **RadFrac**[®] solution, the pressures used to evaluate the column performance are also outputs of the simulation. This is not the case for **RateFrac**[™] where segment pressures are *constants*. After the column performance is calculated using the pressure specification given by the user, Aspen Plus[®] uses the results to estimate a pressure drop for each segment. There is thus a disconnect between the reported column pressure profile and the rest of the column results.

It is possible to obtain estimates of actual column pressure profiles using **RateFrac**[™] but at the cost of additional computation. Several iterations are required where the estimated pressure drops of one run are used to construct the input pressure profile of the subsequent run until convergence is achieved.

Specifying RateFrac[™] In specifying the *Absorber* and *Stripper*, the model developer needs to make decisions regarding four different aspects of the units: column configuration, column type, internal geometry, and column pressure.

Column configuration In the case of the *Absorber*, the inlets and outlets are connected to the top and bottom of the column.

The *Stripper* will have both a partial condenser and a conventional reboiler. The feed enters the column above the mass-transfer region. The molar reflux ratio is varied to achieve a specified condenser temperature (typically 40°C); the bottoms-to-feed ratio is adjusted such that the desired molar flow of CO₂ in the distillate is obtained (nominally 85% of the CO₂ in the flue gas).

Column type Both columns are modelled with sieve trays.

There are other column types to choose from within Aspen Plus[®]. **RateFrac[™]** has built-in routines for bubble-cap and valve trays and for a plethora of random and structured packings.¹³ Sieve trays are selected because they are commonly used and correlations exist for characterizing their hydrodynamic performance. They thus provide a good basis from which to compare more sophisticated column types.

Internal configuration The diameter of the column is an output of the model and is therefore not specified. A diameter estimate (20 m), though, is required as is the number of trays. In addition, the approach to entrainment flooding, tray spacing, and weir height need to be given (or the default values of 80%, 24 in, and 2 in, respectively, used) in order to completely specify the tray geometry. The elucidation for the number of trays, tray spacing, and weir height used in the model is provided in Section 4.5.2.

Column pressure Chakma *et al.* [14] originally hypothesized that increasing CO₂ pressure in the *Absorber* would be a good thing because it increases reactivity of MEA with CO₂. However, they discovered that any benefits accrued due to increased reactivity are more than offset by the increased cost of pressurizing the flue gas. Therefore, the pressure at the top of the *Absorber* is fixed at 101.3 kPa.

In the case of the *Stripper*, increasing the pressure, which raises the column temperature, has been shown to promote less energy-intensive solvent regeneration. However, above temperatures of 122°C, thermal degradation of 30 wt% MEA becomes intolerable. Therefore, in the process model, the pressure of the *Stripper* reboiler is set such that the reboiler temperature approaches, but does not exceed, 122°C.

The actual pressure profile is determined using the iterative procedure mentioned above. At the beginning of each iteration, the input pressure profile of each **RateFrac[™]**

¹³A table listing the complete selection is given in the user documentation [12, p 17-34–17-35].

block is constructed using the segmental pressure drops reported for that particular block from the previous run. The criteria for convergence is a difference between $(\Delta P)_{col}$ of consecutive runs of less than 1 kPa or 3% of the total pressure drop:

$$(\Delta P)_{col}^i - (\Delta P)_{col}^{i-1} < \begin{cases} 1 \text{ kPa} \\ 0.03 (\Delta P)_{col}^{i-1} \end{cases}$$

Calculations for tray-by-tray pressure drop and % downcomer flooding are taken from literature [29, p 14-24–14-34] and are implemented as a Fortran subroutine that is called during **RateFrac**TM execution. **RateFrac**TM contains a built-in routine for these same calculations but initial testing gave calculated pressure drops that were an order of magnitude greater than what was expected. Because the **RateFrac**TM UOM is developed by a third-party, it was not possible to obtain documentation describing the routines and, thus, it was felt best to replace them with a well-known formulation. For reference, the exact calculations used are shown in Appendix B.

Table 4.4 summarizes the parameters and stream properties that are required to size the column and evaluate its hydrodynamics.

Table 4.4: Design parameters for sizing and hydrodynamic evaluation of tray columns

symbol	units	typical value	nominal value
EFA	%	60–85	75
TS	mm	300–600	609.6
ϵ	mm	0.046	0.046
d_h	mm	6.5–13	13
h_c	mm	25.4	25.4
h_w	mm	50	50.8
t_i	mm	2.0–3.6	3.6
A_h/A_a		0.05–0.15	0.15
f		0.75	0.75

Blower

The *Blower* is required to overcome the pressure drop in the cooler and the absorption column and is implemented in Aspen Plus[®] using the **COMPR** UOM. **COMPR** is used to change stream pressure when power requirement is needed and represents a single compressor stage. It requires that the stream pressure rise and the performance characteristics be specified.

The pressure rise is initially set consistent with the initial pressure conditions in the *Absorber*. Then, at the beginning of each iteration, the pressure rise in this block is changed such that

$$(\Delta P)_{Blower}^n = (\Delta P)_{Absorber}^n$$

The performance characteristics for a blower of the size needed to accommodate some $4 \times 10^6 m^3/hr$ of flue gas are not readily available. Below are listed the design choices made by other researchers.

CO₂ Compressor

The *CO₂ Compressor* is required to compress the CO₂ for transportation via pipeline and is implemented in Aspen Plus[®] using the **MCOMPR** UOM. Conceptually, **MCOMPR** is a series of **COMPR** blocks interspersed with heat exchangers and is therefore suitable for modelling a multi-stage compressor with inter-cooling. This block requires that the outlet pressure, compression performance, and interstage temperatures be specified.

The outlet pressure depends upon the pipelining requirements; the choice of conditions by previous researchers is varied and is shown in Table 4.5. Ultimately, the outlet pressure is determined by the pipeline length and design, the location and design of “booster” compressors, and ultimate end-use of the CO₂.

In this study, the CO₂ is compressed to 110 bar at a temperature of 25°C.

Table 4.5: Survey of CO₂ delivery pressures used in MEA absorption studies

Study	CO ₂ conditions
Iijima and Kamijo [33]	2000 psig (136 bar)
Marion <i>et al.</i> [38]	2000 psig (136 bar), 82°F (28°C)
Desideri and Paolucci [20]	140 bar, ambient temperature
David Singh [55]	150 bar, 40°C
Simmonds <i>et al.</i> [53]	220 bar
Slater <i>et al.</i> [56]	220 bar

H₂O Pump and Rich Pump

The *H₂O Pump* and *Rich Pump* are both modelled with the **PUMP** UOM. In this work, **PUMP** only requires that the outlet pressure be specified; by default, **PUMP** calculates

the power requirement using efficiency curves for water in a centrifugal pump [12] which provides sufficient accuracy for this work.

The outlet pressure of *H₂O Pump* and *Rich Pump* are determined by the upstream units. For *H₂O Pump*, the pressure rise is effectively that required to overcome the pressure drop of the *Direct Contact Cooler* and the *Absorber*. For *Rich Pump*, the *rich* solvent pressure is increased, if required, to equal the *Stripper* pressure at the feed segment. In both cases, values are updated along with the *Absorber* and *Stripper* pressure profiles at the beginning of each iteration.

Direct Contact Cooler

The *Direct Contact Cooler* is modelled in the same manner as Desideri and Paolucci [20]: it is a two-stage, Rashig-ring packed column with a pressure loss of 0.1 bar.

Cooler

The *Cooler* cools the *lean* solvent to the desired *Absorber* inlet temperature (typically 40°C). It is modelled with the **HEATER** UOM.

The outlet temperature of *Direct Contact Cooler* and *Cooler* is set at 40°C as this allegedly maximizes CO₂ absorption. Aroonwilas *et al.* found that, from 20°C to 37°C, increasing temperature increased CO₂ take-up due to an increase in the rate of the reaction between CO₂ and MEA and, from 40°C to 65°C, increasing temperature decreased CO₂ absorption because of Henry's constant increasing with temperature.

4.5 Model Parameter elucidation

4.5.1 Property method selection

At the 2nd workshop of the International Test Network for CO₂ capture,¹⁴ it was proposed that the Aspen Plus[®] “out of the box” could not accurately model the MEA absorption process. The assertion was made that Aspen Plus[®] does not ship with a physical property method or model capable of predicting VLE (vapour-liquid equilibrium) of the CO₂-MEA-H₂O system.

¹⁴This “network” is a collaborative effort amongst researchers from industry, academia, and government to develop technologies for capturing CO₂ from power plant flue gases. Its inaugural meeting was held in Gaithersburg, USA in October 2000 and meetings have been held biannually since.

The experimental work of Jou *et al.* [36] has produced what is held to be the most accurate set of data of CO₂ solubility in 30 wt% MEA solution. Jou *et al.* measured the solubility of CO₂ in a 30 wt% solution of aqueous MEA at partial pressures of CO₂ ranging from 0.001–20000 kPa and temperatures between 0–150°C. Their results are shown in Figure 4.6. CO₂ solubility in aqueous MEA is a strong function of temperature and a moderate function of pressure.

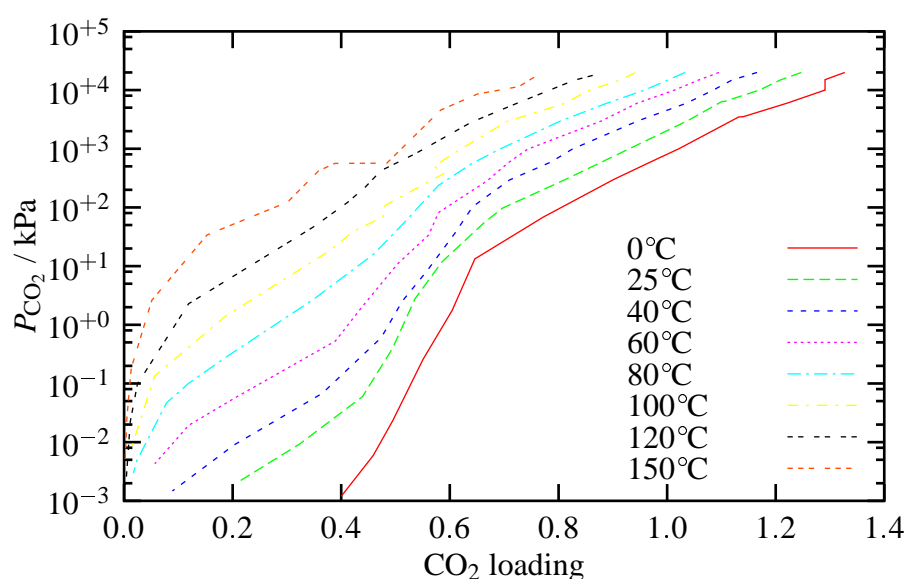


Figure 4.6: Solubility of CO₂ in 30 wt% MEA solution (Jou *et al.* [36])

Using Aspen Plus[®], CO₂ solubility in 30 wt% MEA solution is estimated using representative property methods and models from the different classes shown in Table 4.2. This data is compared to the results of Jou *et al.* in two ways.

1. Figure 4.7 and Figure 4.8 contain plots of P_{CO_2} versus α at 40°C and 120°C, respectively, for the entire range of P_{CO_2} considered by Jou *et al.*¹⁵
2. In Figure 4.9 and Figure 4.10, CO₂ solubility is revisited but, in these cases, only data points for which $P_{\text{CO}_2} < 2$ bar are included in the graphs as the ability of Aspen Plus[®] to accurately predict high-pressure VLE of the CO₂-MEA-H₂O system

¹⁵The temperatures of 40°C and 120°C are the low and high temperatures expected in the MEA absorption process. The reader is referred to Appendix D for comparisons between experimental and simulation data at other temperatures.

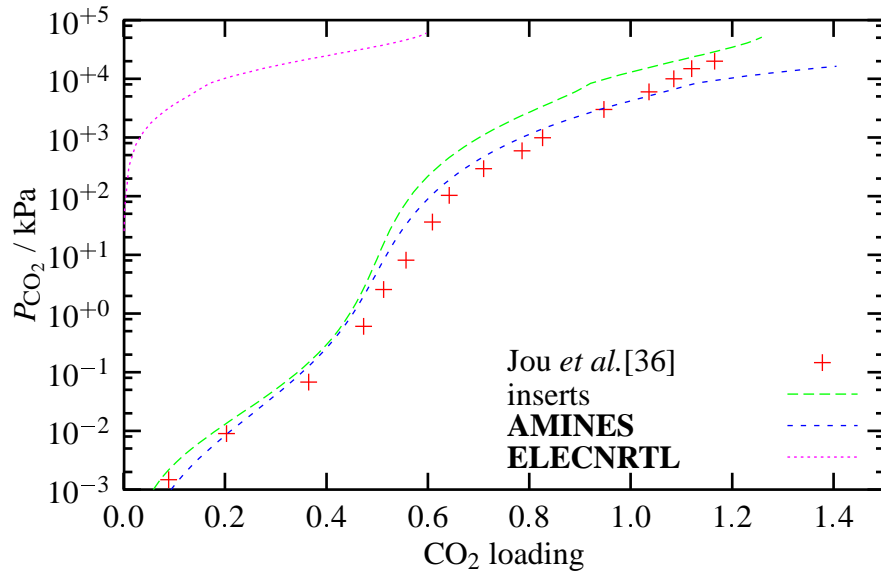


Figure 4.7: Comparison of calculated VLE with experimental values at 40°C

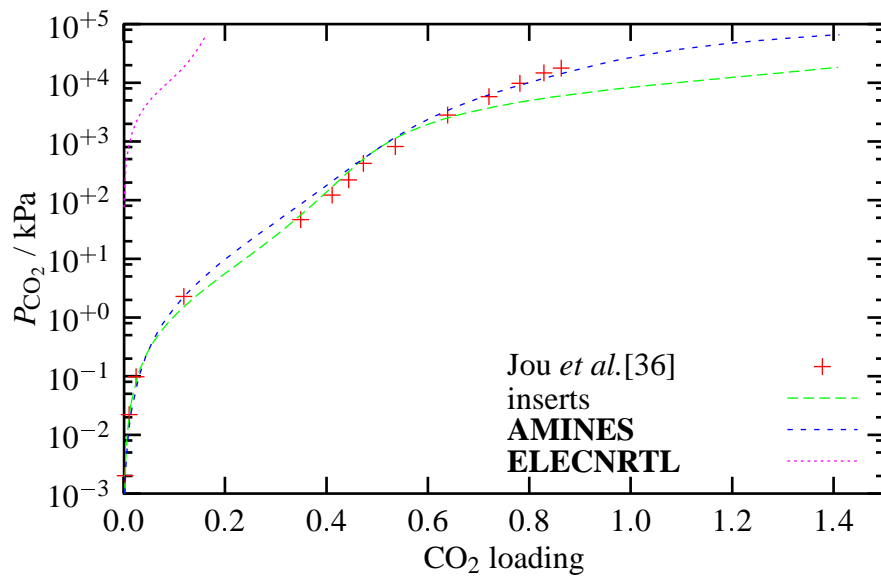


Figure 4.8: Comparison of calculated VLE with experimental values at 120°C

is not of immediate interest.¹⁶ The graphs show the percent difference between predicted CO₂ partial pressures and experimental values plotted versus α at 40°C and 120°C.

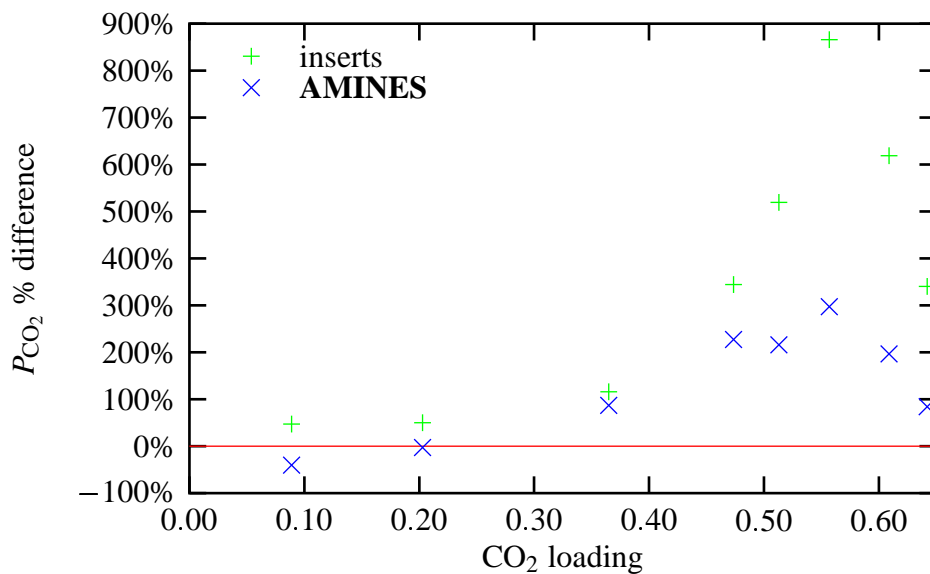


Figure 4.9: Residual analysis of VLE data — ΔP_{CO_2} vs α_{lean} at 40°C

In Figures 4.7 and 4.8, Aspen Plus[®], with the correct property method selected, appears reasonably capable of modelling the solubility of CO₂ in 30 wt% MEA. The following observations regarding the property methods and models are worth noting:

- When developing the Aspen Plus[®] simulation with the user interface, it is recommended that the *Electrolyte Wizard* be used. This feature assists the development of the model by specifying an appropriate property method (*i.e.*, **ELECNRTL**), adding any missing ionic components, defining the solution chemistry, retrieving binary interaction parameters, and inputting parameters for equilibrium constants. This last point is critical as equilibrium constants, unlike interaction parameters, will not be retrieved at run-time. The abysmal **ELECNRTL** curves in Figures 4.7 and 4.8 result from simulations for which the *Electrolyte Wizard* was not used.

¹⁶In the MEA absorption process, CO₂ partial pressure can be expected not to exceed 2 bar; to do so would require *Stripper* pressures in excess of this which, in turn, would force reboiler temperatures to exceed 125°C — a temperature above which MEA thermal degradation is a show-stopper.

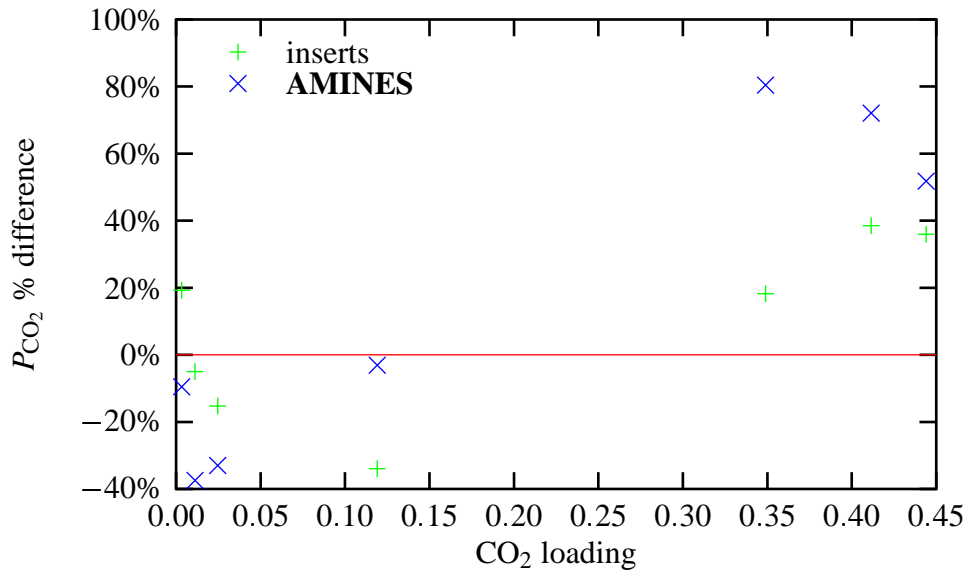


Figure 4.10: Residual analysis of VLE data — ΔP_{CO_2} vs α_{lean} at 120°C

- The four “MEA” property inserts — **mea**, **kmea**, **emea**, **kemea** — all predicted identical VLE. This is also the same VLE generated using a simulation developed using the Aspen Plus® *Electrolyte Wizard*.

Figures 4.9 and 4.10 allow one to more clearly observe the deviation between the experimental and predicted values. The horizontal line is provided as a point of reference; a perfectly behaved model would have its points evenly scattered around this line and, in the extreme case, the data points would be coincident with it. At 40°C, Aspen Plus® severely misstates the vapour phase concentration of CO₂. The **AMINES** property model performs better than the property inserts, but as evidenced, **AMINES** can still overstate vapour phase CO₂ concentration by factors of 2–4×. At 120°C, the fit between the predicted and experimental results better than at 40°C but is still poor. At the higher temperature, the property inserts outperform the **AMINES** property model.

4.5.2 Absorber and Stripper internal configuration

A method of decomposing the MEA absorption process flowsheet was developed as part of this work and has already been reported elsewhere [1]. It is applied to the particular flowsheet shown in Figure 4.5 with the hope of obtaining:

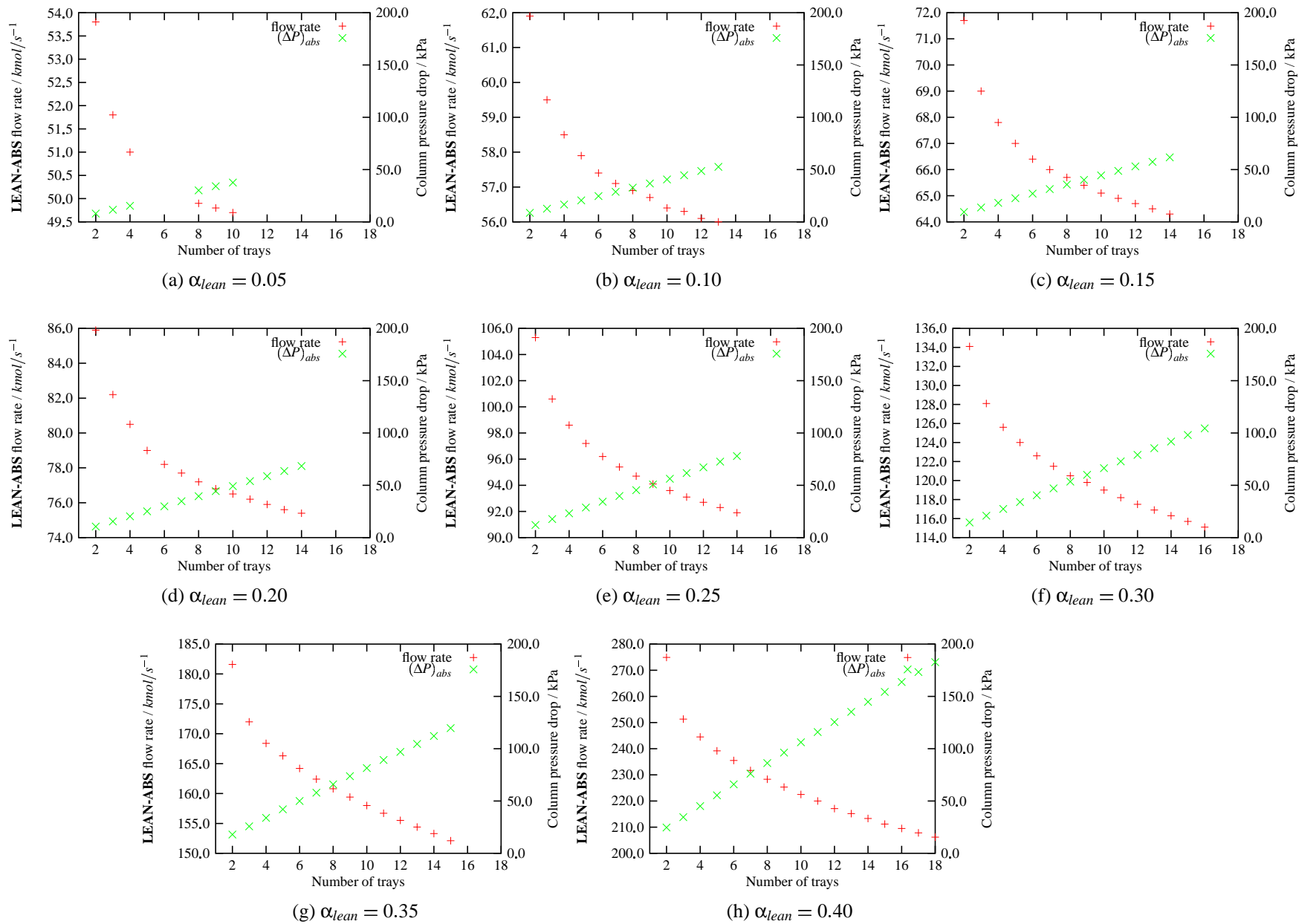
- a realistic indication of the internal configuration for the *Absorber* and *Stripper* and
- ‘good’ initialization values for tear streams, *Stripper* reflux ratio, *Stripper* bottoms-to-feed ratio, and *Absorber* and *Stripper* pressure profiles.

A synopsis of the decomposition concept is given below:

1. The total cost of CO₂ capture is more sensitive to the operating costs than the annualized capital costs.
2. In regards to the operating costs, it is the cost of fulfilling Q_{reb} that dominates.
3. For a particular recovery and α_{lean} , Q_{reb} will be minimized when the *Stripper* inlet flow rate is minimized. Well, the inlet flow rate is solely determined by the design of the *Absorber*.
4. As the number of trays in the *Absorber* is increased, the solvent flow rate needed for a particular recovery will decrease asymptotically to F_{lean}^{min} as $N_{Absorber}$ approaches infinity. It makes sense that at some $N_{Absorber} < \infty$, the reduction in solvent flow rate from adding an additional tray will be negligible and this $N_{Absorber}^*$ will be the design number of trays for the *Absorber*.
5. At this minimum inlet flow rate, the reboiler heat duty is controlled by the design of the *Stripper*.
6. As the number of trays in the *Stripper* is increased, the reboiler heat duty will decrease. At some $N_{Stripper} < \infty$, the reduction in reboiler heat duty from adding an additional tray will be negligible and this $N_{Stripper}^*$ will be the design number of trays for the *Stripper*.

***Absorber* study**

Number of trays With a ‘stand-alone’ *Absorber* model, F_{lean} required to achieve 85% recovery of CO₂ is determined for $0.05 \leq \alpha_{lean} \leq 0.40$. The number of trays in the *Absorber* is varied from one run to the next but the tray spacing and weir height values are not; they are kept constant at the **RateFrac**TM default values. The results of this set of simulations is shown in Figure 4.11. The most significant observations are:

Figure 4.11: Sensitivity of F_{lean} to Absorber height

- As is indicated by the increasing scale of the ordinate axes in sub-figures 4.11(a) through 4.11(h), higher CO₂ loadings require greater F_{lean} to achieve the same level of CO₂ recovery.
- F_{lean} decreases asymptotically as more trays are added to the *Absorber*.
- $(\Delta P)_{Absorber}$ is directly proportional to the number of trays in the *Absorber*.

The criteria for selection of $N_{Absorber}^*$ originally presented [1] was as follows:

$$N_{Absorber}^* = N_{Absorber} \left| \frac{F_{lean}^i - F_{lean}^{i+1}}{F_{lean}^i} < 0.005 \right.$$

Why limit the number of trays in the initial *Absorber* design? Well, even without doing the complete economic analysis, at some point the marginal capital cost of an additional tray in the *Absorber* will trump the marginal benefit that a larger column has in reducing F_{lean} . So, adding trays to the *Absorber* until the reduction in *lean* solvent flow rate dropped below 5% seemed like a reasonable thing to do.

The practical limit to the number of trays is tightened with the added consideration of column pressure drop. The benefit of adding ‘just one more tray’ is further reduced in light of the fact that while there is a diminishing return from increasing tray number, the marginal cost associated with overcoming $(\Delta P)_{Absorber}$ appears to be constant. This new reality spurred the modification of the above selection criteria for $N_{Absorber}^*$:

$$N_{Absorber}^* = N_{Absorber} \left| (\Delta P)_{Absorber}^i < 101.3 \text{ kPa} \forall 0.05 \leq \alpha_{lean} \leq 0.40 \right.$$

As it turns out, $N_{Absorber}^* = 10$.¹⁷

Tray spacing and weir height With a ‘stand-alone’ *Absorber* model, F_{lean} required to achieve 85% recovery of CO₂ is determined for $0.05 \leq \alpha_{lean} \leq 0.40$. $N_{Absorber}^*$ trays is used in the *Absorber* and the tray spacing, weir height, and downcomer clearance are varied by adjusting, k , where

$$\begin{aligned} TS &= k \cdot 24 \text{ in} \\ h_w &= k \cdot 2 \text{ in} \\ h_c &= k \cdot 1 \text{ in} \end{aligned}$$

¹⁷For the case of $\alpha_{lean} = 0.05$, a value of $N_{Absorber} = 4$ is used because, at this CO₂ loading, it was impossible to routinely converge the *Absorber* with a greater number of trays.

The results of this set of simulations is shown in Figure 4.12. Of note is that:

- Using the default **RateFrac**TM values for tray spacing and weir height (represented in Figure 4.12 by points lying on the ordinate axes), the *Absorber* downcomer flooding consistently exceeds the typical design value of 50% *TS*.
- As α_{lean} increases, so does $k_{Absorber}^*$.
- Increasing the tray spacing such that $h_{dc} \leq 50\% TS$ causes an accompanying increase in $(\Delta P)_{Absorber}$.¹⁸

An explanation of this observation is as follows. Pressure drop across a tray can be decomposed into the resistance to flow through the holes in the tray, h_d , and the resistance to flow through the effective height of clear liquid on the tray, h_L . Increasing the tray spacing reduces the liquid holdup on the tray (reducing h_L) but turns out to decrease h_d . This latter effect arises from the fact that increasing the tray spacing increases the gas velocity at which entrainment flooding occurs, U_{NF} , and consequently, the gas phase design velocity through the column — the approach to entrainment flooding is a constant design parameter and $U_N = EFA/100\% \times U_{NF}$. And, of course, the faster the gas flows through the holes, the greater the resistance to flow. At higher values of k , h_d dominates over h_L .

Values of $k_{Absorber}^*$ for each α_{lean} examined are given in Table 4.6. Also shown is the state and composition of the *rich* stream leaving the *Absorber*. This information is an input into the *Stripper* study.

Table 4.6: Summary of results from *Absorber* study

α_{lean}	$N_{Absorber}^*$	$k_{Absorber}^*$	T_{rich} [°C]	P_{rich} [kPa]	F_{rich} [kmol/s]	x_{H_2O}	x_{MEA}	x_{CO_2}
0.05	4	5	49.8	118.7	50.4	0.809	0.128	0.063
0.10	10	6	45.4	164.0	54.5	0.807	0.128	0.065
0.15	10	6	46.8	163.3	63.4	0.810	0.126	0.064
0.20	10	7	48.7	170.1	74.8	0.813	0.124	0.063
0.25	10	8	50.9	177.1	92.0	0.816	0.123	0.062
0.30	10	9	52.7	182.0	117.5	0.818	0.121	0.061
0.35	10	11	52.8	190.8	156.2	0.820	0.120	0.060
0.40	10	13	50.8	190.7	224.9	0.821	0.119	0.060

¹⁸There is one exception to this statement. With $\alpha_{lean} = 0.40$ and $k^* = 13$, $(\Delta P)_{Absorber} = 98.5$ kPa which is less than the 106.1 kPa observed with the **RateFrac**TM default values.

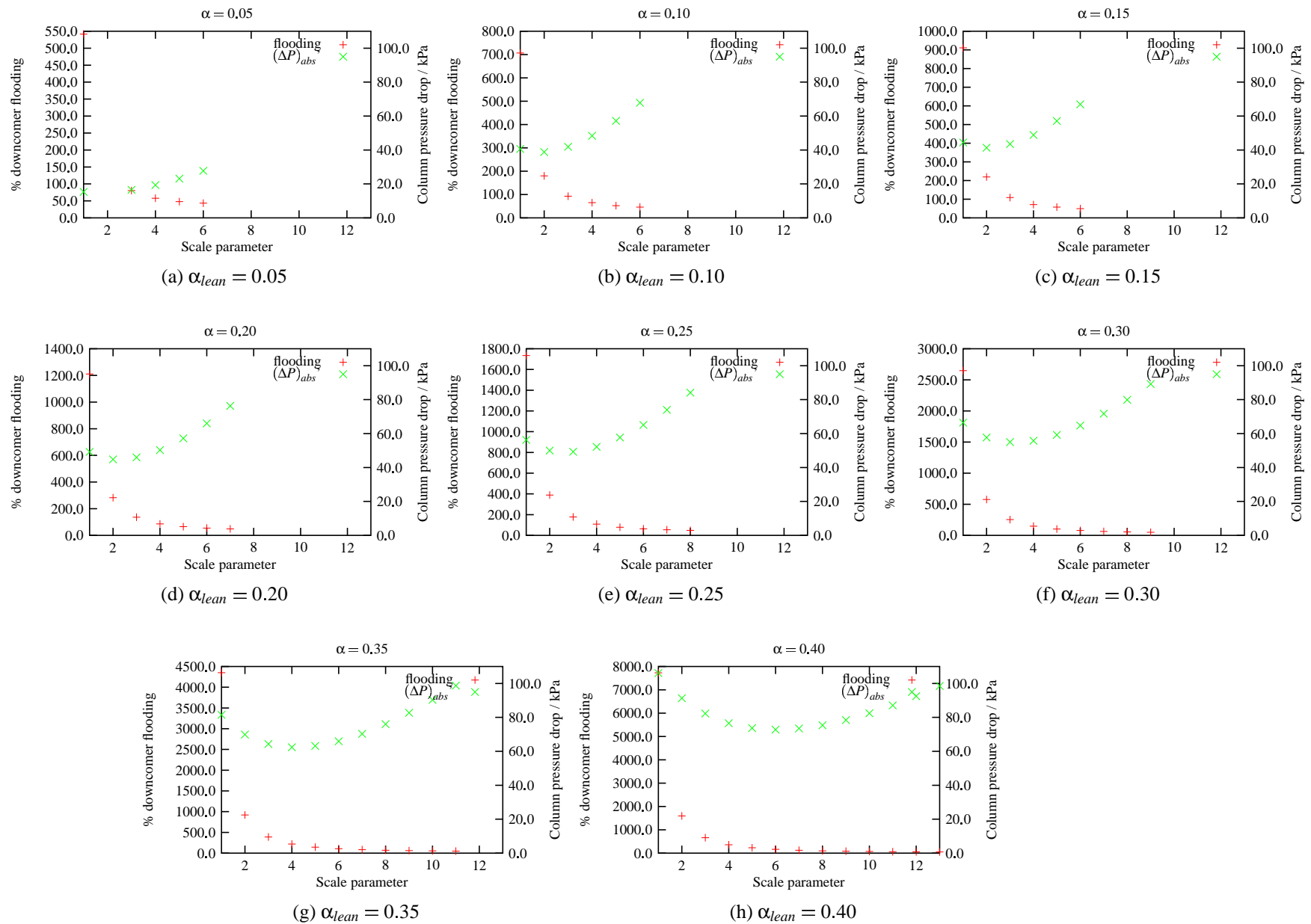


Figure 4.12: Sensitivity of *Absorber* downcomer flooding to *Absorber* tray spacing

Stripper study

Number of trays With a ‘stand-alone’ *Stripper* model, the molar reflux and molar bottoms-to-feed ratios required for the removal of 2.85 kmol/s of CO₂ (*i.e.*, 85% of the CO₂ fed into the bottom of the *Absorber*) are ascertained for $0.10 \leq \alpha_{lean} \leq 0.35$.¹⁹ **RICH-HX** is specified using the results from the *Absorber* study shown in Figure 4.6. The number of trays in the *Stripper* is varied from one run to the next but tray spacing and weir height are not; they are kept constant at the **RateFrac**TM default values. The results from this set of simulations is presented in Figure 4.13. Some points worth mentioning:

- For $\alpha_{lean} < 0.30$, increasing α_{lean} decreases Q_{reb} . Where $\alpha_{lean} \geq 0.30$, Q_{reb} is insensitive to changes in α_{lean} .
- For $\alpha_{lean} \leq 0.25$, Q_{reb} decreases asymptotically as more trays are added to the *Stripper*. Where $\alpha_{lean} \geq 0.25$, there is a point where Q_{reb} is minimized with respect to $N_{Stripper}$.

The ‘5% rule’ criteria used to select $N_{Stripper}^*$ presented in [1] is used here without modification:

$$N_{Stripper}^* = N_{Stripper} \left| \frac{Q_{reb}^N - Q_{reb}^{N+1}}{Q_{reb}^N} \right| < 0.05$$

The value of $N_{Stripper}^*$ for each α_{lean} examined is given in Table 4.7.

Tray spacing and weir height Once again, with a ‘stand-alone’ *Stripper* model, molar reflux and molar bottoms-to-feed ratios are again ascertained for $0.10 \leq \alpha_{lean} \leq 0.35$. However, in this case, for each α_{lean} examined, the number of trays is kept constant at $N_{Stripper}^*$ and it is k that is varied. The results for this set of simulation is given in Figure 4.14. In the main, the observations here are the same as those from the *Absorber* study:

- Using the default **RateFrac**TM values for tray spacing and weir height (represented in Figure 4.14), the *Stripper* downcomer flooding consistently exceeds the typical design value of 50% *TS*.

¹⁹The range of CO₂ loadings examined is narrowed because of the difficulty converging the *Stripper* at very high and very low loadings.

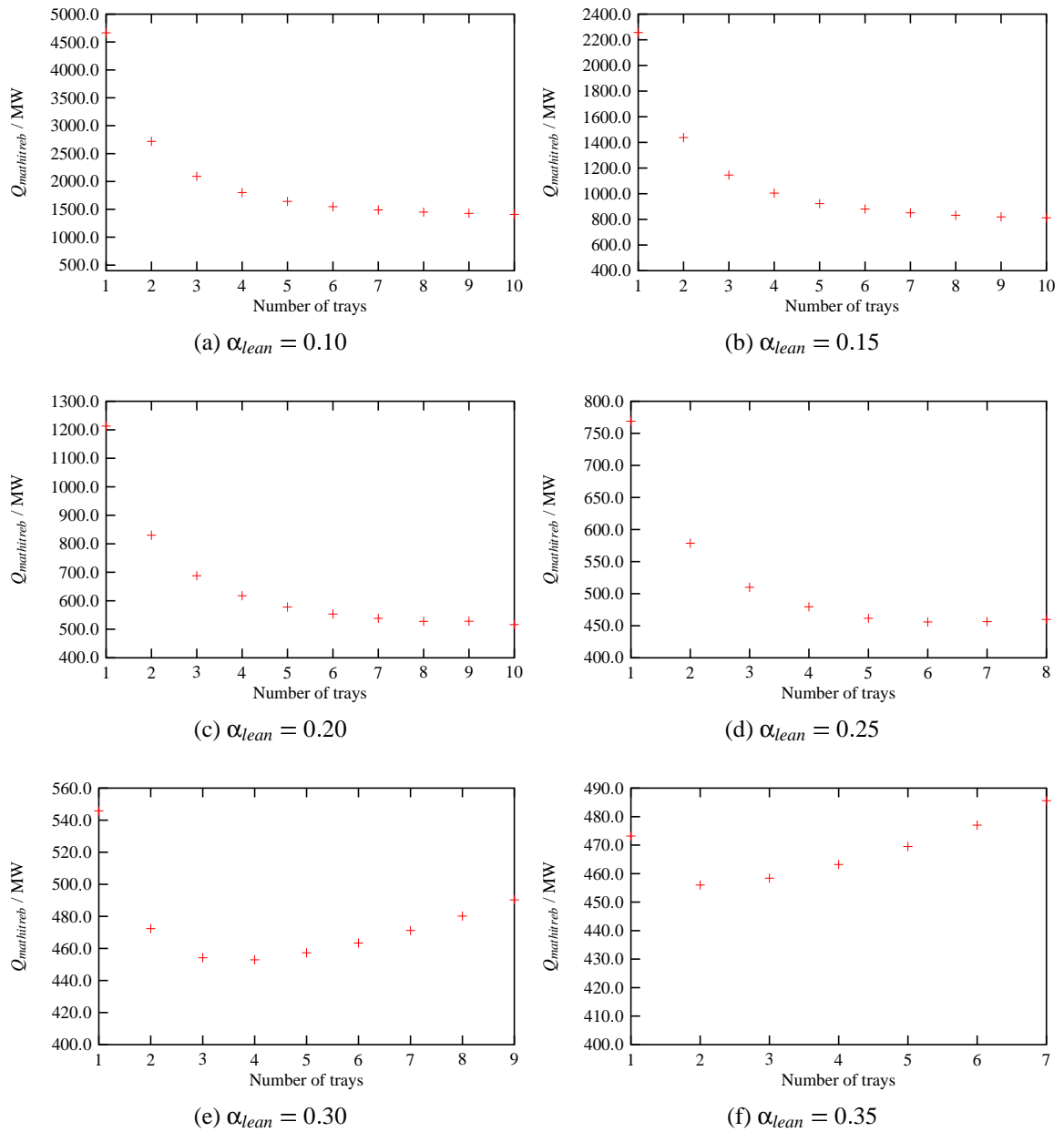


Figure 4.13: Sensitivity of Q_{reb} to *Stripper* height

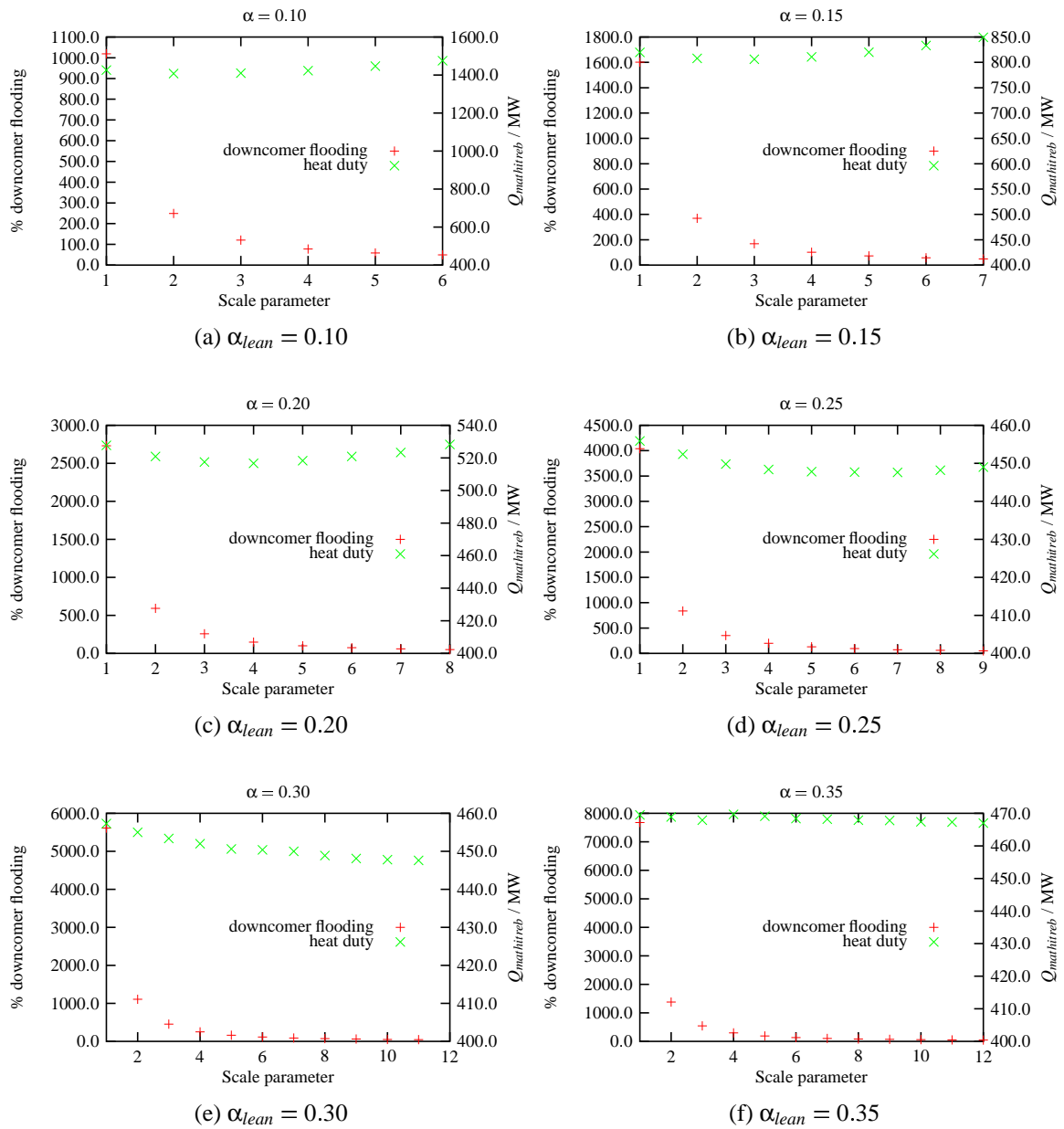


Figure 4.14: Sensitivity of *Stripper* downcomer flooding to *Stripper* tray spacing

- As α_{lean} increases, so does $k_{Stripper}^*$.
- Increasing the tray spacing such that $h_{dc} \leq 50\% TS$ has no significant impact upon Q_{reb} .

Values of $k_{Stripper}^*$ are given in Table 4.7.

Summary of *Absorber* and *Stripper* studies' results

The decomposition methodology has yielded a set of conditions which can be used to initialize the integrated process model. This data is given in Table 4.7.

Table 4.7: MEA absorption process model initialization parameters

α_{lean}	$N_{Absorber}^*$	$k_{Absorber}^*$	F_{lean} [kmol/s]	$N_{Stripper}^*$	$k_{Stripper}^*$	L/D	B/F
0.10	10	6	56.0	9	6	6.75	0.928
0.15	10	6	64.6	9	7	3.05	0.939
0.20	10	7	75.7	8	8	1.22	0.951
0.25	10	8	92.4	6	9	0.68	0.961
0.30	10	9	117.5	5	11	0.59	0.970
0.35	10	11	155.0	5	12	0.54	0.978

4.6 Conclusions and recommendations

1. Generally speaking, Aspen Plus[®], “out of the box”, is not able to predict CO₂ solubility in 30 wt% MEA. At the most favourable conditions — moderate pressure (*i.e.*, those of interest to MEA absorption processes) and higher temperatures (*i.e.*, *Stripper* conditions) — agreement between experimental and predicted values is only mediocre.
2. For simulation of MEA absorption processes, on the basis of predicting CO₂ solubility, either the **AMINES** property model or the property inserts should be used.
3. For modelling an MEA absorption process, especially when handling flue gas volumes typically emitted from power plants and recovering substantial fractions of the CO₂ contained therein, the **RateFrac**[™] default tray geometry is unsuitable.

4. After accumulating data like that shown in Table 4.7 and using it to initialize the MEA absorption model, solving said model is no longer difficult.
5. However, even with seemingly 'good' initialization values, convergence can still be difficult to achieve because of Aspen Plus[®]'s sensitivity to the initial conditions. For example, in initializing the *Stripper*, there were many occasions when, for example, initial (L/D) values of 0.4 and 0.5 are unsuccessful but (L/D) = 0.35 works. The reason for this behaviour is not well understood.

Chapter 5

Integration of Power Plant and MEA Absorption

5.1 Introduction

Objective

The objective of the work in this chapter is to intelligently integrate the combustion, steam cycle, and MEA absorption models such that heat and power from the power plant is used to satisfy the supplemental energy requirements of the CO₂ capture process.

Motivation

Unifying the combustion, steam cycle, and CO₂ capture models creates a platform from which the merits of steam extraction for process heating can be assessed. In addition, the model places the energy requirements of key unit operations — *Blower*, *Stripper* reboiler, and *CO₂ Compressor* — on the same basis which allows different designs to be more easily compared.

Merits of steam extraction for process heating

Figure 32 contains the enthalpy-entropy curve for a unit at operating at base-load.¹ \overrightarrow{AB} , \overrightarrow{CD} , and \overrightarrow{DE} represent expansion through the high-, medium-, and low-pressure sections

¹The arguments presented in this section are influenced heavily by those presented by Mimura *et al.* [43].

of the turbine, respectively.² \overleftarrow{ef} is the enthalpy change that occurs in the *Condenser*. Pre-CO₂ capture, this heat is completely lost to the surroundings. If CO₂ capture using MEA absorption is to be performed, significant amounts of heat will be required by the *Stripper* reboiler. Assuming $T_{reb} = 121^\circ\text{C}$, a 10°C hot-side temperature approach, and saturated inlet and outlet conditions, \overleftarrow{xy} represents the change in process steam enthalpy in the reboiler. Comparing \overleftarrow{ef} and \overleftarrow{xy} , it appears possible to substantially mitigate the impact of large Q_{reb} by diverting steam from the latter stages of the turbine. This, in effect, would translate much of the waste heat into useful energy. However, doing so would reduce the steam flow through the turbine thus *de-rating* the power plant. Obviously, the benefit of extracting steam from the steam cycle for use in the CO₂ capture plant depends upon the tradeoff between the recovery of waste heat and the accompanying reduction in electricity production.

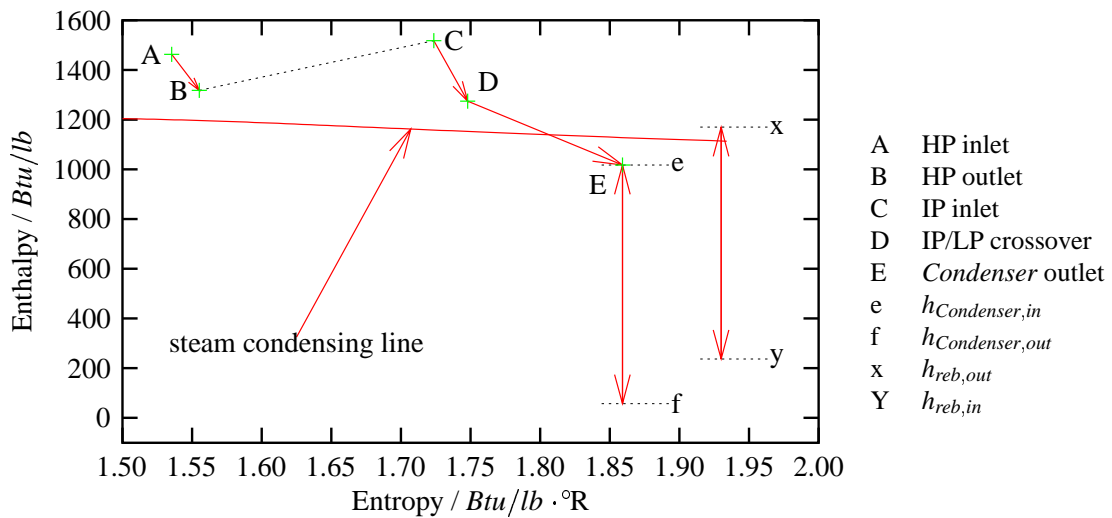


Figure 5.1: Enthalpy-entropy curve for power plant

Figure 5.2 better illustrates the inherent tradeoff mentioned above. Depicted is the utilization of steam internal energy through the steam cycle; Figure 5.2(a) reflects nominal steam cycle operation whereas Figure 5.2(b) represents a case where 50% of the LP section of the turbine is extracted.³

The upper three blocks in Figure 5.2(a) show the energy transfer as the steam expands in the turbine and the area of the lowest region is the energy released in the *Condenser*.

²The actual transitions would not necessarily appear as straight lines on the enthalpy-entropy diagram but this lack of precision does not adversely affect the discussion presented here.

³See Appendix C for a discussion of the development of Figure 5.2.

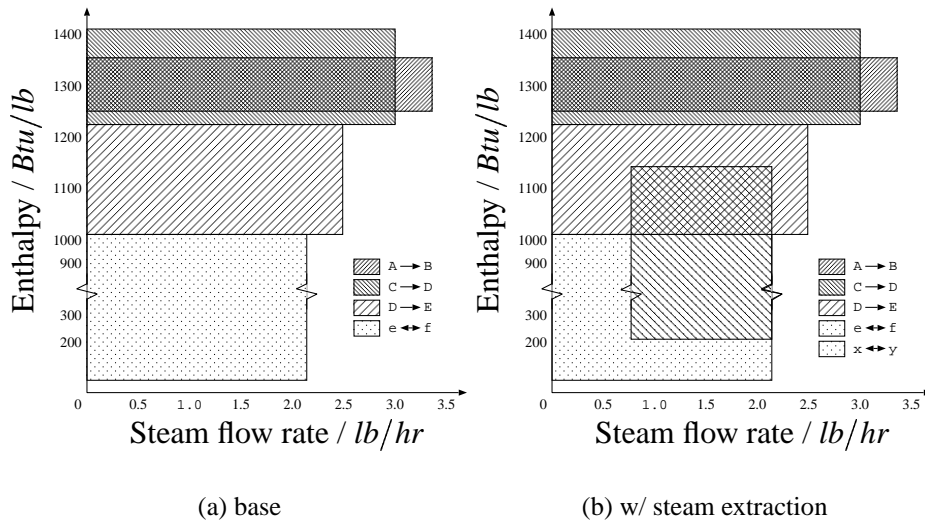


Figure 5.2: Implication of steam extraction on steam cycle work and heat flows

The split between the two ‘sinks’ is approximately 41% for the former and 59% for the latter. The additional shaded region in the adjacent figure, the one straddling \overrightarrow{CD} and \overrightarrow{DE} , is the flow of energy redirected from the turbine and *Condenser* once steam is extracted. What do the figures say in regards to the benefit of extracting steam for reboiler heating?

- Some 49% of otherwise waste heat instead services the reboiler. This represents 86% of the reboiler heat duty.
- The caveat is that the remaining 14% of the reboiler duty is taken from energy that otherwise would go into generating power in the LP section of the turbine. This a little over 30% of the steam internal energy in the \overrightarrow{DE} region.
- Post-CO₂ capture, 70% of the total energy flow is going towards power generation or servicing the *Stripper* reboiler and only 30%, down from 59%, is “thrown out with the bath water”.

Given the above development, steam extraction does seem beneficial. With the integrated model, it becomes possible to quantify the benefits/disadvantages of such a system. In particular, one will be able to ascertain:

- how much steam is required to satisfy the *Stripper* reboiler heat duty?
- and, by how much will this quantity of steam extraction de-rate the power-plant?

Comparison of different process designs and configurations

In Chapter 4, it is stated that a motivation for a detailed and adaptable MEA absorption model is the flexibility it affords. More specifically, such a model allows changes in flowsheet configuration, equipment design, solvent selection, and process operating conditions of the process performance to be studied. However, comparing the results of different case studies can be difficult.

As an example, consider the effect of changing the design CO₂ loading in the *lean* solvent stream. The effect of manipulating this variable has been reported [26, 27, 1] but only in regards to its effect on Q_{reb} . Increasing α_{lean} increases the solvent flow rate through the *Absorber* which, in turn, increases the pressure drop across that column. So, on the one hand, increasing α_{lean} reduces the process heating requirement but, on the other hand, it increases the need for compression power. These quantities are directly incomparable so how is one to truly ascertain the loading where the tradeoff is equal?

There are other variables which create similar problems (*e.g.*, *Absorber* height, *Column* height, *Stripper* pressure) as described above. With the unified model, all process duties, be they work or heat, are ultimately reflected in the plant's electricity output: a concept that is easy to grasp, is sensitive to design changes, and is relevant to the bigger question of "does CO₂ capture at an existing coal-fired power plant make sense?" Thus, tradeoffs similar to the one described in the preceding paragraph, are more easily assessed with an integrated model.

5.2 Implementation

The synthesis of the integrated flowsheet required adding new units to simulate flue gas cleanup and the *Stripper* reboiler and, most importantly, deciding from which location in the steam cycle to extract steam and how best to re-inject the condensate. The simulation flowsheet is given in Figure 5.3 and the details of its development are given below.

5.2.1 Location of steam extraction and condensate re-injection

There are two considerations in regards to the identification of the 'right' place to withdraw steam.

1. *Steam needs to be at the right temperature.*

The consensus is that $T_{reb} \leq 122^\circ\text{C}$ as, above this temperature, either thermal degradation of MEA or corrosion [61] becomes intolerable. Therefore, to maintain a “rule-of-thumb” 10°C hot-side temperature approach in the reboiler, the steam conditions must be such that $T^{sat} \geq 132^\circ\text{C}$. In addition, it is desirable to take the lowest quality steam that is available and meets this criteria; steam superheat is more valuable for power generation than heat transfer.

2. *The extraction point must be both accessible and able to accommodate the needed steam flow rate.*

There is limited mention in the literature of steam being extracted from the steam cycle of a power plant for providing heat to the *Stripper* reboiler.

- Mimura *et al.* [43, 44] refer to an “optimum steam system for power plant flue gas CO_2 recovery”. In practice, this consists of extracting steam midway through the low-pressure section of the turbine. In the lone case in which they considered recovering CO_2 from the coal-derived flue gas, some 3.25×10^6 lb/hr of 1208 Btu/lb steam is extracted. As the nominal plant output is 900 MW_e , this represents approximately 54% of the steam leaving the boiler.
- Desideri and Paolucci [20] extract steam for reboiler heating at the same position as deaerating steam is taken — midway through the LP section casing. 7.39×10^5 lb/hr of steam at 5 bar pressure is removed from the turbine causing the 320 MW_e plant to be de-rated by about 17%.
- In their study, Marion *et al.* [38] extract steam from the IP/LP crossover pipe. 2.5×10^6 lb/hr of steam, or 79% of that generated in the boiler, is extracted from the nominally 450 MW_e plant.

Inferred from these results is that it is not merely a “bleed” stream of steam that is required; access to large quantities of steam is necessary if this is going to work.

The schematic of the steam turbine in Figure 5.4 is repeated from Figure 3.6; it shows the location of all the potential steam extraction points. The adjacent table gives the steam flow rate at each location and the steam saturation temperature. From the data, it is (almost?) obvious as to where steam can be taken.

Consider the first requirement that $T^{sat} \geq 132^\circ\text{C}$ but as close to this cutoff as possible. Well, the steam in the IP/LP crossover pipe (position *LP*) and at position *D* have the same conditions and meet the first set of criteria. These positions differ dramatically, though, in terms of accessibility and availability, the second requirement.

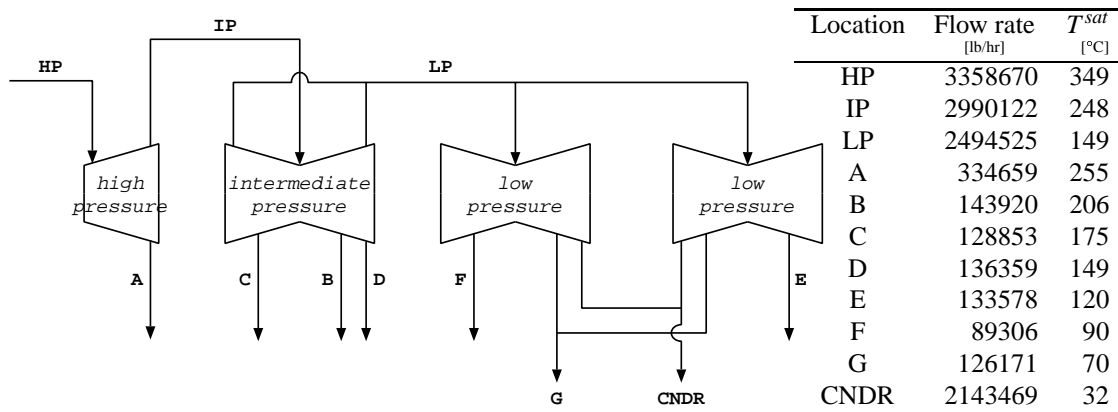


Figure 5.4: Base-load steam conditions in steam cycle

The “bleed” stream *D* is used in the fourth feed water pre-heater. Steam at this location, and at any of the other extraction points for that matter, have several disadvantages that preclude their use for providing for the *Stripper* reboiler:

- They are situated on the underside of the turbine, restricting access.
- The flow paths would not permit significantly increased flow rates than the nominal ones given in Figure 5.4[37].

Therefore, steam for the reboiler is taken from the IP/LP crossover pipe and, consequently, the condensate is re-injected into the cycle at the fourth feed water pre-heater. Doing so effectively splits the turbine into two parts: a base-load part consisting of the high- and intermediate-pressure sections and a part-load part consisting of the low-pressure section. In this manner, the correlations developed in Chapter 3 for predicting the performance of the turbine and feed water pre-heaters as a function of header and heat exchanger inlet flow rates is still applicable, even with steam extraction. Thus, the estimation of the power plant de-rate due to reduced steam flow through the LP section will be accurate.

For illustration purposes, the turbine of one of the units at Nanticoke is depicted in Figures 5.8 through 5.7. The IP/LP crossover pipes are the double-pair of large, longitudinal pipes that come up from the middle of the section shown in Figure 5.6 and extend into Figure 5.7 and is from here that reboiler steam is to be taken.⁴

⁴Apparently, this extraction location is not just feasible on paper. A preliminary estimation is that appropriate access at this position could be added during planned shutdown periods [37].



Figure 5.5: High-pressure section of Nanticoke turbine



Figure 5.6: Intermediate-pressure section of Nanticoke turbine



Figure 5.7: Low-pressure section of Naticoke turbine

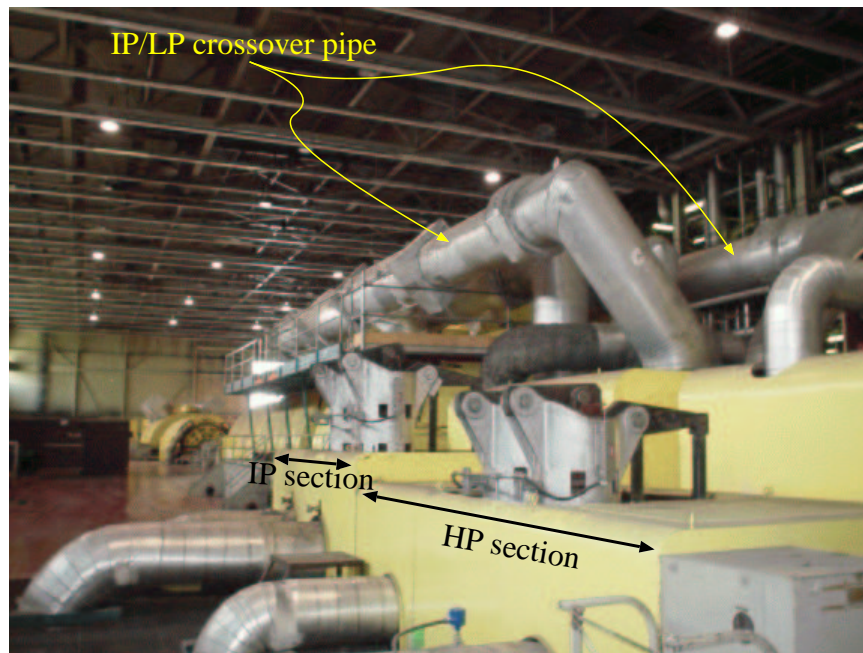


Figure 5.8: Lengthwise view of Naticoke turbine

5.2.2 Maximum available steam for *Stripper* reboiler heating

Deciding to transfer power plant steam to the *Stripper* reboiler imposes a practical limit as to the magnitude of reboiler heat duty that can be accommodated. The specified minimum design load for Nanticoke is 25% [4] however, it should be operationally feasible to go down to 10% flow through the LP section of the turbine [37]. In any case, even if it were possible to extract *all* of the steam, there is a finite amount available and this dictates the reboiler heating possible.

In order to ascertain this maximum heat duty, a series of simulations is performed where the fraction of steam extracted from the IP/LP crossover pipe is slowly increased. The extracted steam is condensed to the saturated liquid at 132°C and is re-injected into the steam cycle. The sensible and latent heat released is recorded and, along with the power plant terminal input, is shown in Figure 5.9.

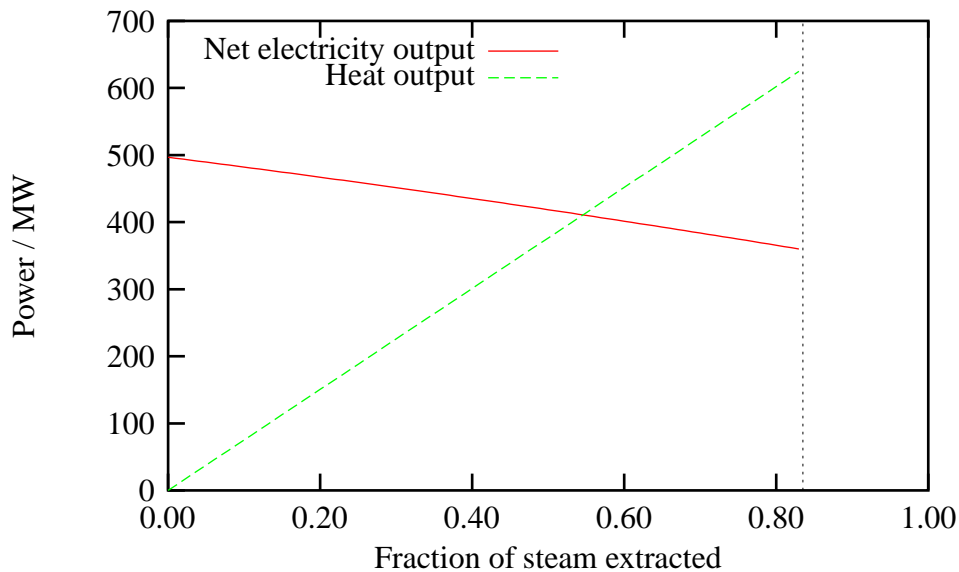


Figure 5.9: Sensitivity of power plant electricity output to steam extraction

Cases with steam extraction up to 90% were examined. However, when more than 83% of steam was diverted to the reboiler, the flow through the lowest-pressure stages of the LP section of the turbine is reduced to zero. The corresponding maximum Q_{reb} is approximately 625 MW and the terminal input is reduced from an initial 496.72 MW_e to 360.02 MW_e.

5.2.3 Flue gas pre-conditioning

Background

The first attempts to capture CO₂ from coal-derived flue gases were made in the 1980's at the Sundance Power Plant in Alberta [64] and, later, at the Boundary Dam Power Station in Saskatchewan [39]. While the efforts showed that large-scale capture of CO₂ from coal power is feasible, operational problems abounded due principally to the presence of fly ash, O₂, NO_x, and SO_x in the flue gas. In the intervening years, practical limits for each of these components in the flue gas have evolved.

Fly ash Fly ash causes foaming in the columns and plugging, scaling, corrosion, erosion in equipment and should be removed to 0.006 gr/dscf [15].

NO_x NO_x needs to be at or below 20 ppm [53].

O₂ O₂ is a problem because it oxidizes carbon steel and degrades MEA [15, 16, 28]. O₂ is dealt with in Fluor Daniel's Econamine FG™ by using oxygen inhibitors. Alternative approaches include using oxygen-tolerant alloys, removal of all oxygen from the flue gas (near-stoichiometric combustion and/or catalytic reduction), and continuous addition of oxygen scavengers to the solvent [15].

SO_x SO_x is a problem because it reacts irreversibly with MEA to form heat-stable salts thus reducing the absorption capacity of the solvent [15, 64, 63]. In systems where 30 wt% MEA solution is used, solvent losses due to SO_x become uneconomic when SO_x is greater than 10 ppmv in the flue gas [15, 39, 40, 38, 53]. With the Kerr-McGee/ABB Lummus Crest process, SO_x removal is necessary if the flue gas contains more than 100 ppmv. In the 50–100 ppmv range, upstream SO_x removal is optional as it can be removed during reclaiming through the addition of caustic. The downside to SO_x removal in the reclaimer is that some MEA loss occurs. Below 50 ppmv, SO_x removal is not justified [13].

Present implementation

Removal of fly ash is already accomplished in the *Separate* block that is part of the coal combustion model. A new block, *Scrubber*, modelled with the UOM's **SEP2** and **FLASH2**, handles the removal of O₂, NO_x, and SO_x from the flue gas as it flows between the coal combustion and MEA absorption parts of the flowsheet.

5.2.4 *Stripper* reboiler

The *Stripper* reboiler is modelled using the **HEATER** UOM. The outlet stream is saturated liquid. A zero pressure-drop is assumed across the unit.

5.2.5 *Blower* and *CO₂ Compressor*

It is assumed that electrical motors are used to drive the *Blower* and *CO₂ Compressor* and motor efficiencies of 90% are assumed.

5.3 Process Simulation

With an integrated process model, it is now possible to evaluate the feasibility of using the power plant as the source of *Stripper* reboiler heating. In Chapter 4 is given a number of different process design considerations that should influence the attractiveness of CO₂ capture using MEA absorption. For clarity, these ‘ideas’ that are evaluated are given in Table 5.1.

Table 5.1: Scope of MEA absorption sensitivity analysis

Design variable	Location
α_{lean}	page 84
$N_{Absorber}$	page 87
$N_{Stripper}$	page 89

As a basis, initial column heights of $N_{Absorber} = 10$ and $N_{Stripper} = 7$ are used.

5.3.1 Sensitivity of CO₂ capture to recycle CO₂ loading

In this study, the effect of changes in α_{lean} to the net electric output of the plant is examined. The results are shown in Figures 5.10 through 5.12.

- At lower CO₂ loading, Q_{reb} decreases quickly with increasing loading. With $\alpha_{lean} \geq 0.23$, Q_{reb} changes very little with CO₂ loading, going through a shallow minimum at $\alpha_{lean} = 0.26$ (Figure 5.10).

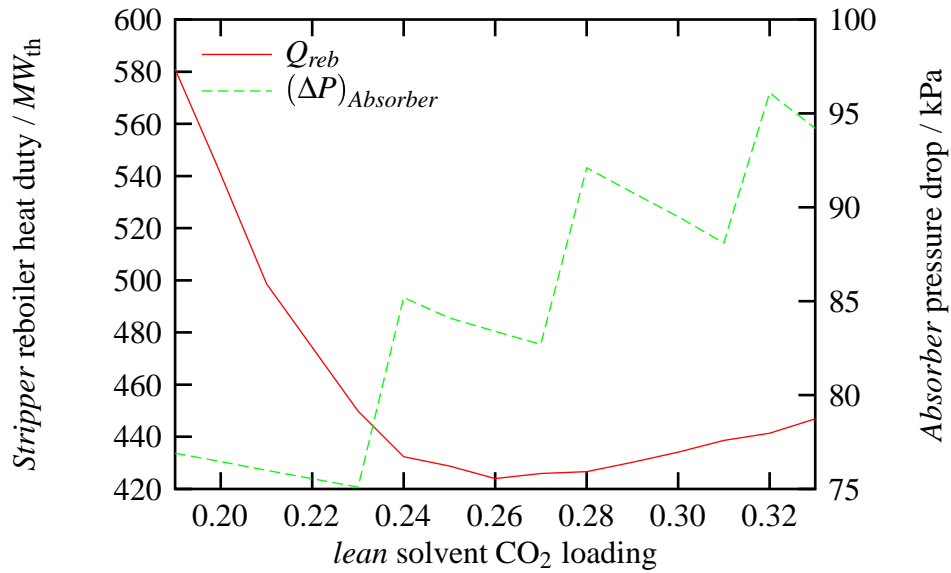


Figure 5.10: Sensitivity of *Absorber* pressure drop and *Stripper* reboiler heat duty to CO₂ loading

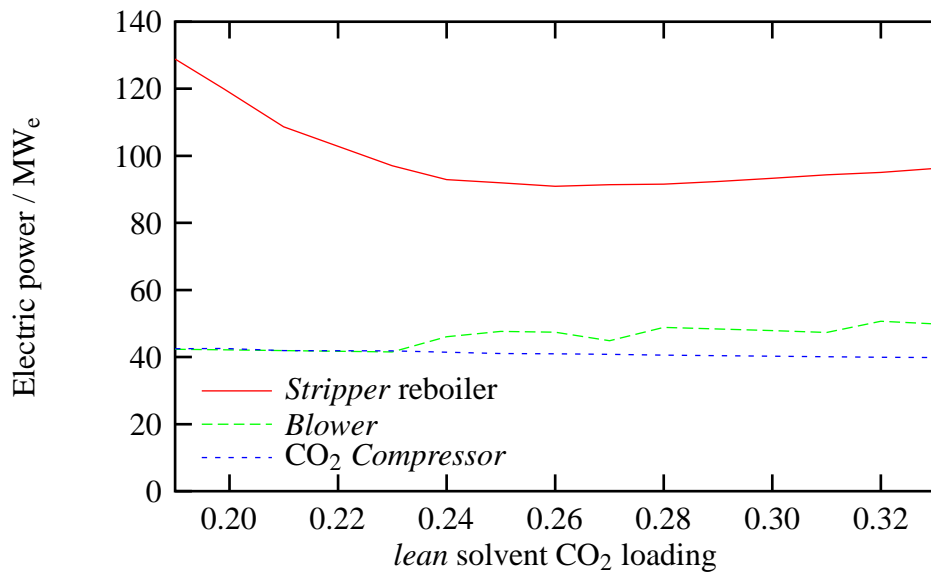


Figure 5.11: Sensitivity of capture plant's electricity demand to CO₂ loading

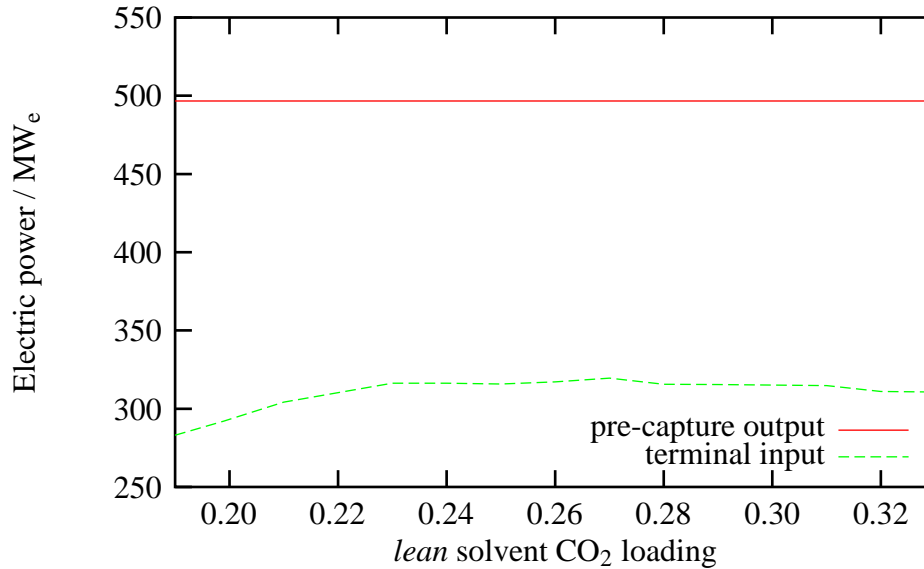


Figure 5.12: Sensitivity of power plant electricity output to CO₂ loading

- The *Absorber* pressure drop tends to increase as loading is increased. This is because F_{lean} increases with α_{lean} and this puts more resistance on the flow of vapour upwards through the column (Figure 5.10).⁵
- $E_{BLOWER} \approx E_{CO_2 COMP}$ (Figure 5.11).
- $(E_{BLOWER} + E_{CO_2 COMP}) \approx (\Delta E)_{reb}$ ⁶ (Figure 5.11).
- With constant design considerations $N_{Absorber}$, $N_{Stripper}$, and % flooding, E_{BLOWER} and $E_{CO_2 COMP}$ are insensitive to α_{lean} ; E_{BLOWER} experiences only a slight increase over the range observed (Figure 5.11).
- Power plant terminal output is less sensitive to changes in CO₂ loading than Q_{reb} . Over the interval $0.22 \leq \alpha_{lean} \leq 0.33$, the change in E_{net} is never more than ± 5 MWe (Figure 5.12).

⁵The stepwise nature of $(\Delta P)_{Absorber}$ curve arises from the constraint that the downcomer flooding must be less than 50% but that the tray spacing and weir height are only adjusted in whole number multiples of the Aspen Plus[®] default values of 24 and 2 inches, respectively.

⁶Just to be clear, $(\Delta E)_{reb}$ represents the decrease in E_{plant} that occurs by the extraction of steam for *Stripper* reboiler service

5.3.2 Sensitivity of CO₂ capture to Absorber height

In this study, the effect of changes in *Absorber* height on the net electric output of the plant is examined. The optimum loading from the Section 5.3.1, $\alpha_{lean} = 0.25$, is used. The results are shown in Figures 5.13 through 5.15.

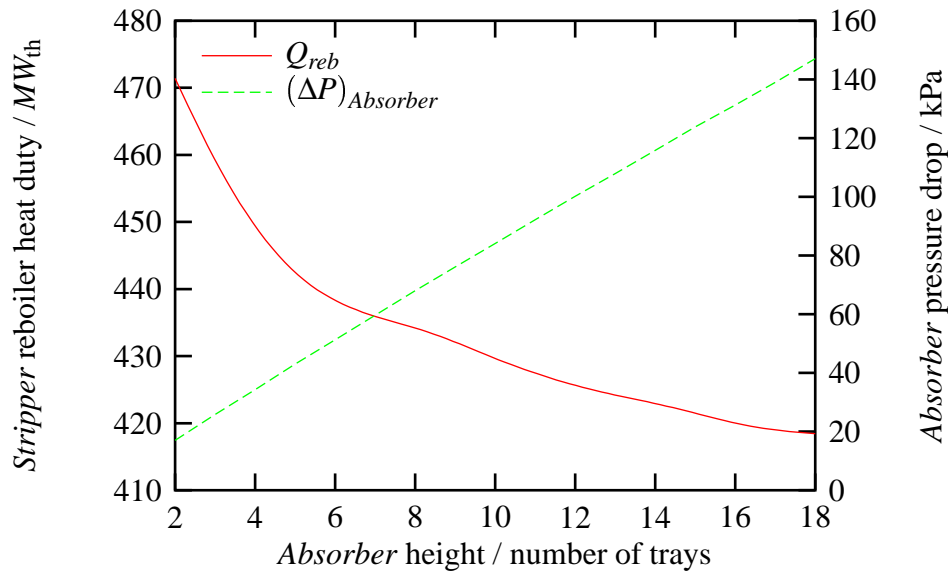


Figure 5.13: Sensitivity of *Absorber* pressure drop and *Stripper* reboiler heat duty to *Absorber* height

- Q_{reb} decreases asymptotically as $N_{Absorber}$ is increased. The overall effect is moderate; from the ‘base case’ at $N_{Absorber} = 10$, it was only possible to obtain a reduction of 10 MW_{th} in Q_{reb} , about 2%, by moving to $N_{Absorber} = 18$ (Figure 5.13).
- $(\Delta P)_{Absorber}$ varies linearly with $N_{Absorber}$; every additional tray increases the column pressure drop by about 8 kPa (Figure 5.13).
- The moderate reduction that increasing $N_{Absorber}$ has on Q_{reb} translates to even less impressive savings in electric power consumption. This is especially true in comparison to the increases in required *Blower* power as the *Absorber* size is increased (Figure 5.14).
- As alluded to by Figure 5.17, the increased $(\Delta P)_{Absorber}$ of making the *Absorber* bigger more than offsets any reductions in Q_{reb} . The power plant de-rate grows in synchronization the *Absorber* (Figure 5.15).

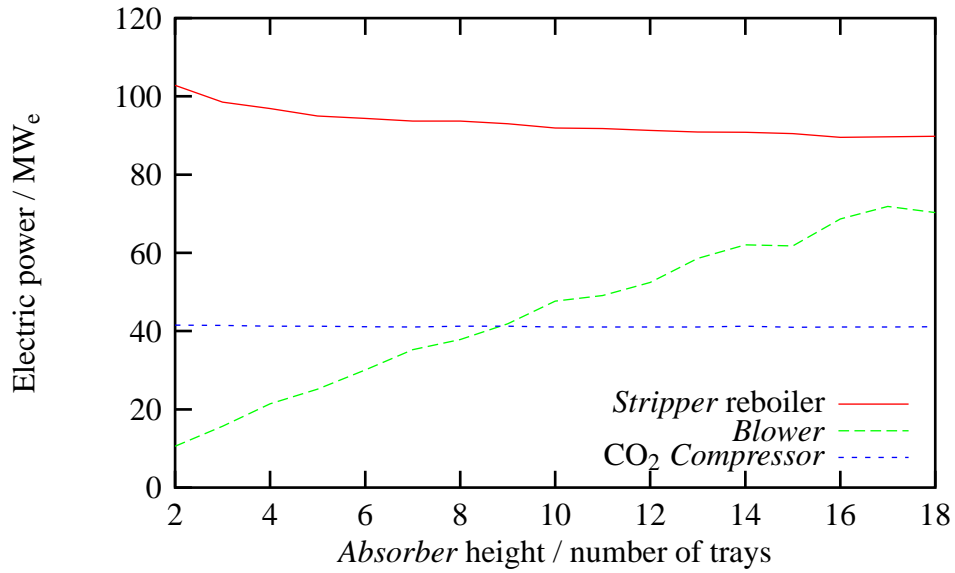


Figure 5.14: Sensitivity of capture plant's electricity demand to *Absorber* height

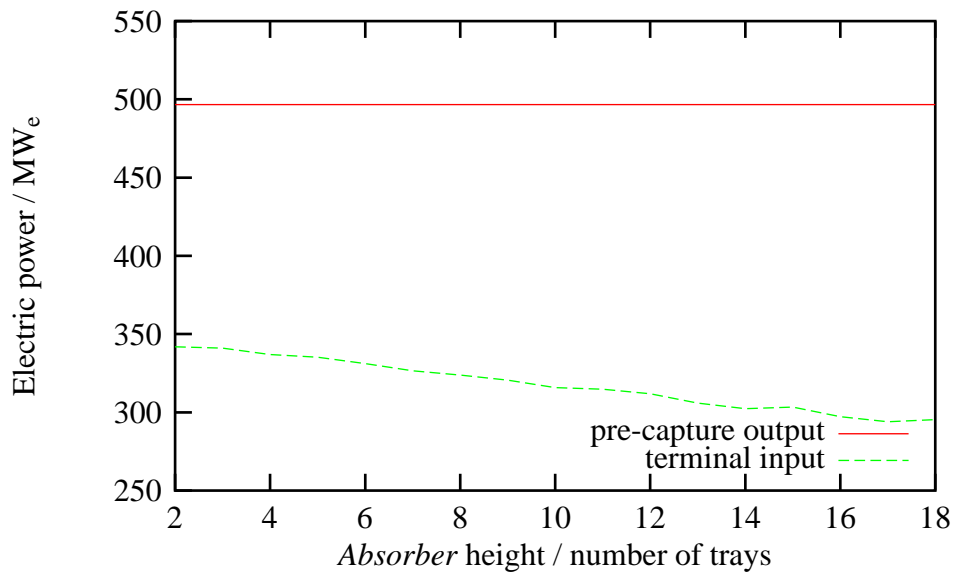


Figure 5.15: Sensitivity of power plant electricity output to *Absorber* height

5.3.3 Sensitivity of CO₂ capture to *Stripper* height

In this study, the effect of changes in *Stripper* height on the net electric output of the plant is examined. The optimum loading from the Section 5.3.1, $\alpha_{lean} = 0.25$, is used. The results are shown in Figures 5.16 through 5.18.

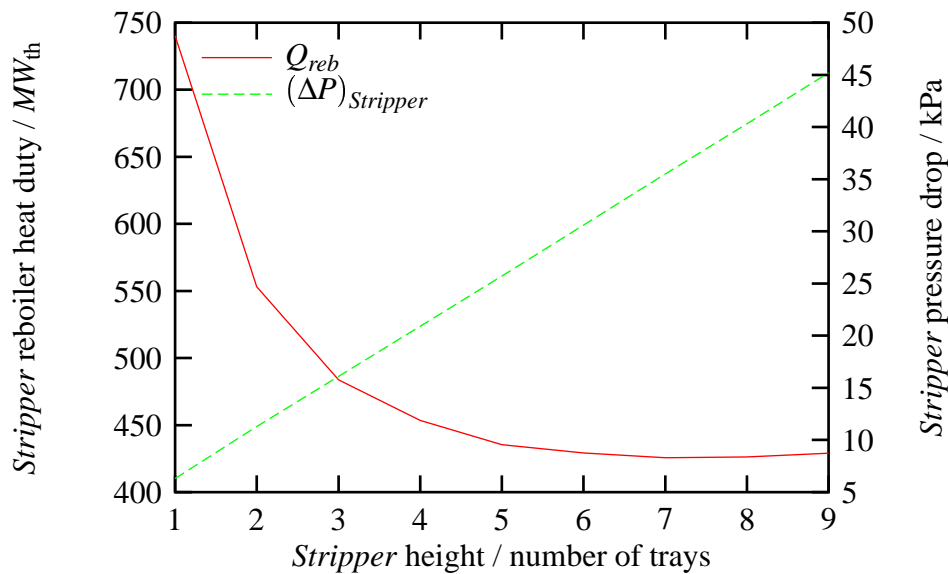


Figure 5.16: Sensitivity of *Stripper* pressure drop and *Stripper* reboiler heat duty to *Stripper* height

- Following the Q_{reb} curve from low to high values of $N_{Stripper}$, there is an immediate and strong benefit to increasing *Stripper* height. This benefit does taper off rather quickly, though; the ‘base case’ value, with just $N_{Stripper} = 7$, has the lowest corresponding Q_{reb} (Figure 5.16).
- $(\Delta P)_{Stripper}$ increases with increasing $N_{Stripper}$ but not as quickly as is the case with the *Absorber*. Here, each additional tray only caused an increase of about 5 kPa (Figure 5.16).
- Reductions in Q_{reb} should translate directly into a reduced electric power consumption and that is indeed the case. In regards to $(\Delta P)_{Stripper}$, smaller values are preferred as this leads to higher pressures in the column distillate which means the *CO₂ Compressor* has to work less hard. While technically, this effect is observed, the magnitude of the change is very small (Figure 5.17).

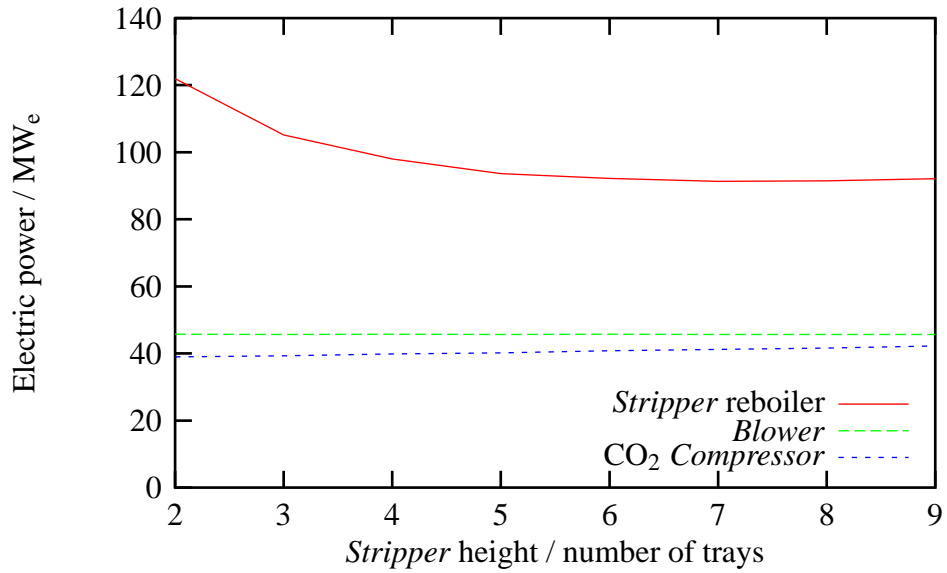


Figure 5.17: Sensitivity of capture plant's electricity demand to *Stripper* height

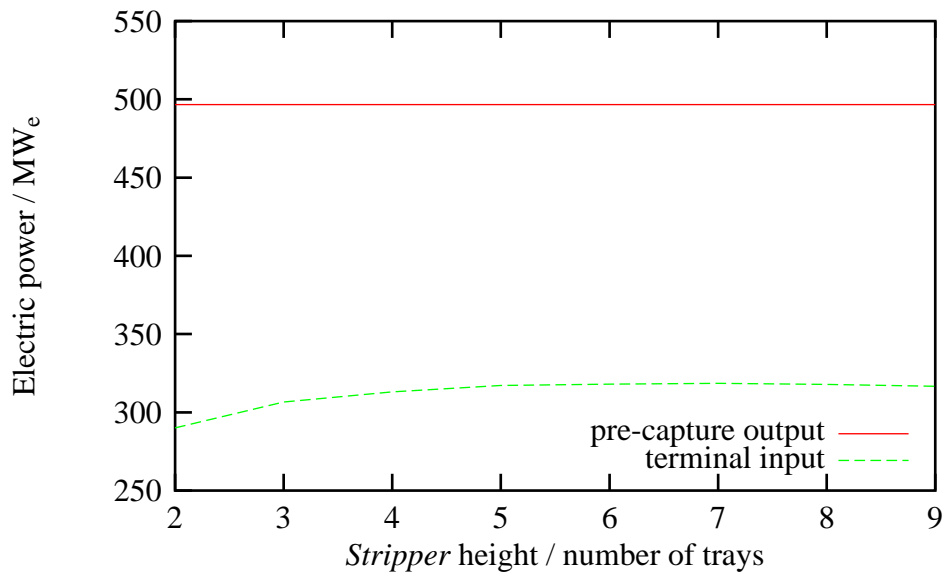


Figure 5.18: Sensitivity of power plant electricity output to *Stripper* height

- The output of the plant tends to increase asymptotically as $N_{Stripper}$ is increased (Figure 5.18).

5.4 Model validation

Table 5.2 compares the best case selected from each study with results from literature.

Table 5.2: MEA absorption process energy duties

Unit capacity [MW _e]	Flue gas		CO ₂ recovery		P_{out} [bar]	E_{Blower} [MW _e]	E_{Comp} [MW _e]	Q_{reb} [MW _{th}]	Source
	[mol% CO ₂]	[tonne/hr]	[%]	[tonne/hr]					
500	13.6	2312	85	426	110	45	41	426	CO ₂ loading study
500	13.6	2312	85	426	110	10	41	474	<i>Absorber</i> study
500	13.6	2312	85	426	110	46	41	426	<i>Stripper</i> study
1000	13.2	3888	60	468		9	56	370	Morimoto <i>et al.</i> [45] ⁷
450	15.0	2619	96	379	135		45	721	Marion <i>et al.</i> [38] ⁸
400	14.6	1664	90	331	150	9	31	351	Singh [55] ⁹
320	13.2	1205	90	234	140	9	20	234	Desideri <i>et al.</i> [20] ¹⁰
300	11.6	1882	88	192	141	12	43	371	Mariz <i>et al.</i> [40] ¹¹
300	11.6	1797	92	192	141	6	43	285	Mariz <i>et al.</i> [40] ¹²
300				333			54	245	Paitoon <i>et al.</i> [60] ¹³
	15.0	565	95	118					Chakma <i>et al.</i> [14]

⁷Only 2/3 of the “emit gas” from the power plant is processed by the capture plant; in actuality, 90% of the CO₂ that enters the absorption process is removed. The blower and compressor are steam-driven so the duties given for these units represent shaft power and not electrical power

⁸In estimating Q_{reb} , the following assumptions are made: $L_{IP} = 3.1 \times 10^6$ lb/hr, $(\Delta P)_{reb} = 0$, and the condensate leaving the reboiler is saturated liquid. The given compressor duty includes the energy required for the blower.

⁹The auxiliary energy equipment emits 84.45 tonne/year of CO₂. Therefore, the CO₂ abatement at the power plant is only 65%.

¹⁰The results reported by Desideri and Paolucci are of questionable quality. For starters, the base efficiency of the power plant in their study is 44.3% and their specific compression power and reboiler heat duty are much lower than observed elsewhere.

¹¹About 75% of the flue gas is from the power plant with the residual generated by the auxiliary coal-fired boiler. In this study, MEA absorption is based on Econamine FGTM process.

¹²About 78% of the flue gas is from the power plant with the residual generated by the auxiliary coal-fired boiler. In this study, MEA absorption is based on MHI/KEPCO KS-1/KP-1 process.

¹³The study is based on capturing 8000 tonne/day from a 300 MW coal-fired power plant. A “back-of-the-envelope” calculation shows that, given the coal-composition given, even at 30% overall thermal efficiency, a 300 MW power plant would produce less than 8000 tonne/day of CO₂. The given compressor duty includes the energy required for the blower.

First, in regards to the electricity consumption, while the *CO₂ Compressor* duties obtained in this study are comparable to what has been observed elsewhere, the *Blower* duties obtained in the *CO₂* and *Stripper* studies are substantially higher than anything seen before. This is attributable to the fact that the MEA absorption model used in this work explicitly calculated pressure drop across the *Absorber* for a given column design. In other studies [54, 20], $(\Delta P)_{abs}$ of approximately 0.2 bar is assumed irrespective of the height of the column or the type of packing used.

For the moment, as most researchers have been apt to do, consider only \bar{Q}_{reb} . In Table 5.3 is required specific reboiler heat duty as reported in this study, and by others.

Table 5.3: *Stripper* reboiler specific heat duty

Source	\bar{Q}_{reb} [kJ/kg CO ₂]
CO ₂ loading study	1.00
<i>Absorber</i> study	1.11
<i>Stripper</i> study	1.11
Morimoto <i>et al.</i> [45]	0.37
Desideri and Paolucci [20]	0.73
Singh [55]	1.06
Mariz <i>et al.</i> [40] ^a	1.48
Marion <i>et al.</i> [38]	1.90
Mariz <i>et al.</i> [40] ^b	1.93

^aIn this study, MEA absorption is based on MHI/KEPCO KS-1/KP-1 process.

^bIn this study, MEA absorption is based on Econamine FGTM process.

The values of \bar{Q}_{reb} obtained in this study fall in line with expectations regarding the effect of flue gas CO₂ concentration and absorption solvent performance:

1. CO₂ capture is facilitated by higher concentrations of CO₂ in the flue gas. Consider the follow studies in which the CO₂ concentration is $\approx 13\%$:
 - $\bar{Q}_{reb} = 1.48$ kJ/kg CO₂ for Mariz *et al.* versus 0.37 for Morimoto *et al.* (both studies use KS-1 as a solvent).
 - $\bar{Q}_{reb} = 1.93$ kJ/kg CO₂ for Mariz *et al.* versus 0.73 and 1.00–1.11 found by Desideri and Paolucci and in this study (all studies used 30 wt% CO₂ as a solvent).

2. KS-1 (Morimoto *et al.*, 0.37 kJ/kg CO₂) outperforms 30 wt% aqueous MEA (Desideri and Paolucci, 0.73 kJ/kg CO₂; this study, 1.00–1.11 kJ/kg CO₂; Singh, 1.06 kJ/kg CO₂) which outperforms 15 wt% aqueous MEA (Marion, 1.90 kJ/kg CO₂).

5.5 Conclusions and recommendations

- The integration of the coal combustion, steam cycle, and MEA absorption models is accomplished in a straight-forward manner.
- The IP/LP crossover pipe is the preferred extraction location from which to extract steam for *Stripper* reboiler as it is easily accessible and furnishes steam at conditions relatively close to those required.
- The following table summarizes the best conditions observed in each of the sensitivity analyses performed to date:

Table 5.4: Summary of best cases from sensitivity studies

Study	α_{lean}	$N_{Absorber}$	$N_{Stripper}$	x_{steam}	E_{net} [MW _e]	de-rate [%]
α_{lean}	0.27	10	7	0.58	320	35.7
$N_{Absorber}$	0.25	2	7	0.64	342	31.2
$N_{Stripper}$	0.25	10	7	0.58	319	35.9

Chapter 6

Conclusion and Future Work

6.1 Conclusion

As mentioned in the Introduction, the more conventional method of satiating the *Stripper* reboiler is by generating steam in a boiler dedicated to this purpose. This thesis seeks to evaluate the feasibility of obtaining the heat required for MEA absorption for the existing power plant which implicitly poses the question, “Is extracting steam from the existing power plant a superior alternative to disassociated units?” It seems a direct comparison is in order. . .

The efficacy of the approaches can be compared using thermal efficiency defined by:

$$\eta_{th} = \frac{E_{net}}{Q_b}$$

For the particular cases of concern here, η_{th} is evaluated in terms of model outputs as follows:

$$\eta_{th} = \begin{cases} \frac{E_{net}}{Q_{boil} + Q_{reht}} & \text{integrated power plant w/ CO}_2 \text{ capture} \\ \frac{E_{net}}{Q_{boil} + Q_{reht} + Q_{reb}/\eta_{aux}} & \text{configuration w/ auxillary boiler} \end{cases}$$

The analyses from Chapter 5, with two modifications, are repeated; this time, a CO₂ capture plant that produces its own steam, as required, using an auxiliary boiler is considered and the measured variable is η_{th} . The results are tabulated and compared with

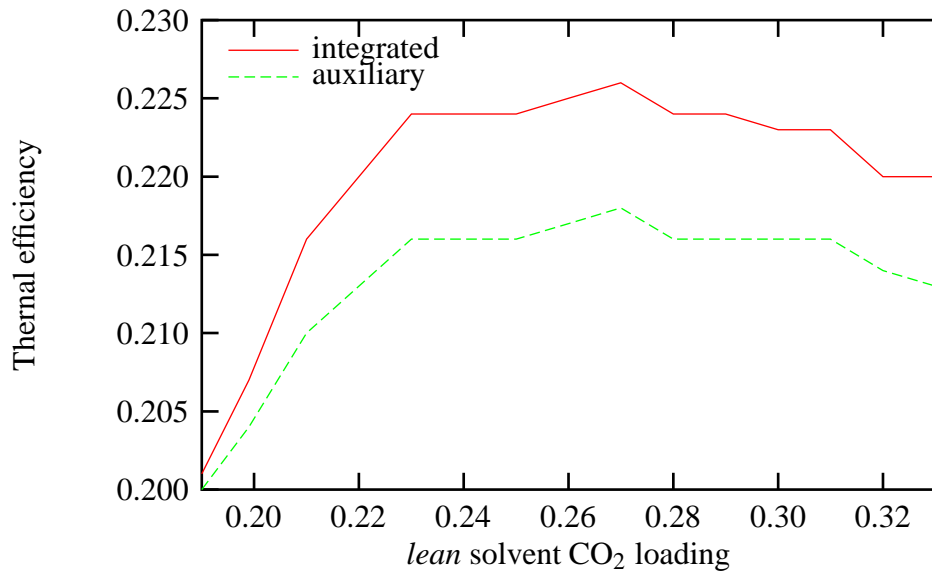


Figure 6.1: Influence of CO₂ loading on plant thermal efficiency

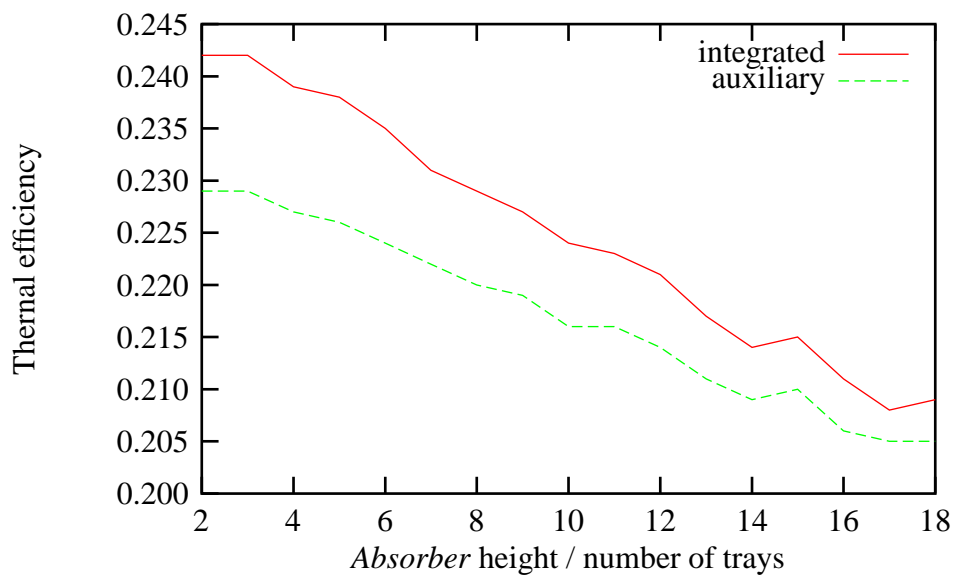


Figure 6.2: Influence of Absorber height on plant thermal efficiency

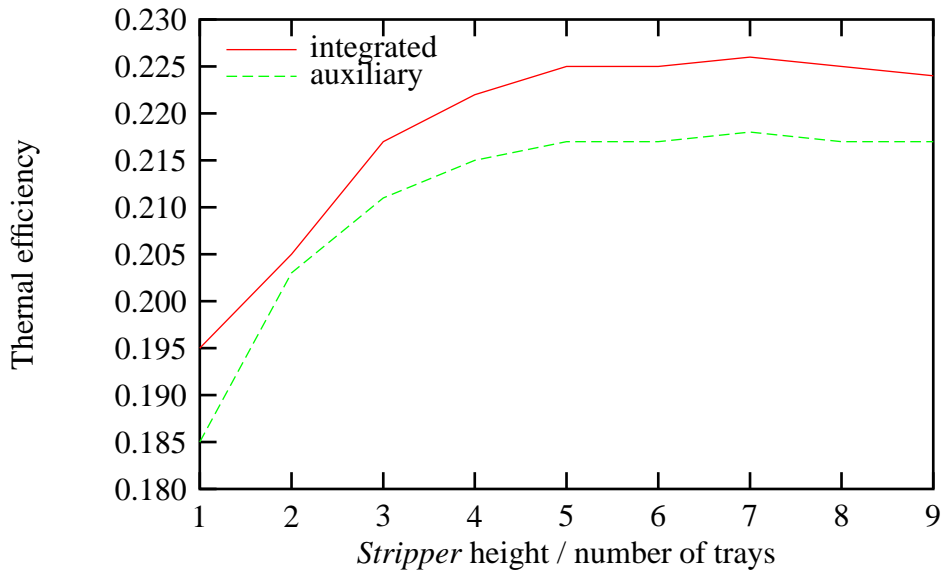


Figure 6.3: Influence of *Stripper* height on plant thermal efficiency

computed thermal efficiencies for the proposed capture plant with integrated CO₂ capture in Figures 6.1 through 6.3.

In all cases, extracting steam from the steam cycle is a Good Thing™. As a general rule, it can be said that doing so improves the plant's energy utilization by a full percentage point. The conclusion of this work is that, for the case of adding CO₂ capture using MEA absorption to the existing coal-fired power plant at Nanticoke Generating Station, satisfying the supplemental heat demand by using steam from the power plant is the way to go.

6.2 Future work

The following are suggestions as to projects which build upon the successes of this work:

- Researchers at the University of Texas, at Austin have developed a rate-based model for the chemistry of the CO₂-MEA-H₂O system [25, 26, 27]. This is in contrast to the equilibrium model used in this work. It would be interesting to incorporate this kinetic model into the power plant with integrated CO₂ capture model developed here and to measure any changes to the conclusions, if any, brought about by the increased rigour.

- The sequential modular approach of the current MEA absorption model is a disadvantage and complicates the issue of the extreme sensitivity of the **RateFrac**TM UOM to changes in process conditions which makes convergence problematic. Newer versions of Aspen Plus[®] [11] now ship with an equation oriented solver. With such a solution method, iteration, a major source of trouble in this thesis, would no longer be necessary. The model should be re-implemented using the equation oriented approach and efficacy of solving the integrated flowsheet using the two different techniques compared.
- Much of the discussion of improving the design of CO₂ capture processes based on MEA absorption focuses on minimizing Q_{reb} . As is clearly demonstrated in Section 5.3.2, minimizing Q_{reb} does not necessarily optimize the design of the CO₂ capture plant. For this reason, in this study, η_{th} is used as a metric for evaluating designs. Ultimately, though, it is the cost of each strategy that guides the decision as to what eventually to implement. While it is true that costs themselves can be misleading [49], they are required if apple-to-apple comparisons are to be made between different technology options (*e.g.*, PCC versus NGCC). Therefore, the cost of CO₂ capture of the best designs from this work should be costed out.
- A new power plant design with integrated CO₂ capture should realize higher thermal efficiencies than any retrofit case whether steam extraction is implemented as part of the retrofit or not. A new design could preclude the extraction of superheated steam for reboiler heating, make steam available at a variety of conditions by including extraction ports in the turbine casing, include additional auxiliary turbines to produce power for the *Blower* and *Compressor*, and increase the number and quality of heat-integration opportunities. To date, there is limited, if any, work being done in this area.¹ One of the more useful outcomes would be a PCC case for comparison with new NGCC and IGCC power plants (both with and without CO₂ capture) that are being proposed for construction in Ontario and North America at large.

¹The only mention in the literature is of work done as part of a joint venture by the Japanese companies Mitsubishi Heavy Industries and Kansai Electric Power Company [43, 44]

Appendix A

Conditions of steam at potential extraction locations

Table A.1: Base and part-load conditions in Nanticoke steam cycle

Stream	100%			75%			50%		
	T [°F]	P [psia]	L [10 ⁶ lb/hr]	T [°F]	P [psia]	L [10 ⁶ lb/hr]	T [°F]	P [psia]	L [10 ⁶ lb/hr]
ST_MAIN	1000.0	2365.0	3.36	1000.0	2365.0	3.26	1000.0	2365.0	3.24
ST-FPT1	1000.0	2365.0	0.01	1000.0	2365.0	0.01	1000.0	2365.0	0.01
ST-HP	994.6	2236.2	3.34	962.1	1631.5	3.24	930.0	1080.7	3.21
ST-REHT	646.7	622.4	2.99	629.4	460.8	2.94	611.7	309.9	2.95
ST-FWPA	646.7	622.4	0.33	629.4	460.8	0.29	611.7	309.9	0.24
ST-IP	1000.0	560.2	2.99	1000.0	414.5	2.94	1000.0	278.7	2.95
ST-FWPC	624.1	129.3	0.13	627.7	96.6	0.11	631.1	65.4	0.10
ST-FPT2	787.9	253.9	0.08	788.9	188.8	0.08	790.9	127.3	0.09
ST-FWPB	787.9	253.9	0.14	788.9	188.8	0.14	790.9	127.3	0.12
ST-FWPD	484.0	66.6	0.14	488.2	49.9	0.12	491.9	34.0	0.11
ST-LP	484.0	66.6	2.49	488.2	49.9	2.48	491.9	34.0	2.52
ST-FWPF	193.4	10.1	0.09	179.9	7.5	0.08	176.1	5.2	0.08
ST-FWPE	330.8	28.8	0.14	335.0	21.7	0.13	339.6	14.9	0.12

Base and part-load conditions in Nanticoke steam cycle cont...

Stream	100%			75%			50%		
	<i>T</i> [°F]	<i>P</i> [psia]	<i>L</i> [10 ⁶ lb/hr]	<i>T</i> [°F]	<i>P</i> [psia]	<i>L</i> [10 ⁶ lb/hr]	<i>T</i> [°F]	<i>P</i> [psia]	<i>L</i> [10 ⁶ lb/hr]
ST-CNDR	89.5	0.7	2.14	79.0	0.5	2.15	79.0	0.5	2.23
ST-FWPG	157.8	4.5	0.13	145.9	3.4	0.13	131.9	2.3	0.10
H2O-FWPA	400.6		3.36	379.1		3.26	350.7		3.24
H2O-BOIL	487.9		3.36	461.1		3.26	425.6		3.24
H2O-FWPB	351.2	2700.0	3.36	329.6	2550.0	3.26	303.9	2500.0	3.24
H2O-FWPC	293.2		2.74	276.8		2.71	255.2		2.75
H2-PUMP	345.4		3.36	324.2		3.26	297.7		3.24
H2O-FWPD	241.6		2.74	228.0		2.71	209.9		2.75
H2O-FWPE	186.4		2.74	175.0		2.71	160.3		2.75
H2O-FWPF	150.0		2.74	140.7		2.71	129.1		2.75
H2O-FWPG	90.2		2.74	79.9		2.71	80.3		2.75
STFPT_CN	89.5	0.7	0.09	79.0	0.5	0.09	79.0	0.5	0.09
H2O-MAIN	89.5		2.74	79.0		2.71	79.0		2.75

Appendix B

Sieve Tray Column Hydrodynamic Design Recipe

Table B.1 summarizes the parameters and stream properties that are required to size the column and evaluate its hydrodynamics.

B.1 Tower diameter

The tower diameter is equal to the diameter of the largest tray. The following steps are required to calculate tray diameter:

1. Calculate constant F_{LG} .

$$F_{LG} = \frac{L}{G} \left(\frac{\rho_G}{\rho_L} \right)^{0.5}$$

2. Calculate C_{sbf} .

$$C_{sbf} = 0.0105 + 8.127 \times 10^{-4} TS^{0.755} \exp(-1.463 F_{LG}^{0.842})$$

TS is usually 300–600 mm.

Table B.1: Required input for sizing and hydrodynamic evaluation of tray columns

Parameters		Properties	
symbol	nominal	symbol	units
EFA	60–85%	L	kg/s
TS	300–600 mm	G	kg/s
ε	0.046 mm	q_L	m^3/s
d_h	6.5–13 mm	q_G	m^3/s
g	$9.8 m/s^2$	ρ_L	kg/m^3
h_c	25.4 mm	ρ_G	kg/m^3
h_w	50 mm	σ	$dynes/cm$
t_t	2.0–3.6 mm	μ_L	$kg/m \cdot s$
A_h/A_a	0.05–0.15		
f	0.75		

3. Calculate the gas velocity through the net area at entrainment flooding, u_{NF} .

$$U_{NF} = C_{sbf} \left(\frac{\sigma}{20} \right)^{0.2} \left(\frac{\rho_L - \rho_G}{\rho_G} \right)^{0.5}$$

4. The design gas velocity through the net area, U_N , is selected as a percentage of U_{NF} . Perry's [29] says that prudent designs call for approaches to flooding of 75–85%. Course notes [2] give typical design values of 60–80%.

$$U_N = \frac{EFA}{100\%} U_{NF}$$

This calculation is valid provided that the following conditions are met:

- system is low- or non-foaming
- $h_w < 0.15 TS$
- $d_h < 13 \text{ mm}$
- $A_h/A_a > 0.1$

5. The net area of the column is the portion through which gas flows. Therefore, the magnitude of this area, A_N is the quotient of the gas volumetric flow rate and U_N .

$$A_N = \frac{qG}{U_N}$$

6. The net area is the difference between the total cross-sectional area, A_{total} , and the area under the downcomer, A_d . The area of the downcomer is determined by specifying the weir length which is specified as a fraction f of the diameter, usually 75% [2].

$$A_{total} = \frac{A_N}{1 - \frac{1}{\pi} \left(\sin^{-1} f - f \sqrt{1 - f^2} \right)}$$

7. Calculate the diameter, d .

$$d = \sqrt{\frac{4A_{total}}{\pi}}$$

B.2 Downcomer flooding

The depth of liquid in a downcomer should be such that it is less than 50% full. The following *recipe* calculates the height of clear liquid in a downcomer, h_{dc} .

1. Calculate the height due to the downcomer apron, h_{da} .
 - (a) Calculate the area for flow under the downcomer apron, A_{da} .

$$A_{da} = \ell_w \times h_c$$

As stated above, $\ell_w = f \cdot d$. h_c , as a rule of thumb, is 1'' [2].

- (b) Then, calculate h_{da} .

$$h_{da} = 165.2 \left(\frac{qL}{A_{da}} \right)^2$$

2. Calculate the height due to the hydraulic gradient across the tray, h_{hg} .

(a) Calculate the gas velocity through the active area, U_a .

$$U_a = U_N \frac{A_N}{2A_N - A_{total}}$$

(b) Calculate K_s .

$$K_s = U_a \left(\frac{\rho_G}{\rho_L - \rho_G} \right)^{0.5}$$

(c) Calculate the effective froth density on the plate, ϕ_e .

$$\phi_e = \exp(-12.55K_s^{0.91})$$

(d) Calculate the effective clear-liquid height (*i.e.*, liquid holdup), h_L .

i. Calculate the constant C .

$$C = 0.0327 + 0.0286 \exp(-0.1378 h_w)$$

ii. Then use C to calculate h_L .

$$h_L = \phi_e \left[h_w + 15330C \left(\frac{q_L}{\phi_e} \right)^{\frac{2}{3}} \right]$$

h_w is usually 50 mm and less than 15% of tray spacing [2].

(e) Calculate the froth height, h_f .

$$h_f = \frac{h_L}{\phi_e}$$

(f) Calculate the average width of the flow path, D_f .

$$D_f = \frac{L_w + d}{2}$$

(g) Calculate the hydraulic radius of the aerated mass, R_h .

$$R_h = \frac{h_f D_f}{2h_f + 1000D_f}$$

(h) Calculate the velocity of the aerated mass, U_f .

$$U_f = \frac{1000 q_L}{h_L D_f}$$

(i) Calculate the Reynolds number for the flow, $N_{Re,h}$.

$$N_{Re,h} = \frac{R_h U_f \rho_L}{\mu_L}$$

(j) Calculate the Fanning friction factor, f_F , for the flow.

$$f_F = \left\{ -1.737 \ln \left[0.269 \frac{\varepsilon}{R_h} - \frac{2.185}{N_{Re,h}} \ln \left(0.269 \frac{\varepsilon}{R_h} + \frac{14.5}{N_{Re,h}} \right) \right] \right\}^{-2}$$

ε is 0.046 mm for commercial steel [62].

(k) The length of the flow path across the plate, ℓ_f , is given by $L_f = k \cdot d$. Find k such that

$$f \cdot k = \frac{\pi}{4} \left\{ 1 - \frac{2}{\pi} \left[\left(\sin^{-1} f - f \sqrt{1 - f^2} \right) + \left(\sin^{-1} k - k \sqrt{1 - k^2} \right) \right] \right\}$$

(l) Calculate h_{hg} .

$$h_{hg} = \frac{1000 f_F U_f^2 \ell_f}{g R_h}$$

3. Calculate the height caused by liquid pushing up in order to flow over the weir, h_{ow} .

$$h_{ow} = 664 \left(\frac{q_L}{\ell_w} \right)^{\frac{2}{3}}$$

4. Calculate the height caused by the pressure drop across plate, h_t .

(a) Calculate the pressure drop that would exist across the dry dispersion plate, h_d .

- i. Firstly, calculate the gas phase velocity through the tray perforations, U_h .

$$U_h = U_a \left(\frac{A_h}{A_a} \right)^{-1}$$

The hole area is usually 5–15% of the active area (*i.e.*, $A_h/A_a \approx 0.1$).

- ii. Then calculate the constant C_v .

$$C_v = 0.74 \left(\frac{A_h}{A_a} \right) + \exp \left[0.29 \left(\frac{t_t}{d_h} \right) - 0.56 \right]$$

t_t is usually 2–3.6 mm. d_h is 6.5–13 mm.

- iii. Finally, calculate h_d .

$$h_d = \left(\frac{50.8}{C_v^2} \right) \left(\frac{\rho_G}{\rho_L} \right) U_h^2$$

- (b) Calculate the pressure drop across the aerated liquid on the tray, h'_L . The procedure of Bennet *et al.* as described in [29] is followed.

- i. Calculate the pressure drop for surface generation, h'_σ .

$$h'_\sigma = \left(\frac{472 \sigma}{g \rho_L} \right) \left[\frac{g(\rho_L - \rho_G)}{d_h \sigma} \right]^{\frac{1}{3}}$$

- ii. Using the value of h_L calculated during the determination of h_{hg} , calculate h'_L .

$$h'_L = h_L + h'_\sigma$$

- (c) Calculate h_t .

$$h_t = h_d + h'_L$$

5. Calculate the height of liquid in the downcomer, h_{dc} .

$$h_{dc} = h_t + h_w + h_{ow} + h_{da} + h_{hg}$$

B.3 Tray pressure drop

The total pressure drop across the tray, ΔP_t , is expressed as a pressure head, h_t , as follows:

$$\Delta P_t = \frac{h_t \rho_L g}{1000}$$

B.4 Downcomer seal

The downcomer seal, h_{ds} must be great enough to prevent vapour from propagating upwards along this channel.

$$h_{ds} = h_w + h_{ow} + 0.5 h_{hg}$$

As rule of thumb, $h_{ds} > h_a + 13\text{--}38$ mm [2].

B.5 Weeping

Weeping occurs when there is insufficient pressure to maintain a froth on the tray surface. Deleterious weeping occurs when a significant amount of liquid flows through the tray, thereby diminishing contact between the vapour and liquid phases. Weeping is checked for the minimum expected flow rates for a particular column design using Figure 14-27 in [29]. The abscissa and ordinate values are calculated as follows:

$$x = h_w + h_{ow}$$

$$y = \frac{4\sigma}{d_h} + \frac{409\sigma}{\rho_L d_h}$$

Appendix C

Steam Energy Calculations

Expansion in turbine

By definition,¹

$$H = U + PV$$

Taking the partial differential of both sides and rearranging gives,

$$dH = dU + d(PV)$$

$$dU = dH - d(PV)$$

Assuming that the steam behaves ideally, *i.e.*,

$$PV = nRT$$

an expression for steam internal energy in terms of enthalpy and temperature is easily obtained

¹Please note the following that in this Appendix the *overline* is used to distinguish between the absolute and mass-relative forms of internal energy and enthalpy.

$$\begin{aligned}dU &= dH = nRdT \\ \frac{dU}{m} &= \frac{dH}{m} = \frac{RdT}{M}\end{aligned}$$

Integrating both sides gives the final expression:

$$\Delta\bar{U} = \Delta\bar{H} - \frac{R\Delta T}{M}$$

Condensing heat transfer

Starting with the final expression for specific internal energy calculated above

$$\Delta\bar{U} = \Delta\bar{H} - \frac{R\Delta T}{M}$$

it is apparent that, in the case of condensing heat transfer, the expression simplifies to

$$\Delta\bar{U} = \Delta\bar{H}$$

as this is a constant temperature process.

Changes in internal energy encountered in Nanticoke steam cycle

Table C.1: Changes in steam internal energy in steam cycle

Process	\bar{H}_{in}	\bar{H}_{out}	T_{in}	T_{out}	$\Delta\bar{U}$
	Btu/lb	Btu/lb	°F	°F	Btu/lb
\overrightarrow{AB}	1462.83	1318.33	1000	646.7	-105.5
\overrightarrow{CD}	1517.88	1274.65	1000	484.0	-186.3
\overrightarrow{DE}	1274.65	1017.84	484	89.5	-213.3
\overleftarrow{ef}	1017.84	57.52			-960.3
\overleftarrow{xy}	1169.93	236.70			-933.2

Appendix D

Comparison of Calculated CO₂ Solubility With Experimental Values

Figures D.1 through D.8 compare the solubility of CO₂ in 30 wt% aqueous MEA over the complete range of temperatures investigated by Jou *et al.* [36].

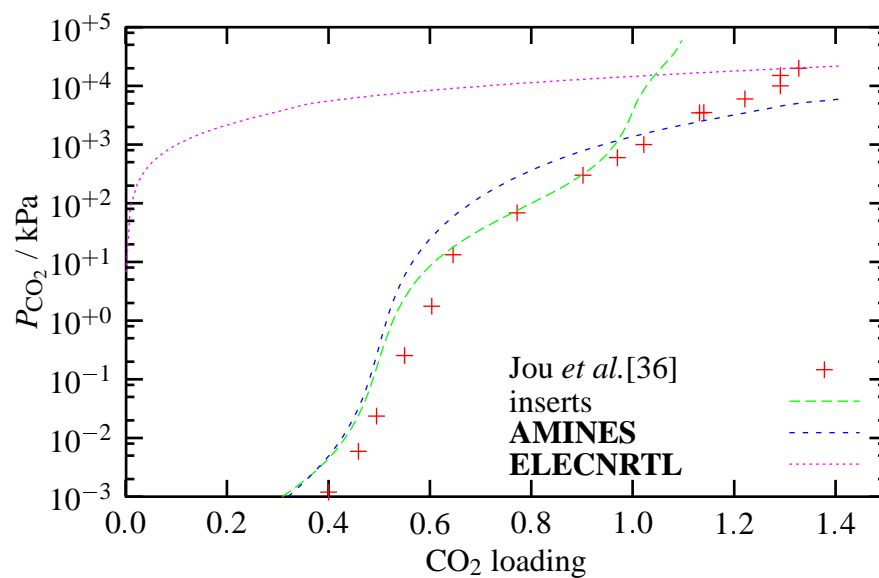


Figure D.1: Comparison of calculated VLE with experimental values at 0°C

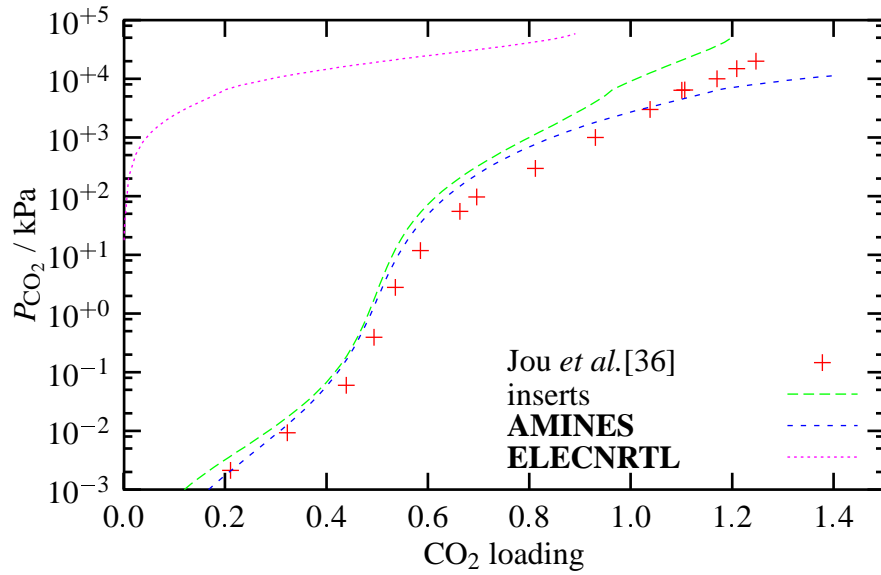


Figure D.2: Comparison of calculated VLE with experimental values at 25°C

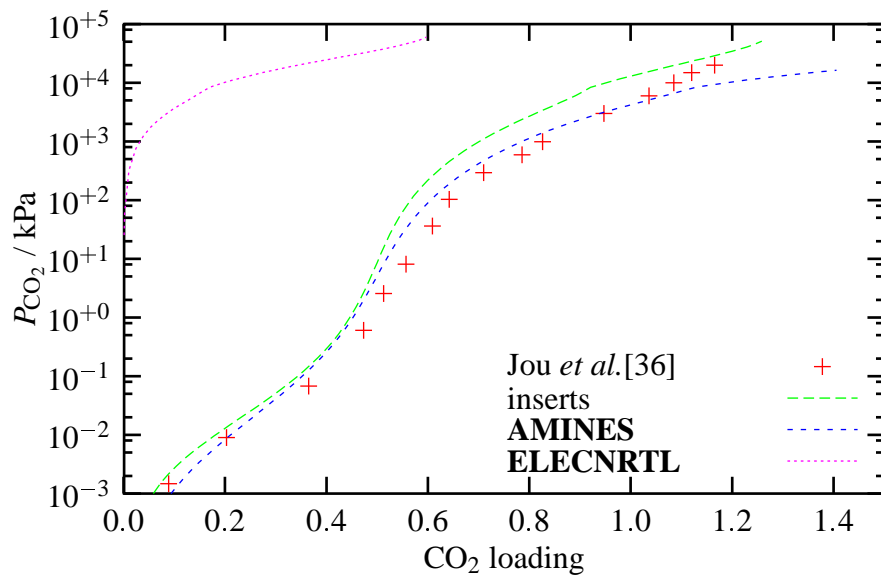


Figure D.3: Comparison of calculated VLE with experimental values at 40°C

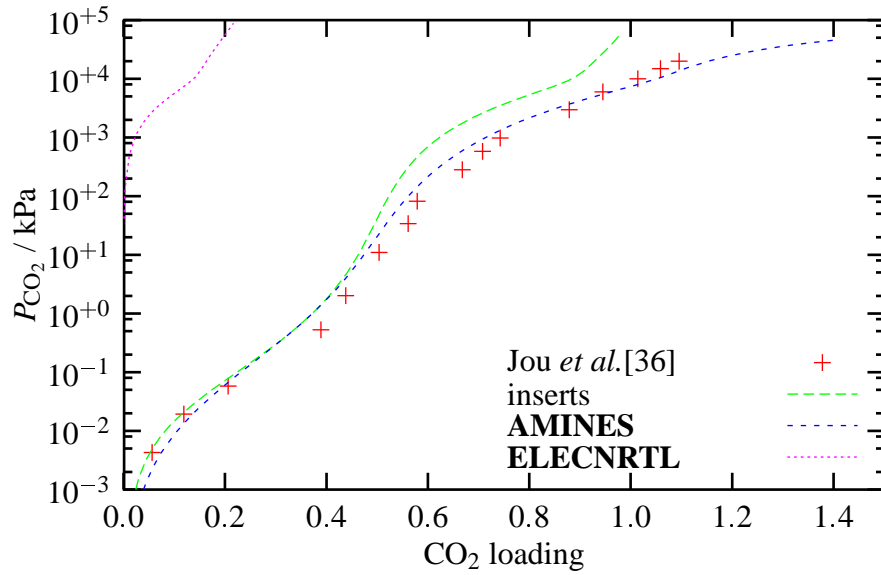


Figure D.4: Comparison of calculated VLE with experimental values at 60°C

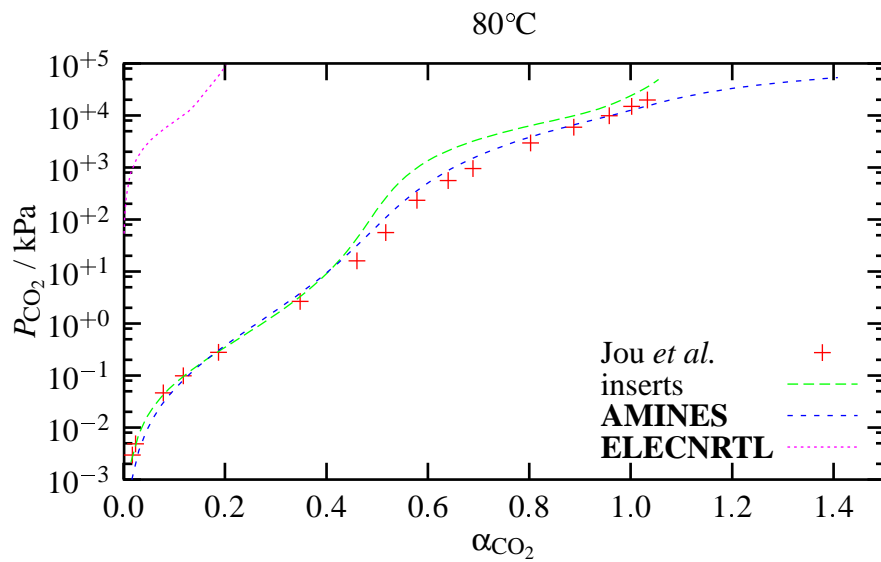


Figure D.5: Comparison of calculated VLE with experimental values at 80°C

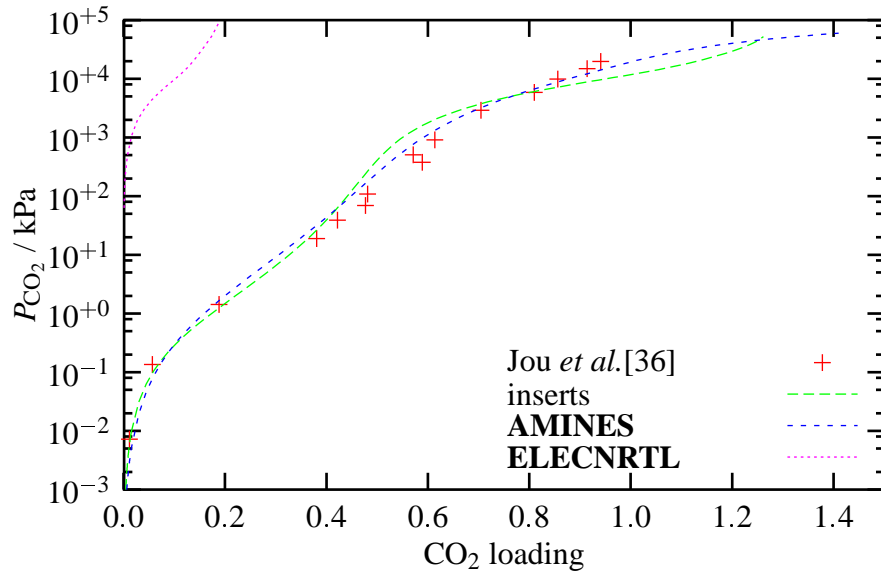


Figure D.6: Comparison of calculated VLE with experimental values at 100°C

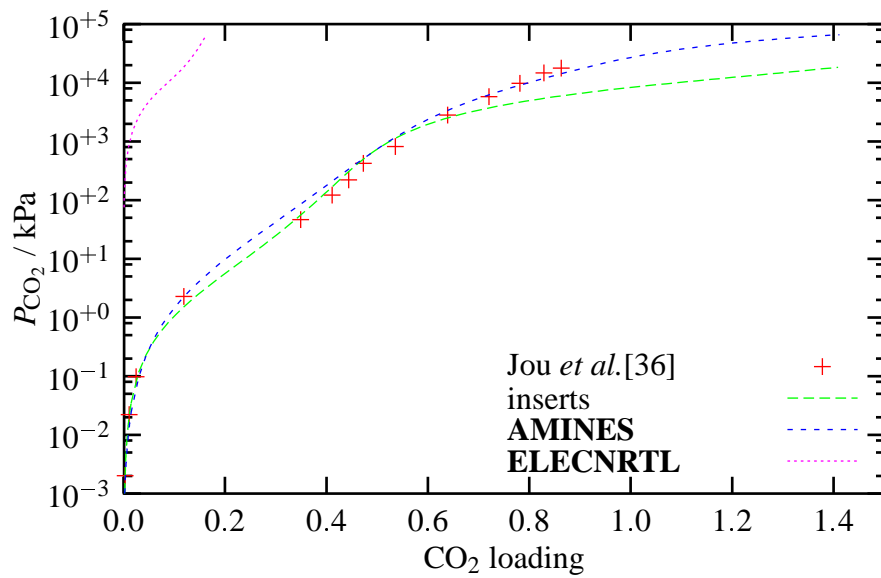


Figure D.7: Comparison of calculated VLE with experimental values at 120°C

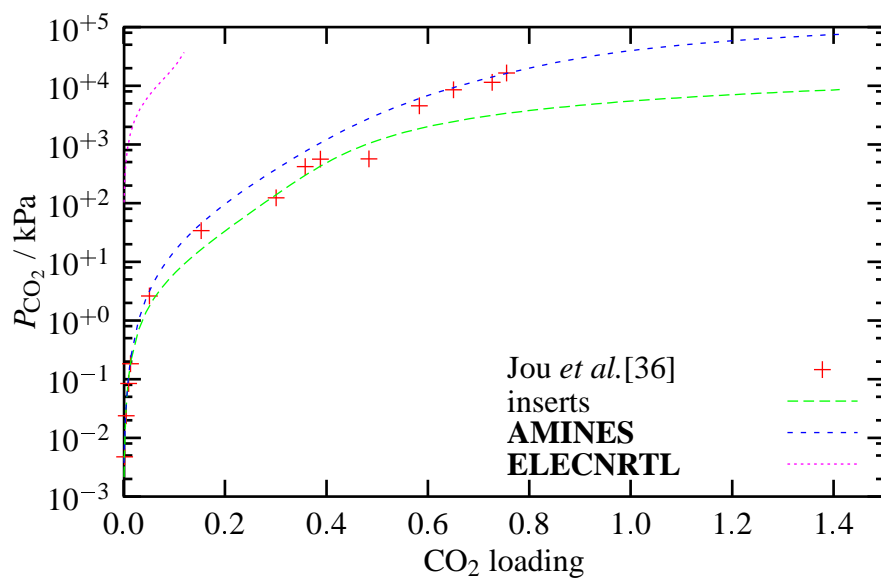


Figure D.8: Comparison of calculated VLE with experimental values at 150°C

Appendix E

Aspen Plus Input file for Power Plant With Integrated MEA Absorption

```
; File:  plant_w_capture_w_steam_extract.inp
; -----
; This file simulates the part-load performance of a nominal 500 MW
; power plant with CO2 capture.  Steam is extracted from the IP/LP
; crossover pipe to supply the stripper reboiler.

;-----
; Report options
;-----
STREAM-REPOR MOLEFLOW MASSFLOW PROPERTIES=ALL-SUBS CPCVMX

;-----
; Diagnostic specifications
;-----
DIAGNOSTICS
    HISTORY SIM-LEVEL=4 CONV-LEVEL=4
    MAX-PRINT SIM-LIMIT=9999

; This paragraph specifies time and error limits.
RUN-CONTROL MAX-TIME=84600 MAX-ERRORS=1000

; This paragraph will cause AspenPlus to include FORTRAN tracebacks in the
; history file.
SYS-OPTIONS TRACE=YES
```

```

;-----
; Units
;-----
IN-UNITS  ENG  POWER=KW
OUT-UNITS  SI  PRESSURE=kPa  TEMPERATURE=C  PDROP=kPa

;-----
; Components
;-----

COMPONENTS
; The property inserts component list contains:  H2O, MEA, H2S, CO2, N2,
; HCO3-, MEACOO-, MEA+, CO32-, HS-, S2-, H3O+, and OH-.  All other
; components need to be listed below:

; These components are involved in coal combustion.
; different types of coal
COAL-IEA /
COAL-PRB /
COAL-USL /
ASH /

; elements contained within coal
C      C /
H2     H2 /
CL2    CL2 /
HCL    HCL /
S      S /
;      H2O    H2O /

; components of air
;      N2     N2 /
O2     O2 /
AR     AR /
NE     NE /
HE     HE-4 /
CH4    CH4 /
KR     KR /
XE     XE /

; combustion products
CO     CO /

```

```

;      CO2      CO2 /
      NO       NO /
      NO2      NO2 /
      SO2      O2S /
      SO3      O3S

```

```

; This paragraph specifies the physical property method and model for each
; non-conventional component.

```

```

NC-COMPS COAL-IEA ULTANAL SULFANAL PROXANAL
NC-PROPS COAL-IEA ENTHALPY HCOALGEN 6 1 1 1 / DENSITY DCOALIGT

```

```

NC-COMPS COAL-PRB ULTANAL SULFANAL PROXANAL
NC-PROPS COAL-PRB ENTHALPY HCOALGEN 6 1 1 1 / DENSITY DCOALIGT

```

```

NC-COMPS COAL-USL ULTANAL SULFANAL PROXANAL
NC-PROPS COAL-USL ENTHALPY HCOALGEN 6 1 1 1 / DENSITY DCOALIGT

```

```

NC-COMPS ASH PROXANAL ULTANAL SULFANAL
NC-PROPS ASH ENTHALPY HCOALGEN / DENSITY DCOALIGT

```

```

;-----
; Properties
;-----

```

```

; This insert specifies property method and data for aqueous MEA-CO2 system.
; ELECNRTL becomes the default property method...
INSERT MEA CEMEA H2O MEA H2S CO2 N2 NO

```

```

; Specify the property method to use in each section.
PROPERTIES PR-BM COAL
PROPERTIES STEAM-TA HP IP LP FPT FWP CNDR

```

```

; This section specifies which databanks to use.
DATABANKS PURE11 / AQUEOUS / SOLIDS / INORGANIC / NOASPENPCD
PROP-SOURCES PURE11 / AQUEOUS / SOLIDS / INORGANIC

```

```

PROP-SET ALL-SUBS VOLFLMX MASSVFRA MASSSFRA RHOMX MASSFLOW &
      TEMP PRES UNITS='lb/cuft' SUBSTREAM=ALL
; "Entire Stream Flows, Density, Phase Frac, T, P"

```

```

; This paragraph specifies the gross calorific value for each type of

```

```

; coal (Btu/lb) on a dry, mineral-matter free basis.
PROP-DATA HEAT
    IN-UNITS SI MASS-ENTHALPY="KJ/KG"
    PROP-LIST HCOMB
    PVAL COAL-IEA 27060      ; 11632
    PVAL COAL-PRB 27637      ; 11880
    PVAL COAL-USL 31768      ; 13656

PROP-SET VFLOW VOLFLMX

PROP-SET LPHASE MUMX RHOMX SIGMAMX VOLFLMX MASSFLMX PHASE=L &
    UNITS='KG/CUM' 'DYNE/CM'

PROP-SET VPHASE RHOMX VOLFLMX MASSFLMX PHASE=V UNITS='KG/CUM'

PROP-SET CPCVMX CPCVMX

DEF-STREAMS MIXCINC COAL
DEF-STREAMS CONVEN HP IP LP FPT FWP CNDR MEA

;=====
; BEGIN:  flowsheet specification
;=====

; some globally defined blocks and streams
FLWSHEET GLOBAL
    BLOCK "SHAFT"    IN="W_HP" "W_IP" "W_LP" OUT="P_INTERN"

; globally defined streams
DEF-STREAMS WORK "P_INTERN"

; globally defined blocks
BLOCK SHAFT MIXER

;*****
;
;                               COAL COMBUSTION
;*****

;-----
; Flowsheet
;-----

```

```

FLOWSHEET COAL
  BLOCK DECOMP          IN=COAL-IN          OUT=COAL-OUT "Q_DECOMP"
  BLOCK BURN            IN=COAL-OUT AIR "Q_DECOMP" OUT=IN-BURN
  BLOCK HTRANS         IN=IN-BURN          OUT=EXHAUST "Q_FURN"
  BLOCK SEPARATE       IN=EXHAUST          OUT=FLUE-AHT SOLIDS
  BLOCK AIR-HEAT       IN=FLUE-AHT         OUT=FLUE-SCR
  BLOCK SCRUB1         IN=FLUE-SCR         OUT=WASTE1 IN-SCRUB
  BLOCK SCRUB2         IN=IN-SCRUB         OUT=FLUE-GAS WASTE2

```

```

;-----
; Stream Specification
;-----

```

```

; specify the heat and work streams in the flowsheet
DEF-STREAMS HEAT "Q_DECOMP" "Q_FURN"

```

```

; The composition of air is taken from Cooper et al., p 653.

```

```

STREAM AIR TEMP=519 <F> PRES=101.3 <KPA> MOLE-FLOW=1.0
  MOLE-FRAC H2 .000050 / N2 78.090 / O2 20.940 / AR .930 /
  CO2 .0360 / NE .00180 / HE .000520 / CH4 .000170 /
  KR .00010 / NO2 .000030 / XE 8.0000E-06

```

```

STREAM COAL-IN

```

```

  SUBSTREAM NC TEMP=160 <F> PRES=101.30 <KPA> MASS-FLOW=10 <KG/SEC>
  MASS-FRAC COAL-IEA 0.0 / COAL-PRB 0.5 / COAL-USL 0.5

```

```

; PROXANAL          ULTANAL
; water, moisture-included basis    ash (dry-basis)
; fixed carbon (dry-basis)          carbon (dry-basis)
; volatile matter (dry-basis)       hydrogen (dry-basis)
; ash (dry-basis)                   nitrogen (dry-basis)
;                                     chlorine (dry-basis)
;                                     sulfur (dry-basis)
;                                     oxygen (dry-basis)

```

```

; IEA tech specs coal...

```

```

  COMP-ATTR COAL-IEA ULTANAL ( 13.48 71.38 4.85 1.56 0.026 0.952 7.79 )
  COMP-ATTR COAL-IEA PROXANAL ( 9.50 86.52 0.0 13.48 )
  COMP-ATTR COAL-IEA SULFANAL ( 0.0 100 0.0 )

```

```

; Powder River basin coal

```

```

  COMP-ATTR COAL-PRB ULTANAL ( 7.1 69.4 4.9 1.0 0.000 0.4 17.2 )

```

```

COMP-ATTR COAL-PRB PROXANAL ( 28.1 49.95 42.92 7.13 )
COMP-ATTR COAL-PRB SULFANAL ( 0.0 100 0.0 )

; US low-sulphur coal
COMP-ATTR COAL-USL ULTANAL ( 10.4 77.2 4.9 1.5 0.000 1.0 5.0 )
COMP-ATTR COAL-USL PROXANAL ( 7.5 55.95 33.69 10.36 )
COMP-ATTR COAL-USL SULFANAL ( 0.0 100 0.0 )

;-----
; Block Section
;-----

BLOCK DECOMP RYIELD
  PARAM TEMP=298.15 <K> PRES=0.0
  MASS-YIELD MIXED H2O .30 / NC ASH .10 / CISOLID C .10 / MIXED H2 .10 /
  N2 .10 / CL2 .10 / S .10 / O2 .10

  COMP-ATTR NC ASH PROXANAL ( 0.0 0.0 0.0 100 )
  COMP-ATTR NC ASH ULTANAL ( 100 0.0 0.0 0.0 0.0 0.0 0.0 )
  COMP-ATTR NC ASH SULFANAL ( 0.0 0.0 0.0 )

; This block decomposes the coal into a stream of its component elements.
CALCULATOR COAL-DEC
  DEFINE XC BLOCK-VAR BLOCK=DECOMP VARIABLE=YIELD SENTENCE=MASS-YIELD &
    ID1=CISOLID ID2=C
  DEFINE XH2 BLOCK-VAR BLOCK=DECOMP VARIABLE=YIELD SENTENCE=MASS-YIELD &
    ID1=MIXED ID2=H2
  DEFINE XN2 BLOCK-VAR BLOCK=DECOMP VARIABLE=YIELD SENTENCE=MASS-YIELD &
    ID1=MIXED ID2=N2
  DEFINE XCL2 BLOCK-VAR BLOCK=DECOMP VARIABLE=YIELD SENTENCE=MASS-YIELD &
    ID1=MIXED ID2=CL2
  DEFINE XS BLOCK-VAR BLOCK=DECOMP VARIABLE=YIELD SENTENCE=MASS-YIELD &
    ID1=MIXED ID2=S
  DEFINE XO2 BLOCK-VAR BLOCK=DECOMP VARIABLE=YIELD SENTENCE=MASS-YIELD &
    ID1=MIXED ID2=O2
  DEFINE XASH BLOCK-VAR BLOCK=DECOMP VARIABLE=YIELD SENTENCE=MASS-YIELD &
    ID1=NC ID2=ASH
  DEFINE XH2O BLOCK-VAR BLOCK=DECOMP VARIABLE=YIELD SENTENCE=MASS-YIELD &
    ID1=MIXED ID2=H2O

  DEFINE CIEA MASS-FLOW STREAM=COAL-IN SUBSTREAM=NC COMPONENT=COAL-IEA
  DEFINE CPRB MASS-FLOW STREAM=COAL-IN SUBSTREAM=NC COMPONENT=COAL-PRB

```

```

DEFINE CUSL MASS-FLOW STREAM=COAL-IN SUBSTREAM=NC COMPONENT=COAL-USL

; ultimate analyses of the three coals
VECTOR-DEF UIEA COMP-ATTR STREAM=COAL-IN SUBSTREAM=NC &
    COMPONENT=COAL-IEA ATTRIBUTE=ULTANAL
VECTOR-DEF UPRB COMP-ATTR STREAM=COAL-IN SUBSTREAM=NC &
    COMPONENT=COAL-PRB ATTRIBUTE=ULTANAL
VECTOR-DEF UUSL COMP-ATTR STREAM=COAL-IN SUBSTREAM=NC &
    COMPONENT=COAL-USL ATTRIBUTE=ULTANAL

; proximate analyses of the three coals
VECTOR-DEF PIEA COMP-ATTR STREAM=COAL-IN SUBSTREAM=NC &
    COMPONENT=COAL-IEA ATTRIBUTE=PROXANAL
VECTOR-DEF PPRB COMP-ATTR STREAM=COAL-IN SUBSTREAM=NC &
    COMPONENT=COAL-PRB ATTRIBUTE=PROXANAL
VECTOR-DEF PUSL COMP-ATTR STREAM=COAL-IN SUBSTREAM=NC &
    COMPONENT=COAL-USL ATTRIBUTE=PROXANAL

; Stupid fucking Aspen Plus fortran interpreter can't handle lines >
; 72 characters so I have to break up the arithmetic into bite-sized pieces...

; COAL => total coal mass flowrate
F      COAL = CIEA + CPRB + CUSL

; THE VECTOR U___ CONTAINS THE MASS FRACTIONS OF THE COAL CONSTITUENTS
; ON A DRY-BASIS WHEREAS THE COAL FLOW RATE ON A WET-BASIS.  THE factor
; DRY___ is used to make this conversion.
;
; DRY___ => coal "dry" fraction (i.e. 1 - moisture fraction)
; P___(1) => coal moisture content, wt%
F      DRYIEA = (100 - PIEA(1)) / 100
F      DRYPRB = (100 - PPRB(1)) / 100
F      DRYUSL = (100 - PUSL(1)) / 100

F      ASH1 = (UIEA(1) / 100) * DRYIEA * CIEA
F      ASH2 = (UPRB(1) / 100) * DRYPRB * CPRB
F      ASH3 = (UUSL(1) / 100) * DRYUSL * CUSL
F      XASH = (ASH1 + ASH2 + ASH3) / COAL

F      C1 = (UIEA(2) / 100) * DRYIEA * CIEA
F      C2 = (UPRB(2) / 100) * DRYPRB * CPRB
F      C3 = (UUSL(2) / 100) * DRYUSL * CUSL

```



```

F      XC = (C1 + C2 + C3) / COAL

F      HYDRO1 = (UIEA(3) / 100) * DRYIEA * CIEA
F      HYDRO2 = (UPRB(3) / 100) * DRYPRB * CPRB
F      HYDRO3 = (UUSL(3) / 100) * DRYUSL * CUSL
F      XH2 = (HYDRO1 + HYDRO2 + HYDRO3) / COAL

F      FITRO1 = (UIEA(4) / 100) * DRYIEA * CIEA
F      FITRO2 = (UPRB(4) / 100) * DRYPRB * CPRB
F      FITRO3 = (UUSL(4) / 100) * DRYUSL * CUSL
F      XN2 = (FITRO1 + FITRO2 + FITRO3) / COAL

F      CHLOR1 = (UIEA(5) / 100) * DRYIEA * CIEA
F      CHLOR2 = (UPRB(5) / 100) * DRYPRB * CPRB
F      CHLOR3 = (UUSL(5) / 100) * DRYUSL * CUSL
F      XCL2 = (CHLOR1 + CHLOR2 + CHLOR3) / COAL

F      SULFR1 = (UIEA(6) / 100) * DRYIEA * CIEA
F      SULFR2 = (UPRB(6) / 100) * DRYPRB * CPRB
F      SULFR3 = (UUSL(6) / 100) * DRYUSL * CUSL
F      XS = (SULFR1 + SULFR2 + SULFR3) / COAL

F      OXYGN1 = (UIEA(7) / 100) * DRYIEA * CIEA
F      OXYGN2 = (UPRB(7) / 100) * DRYPRB * CPRB
F      OXYGN3 = (UUSL(7) / 100) * DRYUSL * CUSL
F      XO2 = (OXYGN1 + OXYGN2 + OXYGN3) / COAL

F      XH2O=(PIEA(1)*CIEA+PPRB(1)*CPRB+PUSL(1)*CUSL)/(COAL*100)

C      WRITE(NRPT, *) XH2O
C      WRITE(NRPT, *) XH2
C      WRITE(NRPT, *) XN2
C      WRITE(NRPT, *) XCL2
C      WRITE(NRPT, *) XS
C      WRITE(NRPT, *) XO2
C      WRITE(NRPT, *) XC
C      WRITE(NRPT, *) XASH

```

EXECUTE BEFORE BLOCK DECOMP

BLOCK BURN RGIBBS

PARAM PRES=101.3 <kPa>

```

PROD H2O / C SS / H2 / N2 / CL2 / HCL / S / O2 / AR /
      CO / CO2 / NE / HE / CH4 / KR / XE / NO /
      NO2 / SO2 / SO3

```

```

; This block adjusts the air flow rate such that there is 20 mol %
; excess oxygen present during the coal combustion.

```

```

CALCULATOR AIR-FLOW

```

```

  DEFINE AIR STREAM-VAR STREAM=AIR SUBSTREAM=MIXED VARIABLE=MOLE-FLOW
  DEFINE O2COAL MOLE-FLOW STREAM=COAL-OUT SUBSTREAM=MIXED COMPONENT=O2
  DEFINE C MOLE-FLOW STREAM=COAL-OUT SUBSTREAM=CISOLID COMPONENT=C
  DEFINE N2 MOLE-FLOW STREAM=COAL-OUT SUBSTREAM=MIXED COMPONENT=N2
  DEFINE H2 MOLE-FLOW STREAM=COAL-OUT SUBSTREAM=MIXED COMPONENT=H2
  DEFINE S MOLE-FLOW STREAM=COAL-OUT SUBSTREAM=MIXED COMPONENT=S

```

```

F      XS = 0.21

```

```

; CMIXED IS THE MOLE FLOW OF CARBON IN THE COAL-OUT MIXED SUBSTREAM

```

```

F      AIR = ((C + 2*N2 + 0.5*H2 + S)* (1 + XS) - O2COAL) / 0.2094

```

```

EXECUTE BEFORE BLOCK BURN

```

```

BLOCK HTRANS HEATER

```

```

  PARAM TEMP=320 <C> PRES=0.0 NPHASE=2 ; Neill and Gunter

```

```

;      PARAM TEMP=622 <F> PRES=0.0 NPHASE=2 ; Boiler design data

```

```

BLOCK SEPARATE SSPLIT

```

```

  FRAC MIXED FLUE-AHT 1.0

```

```

  FRAC CISOLID FLUE-AHT 0.0

```

```

  FRAC NC FLUE-AHT 0.0

```

```

; The air heater outlet temperature is taken from the Neil and Gunter

```

```

; study.

```

```

BLOCK AIR-HEAT HEATER

```

```

;      PARAM TEMP=134 <C>

```

```

      PARAM TEMP=247 <F>

```

```

BLOCK SCRUB1 SEP2

```

```

  FRAC STREAM=IN-SCRUB COMPS=N2 CO2 H2O FRACS=1 1 1

```

```

  FRAC STREAM=WASTE1 COMPS=H2 S O2 AR NE HE KR XE CO NO NO2 SO2 SO3 &

```

```

      FRACS= 1 1 1 1 1 1 1 1 1 1 1 1 1

```

```

BLOCK SCRUB2 FLASH2

```

```

  PARAM TEMP=40 <C> PRES=0

```

BLOCK CLCHNG1 CLCHNG

```
;*****  
;  
;                               HP turbine and FWP A  
;*****
```

```
;------  
; Flowsheet  
;------
```

FLWSHEET HP

BLOCK BOIL	IN=H2O-BOIL	OUT="ST_MAIN" "Q_BOIL"
BLOCK "HP_SEP1"	IN="ST_MAIN"	OUT=ST-FPT1 ST-HPX
BLOCK VALVE1	IN=ST-HPX	OUT=ST-HP
BLOCK HP1	IN=ST-HP	OUT="HP_1X" "W_HP"
BLOCK "HP_SEP2"	IN="HP_1X"	OUT=ST-REHT ST-FWPA
BLOCK REHT	IN=ST-REHT	OUT=ST-IPX "Q_REHT"

```
;------  
; Streams  
;------
```

; specify the heat and work streams in the flowsheet

DEF-STREAMS HEAT "Q_BOIL" "Q_REHT"

DEF-STREAMS WORK "W_HP"

STREAM H2O-BOIL TEMP=487.91 PRES=2700 MASS-FLOW=3358670
MOLE-FRAC H2O 1

```
;------  
; Blocks  
;------
```

BLOCK VALVE1 VALVE

PARAM P-OUT=2236.19

; This design spec maintains constant volumetric flow rate into HP section

DESIGN-SPEC PRESOUT1

DEFINE F STREAM-PROP STREAM=ST-HP PROPERTY=VFLOW

SPEC "F" TO "1.155e6"

TOL-SPEC "0.001e6"

```

; NB: @ 50% plant load, the ST-HP pressure is 1080.68 psia
VARY BLOCK-VAR BLOCK=VALVE1 SENTENCE=PARAM VARIABLE=P-OUT
LIMITS "900" "2365"

BLOCK "HP_SEP1" FSPLIT
    MASS-FLOW ST-FPT1 7000

BLOCK "HP_SEP2" FSPLIT
    MASS-FLOW ST-FWPA 334659

CALCULATOR "C_HP_SEP"
    DESCRIPTION "Specify steam extracted for FW preheating from HP section"

    DEFINE FREF STREAM-VAR STREAM=ST-HP VARIABLE=MASS-FLOW
    DEFINE FA BLOCK-VAR BLOCK="HP_SEP2" SENTENCE=MASS-FLOW VARIABLE=FLOW &
        ID1=ST-FWPA

F    FA = 0.1231 * FREF - 0.7894e5

    READ-VARS FREF
    WRITE-VARS FA

BLOCK REHT HEATER
    PARAM TEMP=1000

; This design spec maintains outlet temperature of 1000 F from VALVE2
DESIGN-SPEC TEMPOUT
    DEFINE T STREAM-VAR STREAM=ST-IP VARIABLE=TEMP

    SPEC "T" TO "1000"
    TOL-SPEC "0.5"

    VARY BLOCK-VAR BLOCK=REHT SENTENCE=PARAM VARIABLE=TEMP
    LIMITS "1000" "1100"

BLOCK BOIL HEATER
    PARAM TEMP=1000 PRES=2365

BLOCK HP1 COMPR
    PARAM TYPE=ISENTROPIC PRATIO=0.282 SEFF=0.904

```

```

CALCULATOR "C_HP1_P"
    DESCRIPTION "Specify the pressure ratio of HP1"

    DEFINE FLOW STREAM-VAR STREAM=ST-HP VARIABLE=MASS-FLOW
    DEFINE PRATIO BLOCK-VAR BLOCK=HP1 SENTENCE=PARAM VARIABLE=PRATIO

F    PRATIO = -0.4820e-02 * (FLOW/1E6) + 0.2944

    EXECUTE BEFORE HP1

;*****
;
;           IP turbine and FWP B, C, and D
;*****

;-----
; Flowsheet
;-----

FLOWSHEET IP
    BLOCK VALVE2      IN=ST-IPX           OUT=ST-IP
    BLOCK "IP_SEP1"  IN=ST-IP           OUT="IP_02" "IP_03"
    BLOCK IP2        IN="IP_02"         OUT="IP_2X" "W_IP2"
    BLOCK "IP_SEP2"  IN="IP_2X"         OUT=ST-FWPC "IP_12"
    BLOCK IP1        IN="IP_12"         OUT=IP-1LP "W_IP1"
    BLOCK IP3        IN="IP_03"         OUT="IP_3X1" "W_IP3"
    BLOCK "IP_SEP3"  IN="IP_3X1"        OUT="IP_3X2" "IP_34"
    BLOCK IP4        IN="IP_34"         OUT="IP_4X" "W_IP4"
    BLOCK "IP_SEP4"  IN="IP_3X2"        OUT="ST-FPT2" "ST-FWPB"
    BLOCK "IP_SEP5"  IN="IP_4X"         OUT=IP-4LP ST-FWPD
    BLOCK "IP_COMB"  IN=IP-1LP IP-4LP    OUT=ST-LPX
    BLOCK EXTRACT    IN=ST-LPX          OUT=ST-REB ST-LP
    BLOCK "IP_SHAFT" IN="W_IP1" "W_IP2" "W_IP3" "W_IP4" OUT="W_IP"

;-----
; Streams
;-----
DEF-STREAMS WORK "W_IP1" "W_IP2" "W_IP3" "W_IP4" "W_IP"

;-----
; Blocks
;-----

```

```

BLOCK VALVE2 VALVE
    PARAM P-OUT=560.18

DESIGN-SPEC PRESOUT2
    DEFINE F STREAM-PROP STREAM=ST-IP PROPERTY=VFLOW

    SPEC "F" TO "4.531e6"
    TOL-SPEC "0.009e6"

    ; NB: @ 50% plant load, the ST-IP pressure is 260 psia
    VARY BLOCK-VAR BLOCK=VALVE2 SENTENCE=PARAM VARIABLE=P-OUT
    LIMITS "250" "600"

BLOCK "IP_COMB" MIXER

BLOCK "IP_SEP1" FSPLIT
    FRAC "IP_02" 0.50

BLOCK "IP_SEP2" FSPLIT
    MASS-FLOW "ST-FWPC" 128853

BLOCK "IP_SEP3" FSPLIT
    MASS-FLOW "IP_3X2" 227662 ;sum of ST-FWPB and ST-FPT2

BLOCK "IP_SEP4" FSPLIT
    MASS-FLOW ST-FWPB 143920

BLOCK "IP_SEP5" FSPLIT
    MASS-FLOW ST-FWPD 136359

BLOCK EXTRACT FSPLIT
    FRAC ST-REB 0.00

CALCULATOR "C_IP_SEP"
    DESCRIPTION "Specify steam extracted for FW preheating from IP section"

    DEFINE FREF STREAM-VAR STREAM=ST-IP VARIABLE=MASS-FLOW

    DEFINE FBP BLOCK-VAR BLOCK="IP_SEP3" SENTENCE=MASS-FLOW VARIABLE=FLOW &
        ID1="IP_3X2"
    DEFINE FB BLOCK-VAR BLOCK="IP_SEP4" SENTENCE=MASS-FLOW VARIABLE=FLOW &
        ID1=ST-FWPB

```

```

DEFINE FD BLOCK-VAR BLOCK="IP_SEP5" SENTENCE=MASS-FLOW VARIABLE=FLOW &
    ID1=ST-FWPD

F      FB = 0.5389e-1 * FREF - 0.1685e5
F      FP = 0.2684e-1 * FREF + 0.1948e4
F      FBP = FB + FP
F      FC = 0.5095e-1 * FREF - 0.2440e5
F      FD = 0.5236e-1 * FREF - 0.2077e5

READ-VARS FREF
WRITE-VARS FB FBP FD

DESIGN-SPEC "C_IPSEP2"
    DEFINE Q BLOCK-VAR BLOCK="FWP_C-C" SENTENCE=RESULTS VARIABLE=NET-DUTY

    SPEC "Q" TO "0"
    TOL-SPEC "1e4"

    VARY BLOCK-VAR BLOCK="IP_SEP2" SENTENCE=MASS-FLOW VARIABLE=FLOW &
        ID1=ST-FWPC
    LIMITS "50000" "150000"

BLOCK IP1 COMPR
    PARAM TYPE=ISENTROPIC PRATIO=0.517 SEFF=0.902 NPHASE=2

BLOCK IP2 COMPR
    PARAM TYPE=ISENTROPIC PRATIO=0.233 SEFF=0.910 NPHASE=2

BLOCK IP3 COMPR
    PARAM TYPE=ISENTROPIC PRATIO=0.455 SEFF=0.895 NPHASE=2

BLOCK IP4 COMPR
    PARAM TYPE=ISENTROPIC PRATIO=0.265 SEFF=0.914 NPHASE=2

BLOCK "IP_SHAFT" MIXER

;*****
;
;          LP turbine and FWP E, F, AND G
;*****
;-----

```

```

; Flowsheet
;-----

FLOWSHEET LP
    BLOCK "LP_SEP1" IN=ST-LP          OUT="LP_012" "LP_056"
    BLOCK "LP_SEP2" IN="LP_012"      OUT="LP_01" "LP_02"
    BLOCK LP1          IN="LP_01"     OUT=ST-FWPF "W_LP1"
    BLOCK LP2          IN="LP_02"     OUT="LP_2X" "W_LP2"
    BLOCK "LP_SEP3"   IN="LP_2X"     OUT="LP_23" ST-2FWPG
    BLOCK LP3          IN="LP_23"     OUT="LP_3CR" "W_LP3"
    BLOCK "LP_SEP4"   IN="LP_056"     OUT="LP_05" "LP_06"
    BLOCK LP6          IN="LP_06"     OUT=ST-FWPE "W_LP6"
    BLOCK LP5          IN="LP_05"     OUT="LP_5X" "W_LP5"
    BLOCK "LP_SEP5"   IN="LP_5X"     OUT="LP_45" ST-5FWPG
    BLOCK LP4          IN="LP_45"     OUT="LP_4CR" "W_LP4"
    BLOCK "LP_COMB1"          IN="LP_3CR" "LP_4CR" OUT=ST-CNDR
    BLOCK "LP_COMB2"          IN=ST-2FWPG ST-5FWPG OUT=ST-FWPG
    BLOCK "LP_SHAFT"         IN="W_LP1" "W_LP2" "W_LP3" "W_LP4" &
        "W_LP5" "W_LP6" OUT="W_LP"
;-----
; Streams
;-----

DEF-STREAMS WORK "W_LP1" "W_LP2" "W_LP3" "W_LP4" "W_LP5" "W_LP6" "W_LP"

; specify the material streams in the flowsheet

;-----
; Blocks
;-----

BLOCK "LP_COMB1" MIXER

BLOCK "LP_COMB2" MIXER

BLOCK "LP_SEP1" FSPLIT
    FRAC "LP_012" 0.50

BLOCK "LP_SEP2" FSPLIT
    MASS-FLOW "LP_01" 89306 ; flow of ST-FWPF

BLOCK "LP_SEP3" FSPLIT

```



```

        MASS-FLOW "ST-2FWPG" 63085 ; half of ST-FWPG

BLOCK "LP_SEP4" FSPLIT
        MASS-FLOW "LP_06" 135578 ; flow of ST-FWPE

BLOCK "LP_SEP5" FSPLIT
        MASS-FLOW "ST-5FWPG" 63086 ; other half of ST-FWPG

CALCULATOR "C_LP_SEP"
        DESCRIPTION "Specify steam extracted for FW preheating from LP section"

        DEFINE FREF STREAM-VAR STREAM=ST-LP VARIABLE=MASS-FLOW

        DEFINE FE BLOCK-VAR BLOCK="LP_SEP4" SENTENCE=MASS-FLOW VARIABLE=FLOW &
                ID1="LP_06"
        DEFINE FF BLOCK-VAR BLOCK="LP_SEP2" SENTENCE=MASS-FLOW VARIABLE=FLOW &
                ID1="LP_01"
        DEFINE FG2 BLOCK-VAR BLOCK="LP_SEP3" SENTENCE=MASS-FLOW VARIABLE=FLOW &
                ID1=ST-2FWPG
        DEFINE FG5 BLOCK-VAR BLOCK="LP_SEP5" SENTENCE=MASS-FLOW VARIABLE=FLOW &
                ID1=ST-5FWPG

F        FE = 0.6311e-1 * FREF - 0.2228e5
F        FF = 0.4162e-1 * FREF - 0.1475e5
F        FG = 0.6170e-1 * FREF - 0.2538e5
F        FG2 = FG / 2
F        FG5 = FG2

        READ-VARS FREF
        WRITE-VARS FE FF FG2 FG5

BLOCK LP1 COMPR
        PARAM TYPE=ISENTROPIC PRATIO=0.151 SEFF=0.910 NPHASE=2

BLOCK LP2 COMPR
        PARAM TYPE=ISENTROPIC PRATIO=0.068 SEFF=0.907 NPHASE=2

BLOCK LP3 COMPR
        PARAM TYPE=ISENTROPIC PRES=0.686 SEFF=0.640 NPHASE=2

BLOCK LP4 COMPR
        PARAM TYPE=ISENTROPIC PRES=0.686 SEFF=0.640 NPHASE=2

```

```

CALCULATOR "C_LP_P"
    DESCRIPTION "Set the outlet P of LP3 and LP4 equal to the condenser"
    DEFINE PCOND BLOCK-VAR BLOCK=CONDENSE SENTENCE=PARAM VARIABLE=PRES
    DEFINE PLP3 BLOCK-VAR BLOCK=LP3 SENTENCE=PARAM VARIABLE=PRES
    DEFINE PLP4 BLOCK-VAR BLOCK=LP4 SENTENCE=PARAM VARIABLE=PRES

F    PLP3 = PCOND
F    PLP4 = PCOND

    EXECUTE BEFORE LP3

CALCULATOR "C_LP_EFF"
    DESCRIPTION "Use correlation to set LP3 and LP4 isentropic efficiency"

    DEFINE QOUT STREAM-PROP STREAM=ST-CNDR PROPERTY=VFLOW
    DEFINE SEFF3 BLOCK-VAR BLOCK=LP3 SENTENCE=PARAM VARIABLE=SEFF
    DEFINE SEFF4 BLOCK-VAR BLOCK=LP4 SENTENCE=PARAM VARIABLE=SEFF

F    ETA = -0.4016 * (QOUT/1e9) + 0.9867
F    SEFF3 = ETA
F    SEFF4 = ETA

    EXECUTE BEFORE CONDENSE
    READ-VARS QOUT
C    WRITE-VARS SEFF3 SEFF4

BLOCK LP5 COMPR
    PARAM TYPE=ISENTROPIC PRATIO=0.068 SEFF=0.907 NPHASE=2

BLOCK LP6 COMPR
    PARAM TYPE=ISENTROPIC PRATIO=0.435 SEFF=0.901 NPHASE=2

BLOCK "LP_SHAFT" MIXER

;*****
;
;                               Feedwater pump turbine
;*****

;-----
; Flowsheet

```

```

;-----
FLOWSHEET FPT
    BLOCK FPT1      IN=ST-FPT1      OUT="FPT_1X" "W_FPT1"
    BLOCK "FPT_COMB"      IN=ST-FPT2 "FPT_1X"      OUT="FPT_12"
    BLOCK FPT2      IN="FPT_12"      OUT=STFPT-CN "W_FPT2"
    BLOCK "FP_SHAFT"      IN="W_FPT1" "W_FPT2"      OUT="W_FPT"

;-----
; Streams
;-----

DEF-STREAMS WORK "W_FPT1" "W_FPT2" "W_FPT"

;-----
; Blocks
;-----

BLOCK "FPT_COMB" MIXER

BLOCK FPT1 COMPR
    PARAM TYPE=ISENTROPIC PRES=100 SEFF=0.153 NPHASE=2

BLOCK FPT2 COMPR
    PARAM TYPE=ISENTROPIC PRES=0.686 SEFF=0.795 NPHASE=2

CALCULATOR "C_FPT_P"
    DESCRIPTION "Specifies the outlet pressure of FPT1 and FPT2"

    DEFINE PREF STREAM-VAR STREAM=ST-FPT2 VARIABLE=PRES
    DEFINE PCOND BLOCK-VAR BLOCK=CONDENSE SENTENCE=PARAM VARIABLE=PRES
    DEFINE PFPT1 BLOCK-VAR BLOCK=FPT1 SENTENCE=PARAM VARIABLE=PRES
    DEFINE PFPT2 BLOCK-VAR BLOCK=FPT2 SENTENCE=PARAM VARIABLE=PRES

F      PFTP1 = PREF
F      PFTP2 = PCOND

    READ-VARS PREF PCOND
    WRITE-VARS PFPT1 PFPT2

BLOCK "FP_SHAFT" MIXER

```

```

;*****
;
;                               Feed water preheater train
;*****

;-----
; Flowsheet
;-----

FLWSHEET FWP
    BLOCK "FWP_A-H" IN=ST-FWPA Q-FWPA          OUT="STFWP_AB"
    BLOCK "FWP_A-C" IN=H2O-FWPA          OUT=H2O-BOIL Q-FWPA

    BLOCK "FWP_B-H" IN=ST-FWPB "STFWP_AB" Q-FWPB      OUT="STFWP_BC"
    BLOCK "FWP_B-C" IN=H2O-FWPB          OUT=H2O-FWPA Q-FWPB

; dearator and pump
    BLOCK "FWP_C"      IN="STFWP_BC" ST-FWPC H2O-FWPC  OUT=H2-PUMP
    BLOCK FWPUMP2     IN=H2-PUMP "W_FPT"          OUT=IN-PUMP
    BLOCK "FWP_C-C"   IN=IN-PUMP          OUT=H2O-FWPB

    BLOCK "FWP_D-H"   IN=ST-FWPD Q-FWPD          OUT="STFWP_DE"
    BLOCK "FWP_D-C"   IN=H2O-FWPD H2O-REB        OUT=H2O-FWPC Q-FWPD

    BLOCK "FWP_E-H"   IN=ST-FWPE "STFWP_DE" Q-FWPE      OUT="STFWP_EF"
    BLOCK "FWP_E-C"   IN=H2O-FWPE          OUT=H2O-FWPD Q-FWPE

    BLOCK "FWP_F-H"   IN=ST-FWPF "STFWP_EF" Q-FWPF      OUT="STFWP_FG"
    BLOCK "FWP_F-C"   IN=H2O-FWPF          OUT=H2O-FWPE Q-FWPF

    BLOCK "FWP_G-H"   IN=ST-FWPG "STFWP_FG" Q-FWPG      OUT="STFWP_GC"
    BLOCK "FWP_G-C"   IN=H2O-FWPG          OUT=H2O-FWPF Q-FWPG

;-----
; Streams
;-----

; I need to define the heat streams in this flowsheet section
DEF-STREAMS HEAT Q-FWPA Q-FWPB Q-FWPD Q-FWPE Q-FWPF Q-FWPG

;-----
; Blocks
;-----

```

```

; feed water preheater "A"
BLOCK "FWP_A-H" HEATER
    PARAM PRES=0

BLOCK "FWP_A-C" HEATER
    PARAM TEMP=487.91

CALCULATOR "T_FWPA"
    DESCRIPTION "Calculate the cold-side outlet temperature for FWPA"

    DEFINE FFWPA STREAM-VAR STREAM=H2O-FWPA VARIABLE=MASS-FLOW
    DEFINE TFWPA BLOCK-VAR BLOCK="FWP_A-C" SENTENCE=PARAM VARIABLE=TEMP

F    TFWPA = 0.8546e2 * dlog(FFWPA) - 0.7963e3

    EXECUTE BEFORE "FWP_A-C"

; feed water preheater "B"
BLOCK "FWP_B-H" HEATER
    PARAM PRES=0

BLOCK "FWP_B-C" HEATER
    PARAM TEMP=400.56

CALCULATOR "T_FWPB"
    DESCRIPTION "Calculate the cold-side outlet temperature for FWPB"

    DEFINE FFWPB STREAM-VAR STREAM=H2O-FWPB VARIABLE=MASS-FLOW
    DEFINE TFWPB BLOCK-VAR BLOCK="FWP_B-C" SENTENCE=PARAM VARIABLE=TEMP

F    TFWPB = 0.6840e2 * dlog(FFWPB) - 0.6272e3

    EXECUTE BEFORE "FWP_B-C"

; feed water preheater "C" (dearator) and feed water pump
BLOCK "FWP_C" MIXER

BLOCK FWPUMP2 PUMP
;    PARAM PRES=2700

BLOCK "FWP_C-C" HEATER
    PARAM TEMP=351.19

```

```

CALCULATOR "T_FWPC"
  DESCRIPTION "Calculate the cold-side outlet temperature for FWPC"

  ; using the outlet mass flow rate is easier than having to sum
  ; the three input mass flow rates
  DEFINE FFWPC STREAM-VAR STREAM=IN-PUMP VARIABLE=MASS-FLOW
  DEFINE TFWPC BLOCK-VAR BLOCK="FWP_C-C" SENTENCE=PARAM VARIABLE=TEMP

F    TFWPC = 0.6468e2 * dlog(FFWPC) - 0.6212e3

  EXECUTE BEFORE "FWP_C-C"

; feed water preheater "D"
BLOCK "FWP_D-H" HEATER
  PARAM PRES=0

BLOCK "FWP_D-C" HEATER
  PARAM TEMP=293.20

CALCULATOR "T_FWPD"
  DESCRIPTION "Calculate the cold-side outlet temperature for FWPD"

  DEFINE FFWPD STREAM-VAR STREAM=H2O-FWPD VARIABLE=MASS-FLOW
  DEFINE FREB STREAM-VAR STREAM=H2O-REB VARIABLE=MASS-FLOW
  DEFINE TFWPD BLOCK-VAR BLOCK="FWP_D-C" SENTENCE=PARAM VARIABLE=TEMP

F    TFWPD = 0.5537e2 * dlog(FFWPD + FREB) - 0.5274e3

  EXECUTE BEFORE "FWP_D-C"

; feed water preheater "E"
BLOCK "FWP_E-H" HEATER
  PARAM PRES=0

BLOCK "FWP_E-C" HEATER
  PARAM TEMP=241.55

CALCULATOR "T_FWPE"
  DESCRIPTION "Calculate the cold-side outlet temperature for FWPE"

  DEFINE FFWPE STREAM-VAR STREAM=H2O-FWPE VARIABLE=MASS-FLOW

```

```

DEFINE TFWPE BLOCK-VAR BLOCK="FWP_E-C" SENTENCE=PARAM VARIABLE=TEMP
F      TFWPE = 0.4602e2 * dlog(FWPE) - 0.4405e3

EXECUTE BEFORE "FWP_E-C"

; feed water preheater "F"
BLOCK "FWP_F-H" HEATER
PARAM PRES=0

BLOCK "FWP_F-C" HEATER
PARAM TEMP=186.37

CALCULATOR "T_FWPF"
DESCRIPTION "Calculate the cold-side outlet temperature for FWPF"

DEFINE FFWPF STREAM-VAR STREAM=H2O-FWPF VARIABLE=MASS-FLOW
DEFINE TFWPF BLOCK-VAR BLOCK="FWP_F-C" SENTENCE=PARAM VARIABLE=TEMP
F      TFWPF = 0.3788e2 * dlog(FFWPF) - 0.3752e3

EXECUTE BEFORE "FWP_F-C"

; feed water preheater "G"
BLOCK "FWP_G-H" HEATER
PARAM PRES=0

BLOCK "FWP_G-C" HEATER
PARAM TEMP=150.01

CALCULATOR "T_FWPG"
DESCRIPTION "Calculate the cold-side outlet temperature for FWPG"

DEFINE FFWPG STREAM-VAR STREAM=H2O-FWPG VARIABLE=MASS-FLOW
DEFINE TFWPG BLOCK-VAR BLOCK="FWP_G-C" SENTENCE=PARAM VARIABLE=TEMP
F      TFWPG = 0.3033e2 * dlog(FFWPG) - 0.2996e3

EXECUTE BEFORE "FWP_G-C"

;*****
;
; Condensor specification

```

```

;*****
;-----
; Flowsheet
;-----

FLOWSHEET CNDR
      BLOCK "CND_COMB"          IN="STFWP_GC" ST-CNDR STFPT-CN  OUT=H2O-CNDR
      BLOCK CONDENSE  IN=H2O-CNDR      OUT=H2O-MAIN
      BLOCK FWPUMP1   IN=H2O-MAIN      OUT=H2O-FWPG

;-----
; Blocks
;-----

BLOCK "CND_COMB" MIXER

BLOCK CONDENSE HEATER
      PARAM VFRAC=0 PRES=0.688

BLOCK FWPUMP1 PUMP
      PARAM PRES=128

;*****
;
;           MEA Absorption specification
;*****
;-----
; Flowsheet
;-----

FLOWSHEET MEA
      BLOCK CLCHNG1   IN=FLUE-GAS          OUT=FLUE-BLO
      BLOCK BLOWER    IN=FLUE-BLO          OUT=FLUE-DCC "P_BLOW"
      BLOCK "H2O_PUMP" IN=H2O-PUMP          OUT=H2O-DCC P-H2OP
      BLOCK DCC        IN=FLUE-DCC H2O-DCC  OUT=FLUE-ABS H2O-OUT
      BLOCK ABSORBER   IN=FLUE-ABS LEAN-ABS  OUT=STACK RICH-PUM
      BLOCK "RICH_PUM" IN=RICH-PUM          OUT=RICH-HX P-RICHP
      BLOCK STRIPPER   IN=RICH-STR          OUT=CO2-COMP LEAN-HX
      BLOCK "CO2_COMP" IN=CO2-COMP          OUT=CO2 ST1 ST2 ST3 "P_COMP"
      BLOCK HEATX      IN=RICH-HX LEAN-HX    OUT=RICH-STR LEAN-MIX
      BLOCK MIXER      IN=MAKE-UP LEAN-MIX   OUT=LEAN-COO

```



```

        BLOCK COOLER      IN=LEAN-COO          OUT=LEAN-ABS
        BLOCK POWER      IN="P_BLOW" P-H2OP P-RICHP "P_COMP"   OUT="P_DEMAND"
        BLOCK REBOIL     IN=ST-REB           OUT=H2O-REB "Q_REB"

;-----
; Stream Specification
;-----

; specify the heat and work streams in the flowsheet
DEF-STREAMS WORK "P_BLOW" P-H2OP P-RICHP "P_COMP" "P_DEMAND"
DEF-STREAMS HEAT "Q_REB"

; Cooling water temperature for Lake Erie is not given. 12C is summer
; mean temperature form IEA technical specifications document...
STREAM H2O-PUMP TEMP=12 <C> PRES=101.3 <kPa>
      IN-UNITS SI PRESSURE=kPa TEMPERATURE=C PDROP=kPa
      MOLE-FLOW H2O 70

; The mole flow of H2O and MEA are adjusted by the calculator block C_MAEKUP
STREAM MAKE-UP TEMP=40 <C> PRES=101.3
      IN-UNITS SI PRESSURE=kPa TEMPERATURE=C PDROP=kPa
      MOLE-FLOW H2O 1 / MEA 1

; tear streams ...
; Note: 12.6 M MEA is 30 wt%
STREAM LEAN-ABS TEMP=40 <C> PRES=101.3 <kPa> MOLE-FLOW=87.1 <KMOL/SEC>
      MOLE-FRAC MEA 0.126 / H2O 0.874 / CO2 .0315

; Note: F is obtained from absorber results
STREAM LEAN-HX PRES=186 <kPa> VFRAC=0 MOLE-FLOW=87.1 <KMOL/SEC>
      IN-UNITS SI PRESSURE=kPa TEMPERATURE=C PDROP=kPa
      MOLE-FRAC MEA 0.126 / H2O 0.874 / CO2 .0315

;-----
; Block Specification
;-----

;<BLOWER>
BLOCK BLOWER COMPR
      PARAM TYPE=ISENTROPIC DELP=83.6 <kPa> SEFF=0.90
;</BLOWER>

```

```

;<H2O_PUMP>
BLOCK "H2O_PUMP" PUMP
    PARAM DELP=83.6 <kPa>
;</H2O_PUMP>

; This block cools the flue gas stream with water.
BLOCK DCC FLASH2
    IN-UNITS SI PRESSURE=kPa TEMPERATURE=C PDROP=kPa
    PARAM TEMP=40 PRES=0 <kPa>

;<ABSORBER>
BLOCK ABSORBER RATEFRAC
    IN-UNITS SI PRESSURE=kPa TEMPERATURE=C PDROP=kPa
    PARAM NCOL=1 TOT-SEGMENT=10 EQUILIBRIUM=NO &
        INIT-MAXIT=30 MAXIT=30 INIT-TOL=1E-2 TOL=9E-3
        ;INIT-OPTION=CHEMICAL

    COL-CONFIG 1 10 CONDENSER=NO REBOILER=NO
    TRAY-SPECS 1 1 10 TRAY-TYPE=SIEVE DIAM-EST=20 &
        PERCENT-FLOOD=70 TRAY-SPACING=192 <IN> &
        WEIRHT=16 <IN>

    FEEDS FLUE-ABS 1 11 ABOVE-SEGMENT /
        LEAN-ABS 1 1 ABOVE-SEGMENT
    PRODUCTS STACK 1 1 V / RICH-PUM 1 10 L

    P-SPEC 1 1 101.3 / 1 10 176.9
    SUBROUTINE PRESS-DROP=trayp

    COL-SPECS 1 MOLE-RDV=1

; Provides information on proximity to flooding conditions and pressure drop
; on each nonequilibrium segment
    REPORT FLOOD-INFO

; The following line causes the Murphree efficiencies to be tabulated.
    SEGMENT-REPORT SEGMENT-OPTION=ALL-SEGMENTS FORMAT=PROFILE &
        COMP-EFF=YES PROPERTIES=LPHASE VPHASE WIDE=YES
;</ABSORBER>

;<RICH_PUM>
BLOCK "RICH_PUM" PUMP

```

```

        PARAM DELP=0 <kPa>
; /RICH_PUM>

; <STRIPPER>
BLOCK STRIPPER RATEFRAC
    IN-UNITS SI PRESSURE=kPa TEMPERATURE=C PDROP=kPa
    PARAM NCOL=1 TOT-SEGMENT=9 EQUILIBRIUM=NO INIT-MAXIT=45 &
        MAXIT=45 INIT-TOL=1E-2 TOL=9E-3 ;INIT-OPTION=CHEMICAL

    COL-CONFIG 1 9 CONDENSER=YES REBOILER=YES
    TRAY-SPECS 1 2 8 TRAY-TYPE=SIEVE DIAM-EST=20 &
        PERCENT-FLOOD=70 TRAY-SPACING=216 <IN> &
        WEIRHT=18 <IN>

    FEEDS RICH-STR 1 2 ABOVE-SEGMENT
    PRODUCTS CO2-COMP 1 1 V / LEAN-HX 1 9 L

    P-SPEC 1 1 101.3 / 1 9 186
    SUBROUTINE PRESS-DROP=trayp

    COL-SPECS 1 MOLE-RDV=1 MOLE-RR=0.4 MOLE-B:F=0.95
    DB:F-PARAMS 1

    SPEC 1 MOLE-FLOW 2.45 COMPS=CO2 STREAMS=CO2-COMP
    VARY 1 MOLE-B:F COL=1

    SPEC 2 TEMP 70 SEGMENT=1 COL=1 PHASE=L
    VARY 2 MOLE-RR COL=1

; Provides information on proximity to flooding conditions and pressure drop
; on each nonequilibrium segment
    REPORT FLOOD-INFO

; The following line causes the Murphree efficiencies to be tabulated.
    SEGMENT-REPORT SEGMENT-OPTION=ALL-SEGMENTS FORMAT=PROFILE &
        COMP-EFF=YES PROPERTIES=LPHASE VPHASE WIDE=YES
; /STRIPPER>

; Shortcut heat exchanger calculation.
; 10 degree temperature approach at the hot stream outlet
; U = 1134 W / m^2 C (taken from Perry's for H2O-H2O liquid-liquid system)
BLOCK HEATX HEATX

```

```
IN-UNITS SI PRESSURE=kPa TEMPERATURE=C PDROP=kPa
PARAM DELT-HOT=10
FEEDS HOT=LEAN-HX COLD=RICH-HX
PRODUCTS HOT=LEAN-MIX COLD=RICH-STR
HEAT-TR-COEF U=1134
```

```
CALCULATOR "C_MAKEUP"
```

```
DESCRIPTION "Set MEA and H2O flow rate in make-up stream"
```

```
; Streams for water balance
```

```
DEFINE H2OFL MOLE-FLOW STREAM=FLUE-ABS COMPONENT=H2O
```

```
DEFINE H2OAB MOLE-FLOW STREAM=STACK COMPONENT=H2O
```

```
DEFINE H2OST MOLE-FLOW STREAM=CO2-COMP COMPONENT=H2O
```

```
DEFINE MEAAB MOLE-FLOW STREAM=STACK COMPONENT=MEA
```

```
DEFINE MEAST MOLE-FLOW STREAM=CO2-COMP COMPONENT=MEA
```

```
DEFINE MEAMU MOLE-FLOW STREAM=MAKE-UP COMPONENT=MEA
```

```
DEFINE H2OMU MOLE-FLOW STREAM=MAKE-UP COMPONENT=H2O
```

```
F MEAMU = MEAAB + MEAST
```

```
F H2OMU = H2OAB + H2OST - H2OFL
```

```
EXECUTE BEFORE BLOCK MIXER
```

```
BLOCK MIXER MIXER
```

```
BLOCK COOLER HEATER
```

```
IN-UNITS SI PRESSURE=kPa TEMPERATURE=C PDROP=kPa
```

```
PARAM TEMP=40 PRES=101.3
```

```
BLOCK "CO2_COMP" MCOMPR
```

```
IN-UNITS SI PRESSURE=kPa TEMPERATURE=C PDROP=kPa
```

```
PARAM NSTAGE=4 TYPE=ISENTROPIC PRES=110 <BAR>
```

```
FEEDS CO2-COMP 1
```

```
PRODUCTS ST1 1 L / ST2 2 L / ST3 3 L / CO2 4 / "P_COMP" GLOBAL
```

```
COMPR-SPECS 1 SEFF=0.90
```

```
COOLER-SPECS 1 TEMP=25
```

```
BLOCK REBOIL HEATER
```

```
IN-UNITS SI PRESSURE=kPa TEMPERATURE=C PDROP=kPa
PARAM PRES=0 VFRAC=0
```

```
BLOCK POWER MIXER
```

```
=====
; END: flowsheet specification
=====

;-----
; Convergence options
;-----
```

```
SIM-OPTIONS RESTART=YES
```

```
CONVERGENCE "ABS_LOOP" BROYDEN
  DESCRIPTION "Converge Absorber-side recycle and set CO2 loading"
  TEAR LEAN-ABS
  SPEC ALPHA
```

```
CONVERGENCE "STR_LOOP" BROYDEN
  DESCRIPTION "Converge Stripper-style recycle and set Stripper P"
  TEAR LEAN-HX
  SPEC "STR_PRES"
```

```
CONVERGENCE "ST_CYCLE" BROYDEN
  DESCRIPTION "Converge steam cycle tear streams and BOILFLOW spec"
  TEAR Q-FWPA / Q-FWPB / Q-FWPD / Q-FWPE / Q-FWPF /
        Q-FWPG / H2O-BOIL
  SPEC "C_IPSEP2"
  SPEC BOILFLOW
  PARAM MAXIT=60
```

```
CONVERGENCE EXTRACT SECANT
  DESCRIPTION "Specifies parameters used to set steam extraction"
  SPEC EXTRACT
```

```
;SEQUENCE FLOW "ABS_LOOP" ABSORBER "RICH_PUM" &
;              "STR_LOOP" HEATX STRIPPER &
;              (RETURN "STR_LOOP")      &
;              "C_MAKEUP" MIXER COOLER  &
;              (RETURN "ABS_LOOP")
```

```

; This paragraph specifies the convergence order for user-defined
; convergence blocks

CONV-ORDER "STR_LOOP" "ABS_LOOP" "ST_CYCLE" EXTRACT

;-----
; Design specification: FCOAL
;-----
; This design specification adjusts adjusts the coal flow rate such that
; there is sufficient heat generated to satisfy the duties of BOIL and REHT.
DESIGN-SPEC FCOAL
    DEFINE QBOIL INFO-VAR INFO=HEAT VARIABLE=DUTY STREAM="Q_BOIL"
    DEFINE QREHT INFO-VAR INFO=HEAT VARIABLE=DUTY STREAM="Q_REHT"
    DEFINE QFURN INFO-VAR INFO=HEAT VARIABLE=DUTY STREAM="Q_FURN"

    ; The boiler efficiency is 90%
F      EFF = 0.815

; 1 kW = 3412.2 Btu/h
F      G = 3412.2

    SPEC "QFURN" TO "-(QBOIL + QREHT) / EFF"
    TOL-SPEC "1*G"

    VARY STREAM-VAR STREAM=COAL-IN SUBSTREAM=NC VARIABLE=MASS-FLOW
    LIMITS "10" "793800"

;-----
; Design Spec: BOILFLOW
;-----
; Adjusts the flow rate of feed water until the desired value is achieved.

DESIGN-SPEC BOILFLOW
    DEFINE FLOW STREAM-VAR STREAM=H2O-BOIL VARIABLE=MASS-FLOW

;      100%    3358670
;      75%     2446607
;      50%     1619896

    SPEC "FLOW - 3358670" TO "0.0"
    TOL-SPEC "1"

```

```
VARY STREAM-VAR STREAM=H2O-BOIL VARIABLE=MASS-FLOW
LIMITS "809948" "3400000"
```

```

;-----
; Calculator block: C_POWER
;-----
; Calculates mechanical losses of main and BFP turbines, generator losses,
; exciter power to generator, and station service. These are required to
; calculate the turbine and unit heat rates.

; MECH, GEN, EXC      [=] MW; x [=] MW
; STA                 [=] MW; x [=] MW
; BFPM                [=] kW; x [=] MW

CALCULATOR "C_POWER"
    DEFINE PSUPP INFO-VAR STREAM="P_INTERN" INFO=WORK VARIABLE=POWER
    DEFINE PDMND INFO-VAR STREAM="P_DEMAND" INFO=WORK VARIABLE=POWER
    DEFINE PBLOW INFO-VAR STREAM="P_BLOW" INFO=WORK VARIABLE=POWER
    DEFINE PCOMP INFO-VAR STREAM="P_COMP" INFO=WORK VARIABLE=POWER
    DEFINE WFPT INFO-VAR STREAM="W_FPT" INFO=WORK VARIABLE=POWER

    ; 1 hp is equal to 0.745699 kW
F      F = 0.7456999

; Convert power from units of kW to MW
F      PMAIN = -PSUPP / 1e3
F      PBFPT = -WFPT / 1e3
F      PREQD = PDMND / 1e3

F      PMECH = 1.919
F      PGEN = (0.1511e-1) * PMAIN + 0.7343
F      PEXC = (0.3437e-2) * PMAIN - 0.4078
F      PSTA = (0.1110e+2) * DEXP(PMAIN/1e3) - 0.3737e+1
F      PBFPM = ((0.4534e+1) * PBFPT + 0.4244e2) / 1000

; For the calculation of net electric power output, I'm assuming a generator
; efficiency of 90%. It's what David Singh used...
F      GEFF = 0.90

F      EGRSS = PMAIN + PEXC - (PMECH + PGEN + PSTA)
F      EBLOW = -(PBLOW / GEFF) / 1e3

```

```

F      ECOMP = -(PCOMP / GEFF) / 1e3
F      ENET = EGRSS - (PREQD / GEFF)

F      WRITE(NRPT, '(A,F9.2,A3)') 'INTERNAL POWER      ', PMAIN, 'MW'
F      WRITE(NRPT, '(A,F9.2,A3)') 'EXCITER POWER      ', PEXC, 'MW'
F      WRITE(NRPT, '(A,F9.2,A3)') 'MECHANICAL LOSSES  ', -PMECH, 'MW'
F      WRITE(NRPT, '(A,F9.2,A3)') 'GENERATOR LOSSES   ', -PGEN, 'MW'
F      WRITE(NRPT, '(A,F9.2,A3)') 'STATION SERVICE    ', -PSTA, 'MW'
F      WRITE(NRPT, '(A,F9.2,A3)') 'ELEC-TY, GROSS     ', EGRSS, 'MW'
F      WRITE(NRPT, '(A,F9.2,A3)') 'ELEC-TY, BLOWER    ', -EBLOW, 'MW'
F      WRITE(NRPT, '(A,F9.2,A3)') 'ELEC-TY, CO2_COMP  ', -ECOMP, 'MW'
F      WRITE(NRPT, '(A,F9.2,A3)') 'ELEC-TY, NET       ', ENET, 'MW'

      EXECUTE AFTER SHAFT

; -----
; Design specification: COOL-FLU
; -----
; This block sets the flow rate of cooling water needed to cool the flue gas
; to the temperature specified in the DCC block.

DESIGN-SPEC COOL-FLU
      DEFINE QDCC BLOCK-VAR BLOCK=DCC SENTENCE=PARAM VARIABLE=QCALC

; 1 kmol/s = 7938 lbmol/h
F      F = 7938

; 1 kW = 3412.2 Btu/h
F      G = 3412.2

      SPEC "QDCC" TO "0"
      TOL-SPEC "1*G"

      VARY STREAM-VAR STREAM=H2O-PUMP VARIABLE=MOLE-FLOW
      LIMITS "1*F" "120*F"

;-----
; Calculator block: C_RECOV
;-----
; This block calculates the CO2 mole flow rate in the output stream
; that corresponds to a desired CO2 recovery.

```



```

CALCULATOR "C_RECOV"
    DEFINE CO2IN MOLE-FLOW STREAM=FLUE-GAS COMPONENT=CO2
    DEFINE FCO2 BLOCK-VAR BLOCK=STRIPPER SENTENCE=SPEC VARIABLE=VALUE &
        ID1=1

; CO2IN has units of lbmol/hr and FCO2 needs to be expressed in kmol/s.
; 1 kmol/s = 7938 lbmol/hr

F      FCO2 = CO2IN * 0.85 / 7938

    EXECUTE BEFORE CONVERGENCE "ABS_LOOP"

; -----
; Design specification:  ALPHA
; -----
; This block sets the CO2 loading of the recycle stream to a specified value.

DESIGN-SPEC ALPHA
    DEFINE CO2 MOLE-FLOW STREAM=LEAN-ABS COMPONENT=CO2
    DEFINE MEA MOLE-FLOW STREAM=LEAN-ABS COMPONENT=MEA

F      ALPHA = CO2 / MEA

    ; 1 kmol/s = 7938 lbmol/h
F      F = 7938

    SPEC "ALPHA" TO "0.25"
    TOL-SPEC "0.0025"

    VARY STREAM-VAR STREAM=LEAN-ABS VARIABLE=MOLE-FLOW
    LIMITS "30°F" "250°F"

; -----
; Design specification:  STR-PRES
; -----
; This block sets the Stripper reboiler pressure such that the reboiler
; temperature is 121C +- 1C.

DESIGN-SPEC "STR_PRES"
    DEFINE TN STREAM-VAR STREAM=LEAN-HX VARIABLE=TEMP

; Temperature is in units of F; pressure is given in psi.

```

```

SPEC "TN" TO "250"
TOL-SPEC "1.8"

VARY BLOCK-VAR BLOCK=STRIPPER SENTENCE=P-SPEC VARIABLE=PRES ID1=1 &
      ID2=9
LIMITS "14.7" "32"

;-----
; Design specification:  EXTRACT
;-----
; This design specification adjusts the amount of steam extracted from
; the IP/LP crossover pipe such that the reboiler heat duty is satisfied.
DESIGN-SPEC EXTRACT
      DEFINE QREB BLOCK-VAR BLOCK=STRIPPER SENTENCE=RESULTS &
            VARIABLE=REB-DUTY ID1=1
      DEFINE QEXT INFO-VAR STREAM="Q_REB" INFO=HEAT VARIABLE=DUTY

; 1 kW = 3412.2 Btu/h
F      G = 3412.2

SPEC "QEXT" TO "QREB"
TOL-SPEC "10*G"

VARY BLOCK-VAR BLOCK=EXTRACT SENTENCE=FRAC VARIABLE=FRAC ID1=ST-REB
LIMITS "0.0" "0.83"

```

Glossary

α *CO₂ loading* An expression of the CO₂ concentration in solution, it is the molar ratio of CO₂ to MEA.

List of References

- [1] Colin Alie, Leslie Backham, Eric Croiset, and Peter L Douglas. Simulation of CO₂ capture using mea scrubbing: a flowhseet decomposition method. Energy Conversion and Management, 2004. in publication. 11, 62, 65, 68, 76
- [2] W. A. Anderson. Che 045 process equipment sizing and selection course notes, 2001. 102, 103, 104, 107
- [3] anon. Coal-fired electricity generation in ontario. Technical report, Ministry of the Environment, March 2001. 10
- [4] Anon. Design basis document for reduction of mercury emissions at Nanticoke generating station. Internal report prepared for OPG, November 2002. Confidential. 13, 15, 20, 82
- [5] Anon. Something about coal. Technical report, American Society for Testing and Materials, 2002. 19
- [6] anon. Canada's energy future: Scenarios for supply and demand to 2025. Technical report, National Energy Board, July 2003. 6
- [7] Adisorn Aroonwilas, Amornvadee Veawab, and Paitoon Tontiwachuwuthikul. Behaviour of the mass-transfer coefficient of structured packings in CO₂ absorbers with chemical reactions. Journal of Industrial Engineering Chemical Research, 38:2044–2050, 1999. 46, 47, 48
- [8] Aspen Technology, Inc., Cambridge, MA, USA. Aspen Physical Property System: Physical Property Methods and Models 11.1, September 2001. 50
- [9] Aspen Technology, Inc., Cambridge, MA, USA. Aspen Plus Version 11.1 Getting Started: Modeling Process with Solids, September 2001. 15
- [10] Aspen Technology, Inc., Cambridge, MA, USA. Aspen Plus Version 11.1 Unit Operation Models, September 2001. 32

- [11] Aspen Technology, Inc., Cambridge, MA, USA. Aspen Plus Version 11.1 User Guide, September 2001. 15, 98
- [12] Aspen Technology, Inc., Cambridge, MA, USA. Aspen Plus Version 11.1 Service Pack 1 Input Language Guide, March 2002. 55, 58
- [13] R Barchas and R Davis. The Kerr-McGee/ABB Lummus Crest technology for the recovery of CO₂ from stack gases. Energy Conversion and Management, 33(5–8):333–340, 1992. 43, 46, 83
- [14] A. Chakma, A. K. Mehrotra, and B. Nielsen. Comparison of chemical solvents for mitigating CO₂ emissions from coal-fired power plants. Heat Recovery Systems and CHP, 15(2):231–240, 1995. 8, 44, 47, 49, 55, 92
- [15] Dan G. Chapel, Carl L. Mariz, and John Ernest. Recovery of CO₂ from flue gases: Commercial trends. In Canadian Society of Chemical Engineers Annual Meeting, Saskatoon, Saskatchewan, October 1999. 44, 46, 83
- [16] Susan Chi and Gary T. Rochelle. Oxidative degradation of monoethanolamine. In First National Conference on Carbon Sequestration, Washington, DC, May 2001. 83
- [17] Chih-Chung Chou and Yen-Shiang Shih. A thermodynamic approach to the design and synthesis of plant utility systems. Industrial & Engineering Chemistry Research, 26(6):1100–1108, June 1987. 26
- [18] C. David Cooper and F. C. Alley. Air pollution control: a design approach. Waveland Press, Inc., U.S.A., second edition, 1994. 1, 18
- [19] Ralph Cos. Capabilities of hyprotech. In 3rd Workshop of International Test Network for CO₂ capture, Apeldoorn, the Netherlands, May 2002. IEA Greenhouse Gas R&D Programme. 11
- [20] Umberto Desideri and Alberto Paolucci. Performance modelling of a carbon dioxide removal system for power plants. Energy Conversion and Management, 40:1899–1915, 1999. 11, 42, 45, 49, 54, 57, 58, 78, 92, 93
- [21] Energy Section, Manufacturing, Construction & Energy Division. Electric power generating stations 2000. Technical Report 57-206-XIB, Statistics Canada, December 2001. 4, 7, 8
- [22] Energy Section, Manufacturing, Construction & Energy Division. Electric power generation, transmission, and distribution. Technical Report 57-202-XIB, Statistics Canada, 2002. 3, 5

- [23] M. R. Erbes and R. H. Eustis. A computer methodology for predicting the design and off-design performance of utility steam turbine-generators. In Proceedings - American Power Conference, volume 48, pages 318–324. Illinois Institute of Technology, 1986. 26
- [24] Paul Feron. CO₂ capture using membrane gas absorption - status report. In 5th Workshop of International Test Network for CO₂ capture, Pittsburgh, U.S.A., June 2002. IEA Greenhouse Gas R&D Programme. 47
- [25] Stefano Freguia and Gary T. Rochelle. Base conditions for modeling of CO₂ capture by MEA absorption/stripping. In 3rd Workshop of International Test Network for CO₂ capture, Apeldoorn, the Netherlands, May 2002. IEA Greenhouse Gas R&D Programme. 11, 42, 49, 54, 97
- [26] Stefano Freguia and Gary T. Rochelle. Modeling of CO₂ absorption/stripping with monoethanolamine. In 4th Workshop of International Test Network for CO₂ capture, Kyoto, Japan, October 2002. IEA Greenhouse Gas R&D Programme. 11, 42, 46, 47, 49, 54, 76, 97
- [27] Stefano Freguia and Gary T. Rochelle. Modeling of CO₂ absorption/stripping with monoethanolamine. AICHE Journal, 49(7):1676–1687, 2003. 11, 42, 46, 47, 49, 54, 76, 97
- [28] George S. Goff and Gary T. Rochelle. Oxidative degradation of aqueous monoethanolamine in CO₂ capture systems under absorber conditions. In J. Gale and Y. Kaya, editors, Greenhouse Gas Control Technologies: Proceedings of the 6th International Conference on Greenhouse Gas Control Technologies, volume 1, pages 115–119. Elsevier Science Ltd., October 2002. 83
- [29] Don W. Green, editor. Perry's chemical engineers' handbook. McGraw-Hill, seventh edition, 1997. 56, 102, 106, 107
- [30] Ontario Hydro. Nanticoke generating station design heat balance, February 1972. 100%, 75%, and 50% load. 20, 26
- [31] Ontario Hydro. Nanticoke generating station units 1–8 boiler design data, October 1978. 100% load. 20
- [32] IEA Greenhouse Gas R&D programme. Technical and Financial Assessment Criteria, November 1999. Revision B. 10, 13, 15, 52

- [33] Masaki Iijima and Takashi Kamijo. Flue gas CO₂ recovery and compression cost study for CO₂ enhanced oil recovery. In J. Gale and Y. Kaya, editors, Greenhouse Gas Control Technologies: Proceedings of the 6th International Conference on Greenhouse Gas Control Technologies, volume 1, pages 109–114. Elsevier Science Ltd., October 2002. 57
- [34] Nobuo Imai. Flue gas CO₂ capture: CO₂ capture technology of KS-1. In 4th Workshop of International Test Network for CO₂ capture, Kyoto, Japan, October 2002. IEA Greenhouse Gas R&D Programme. 46
- [35] IPCC. Climate Change 2001: Mitigation. Cambridge University Press, 2001. Contribution of Working Group III to the Third Assessment Report of the Intergovernmental Panel on Climate Change. 6
- [36] Fang-Yuan Jou, Alan E. Mather, and Frederick D. Otto. The solubility of CO₂ in a 30 mass percent monoethanolamine solution. The Canadian Journal of Chemical Engineering, 73:140–147, February 1995. 59, 60, 111, 112, 113, 114, 115
- [37] Graeme Lamb, May 2003. Personal communication. 79, 82
- [38] John Marion, Nsakala ya Nsakala, Carl Bozzuto, Gregory Liljedahl, Mark Palkes, David Vogel, J. C. Gupta, Manoj Guha, Howard Johnson, and Sean Plasynski. Engineering feasibility of CO₂ capture on an existing US coal-fired power plant. In 26th International Conference on Coal Utilization & Fuel Systems, Clearwater, Florida, March 2001. 47, 57, 78, 83, 92, 93
- [39] Carl Mariz. Carbon dioxide recovery: large scale design trends. Journal of Canadian Petroleum Technology, 37(7):42–47, July 1998. 83
- [40] Carl Mariz, Larry Ward, Garfiled Ganong, and Rob Hargrave. Cost of CO₂ recovery and transmission for EOR from boiler stack gas. In Pierce Riemer and Alexander Wokaun, editors, Greenhouse Gas Control Technologies: Proceedings of the 4th International Conference on Greenhouse Gas Control Technologies. Elsevier Science Ltd., April 1999. 8, 83, 92, 93
- [41] Michael Lynn McGuire. STEAM67. World Wide Web, February 1985. <http://www.winsim.com/steam/>. 24
- [42] Tomio Mimura, Takashi Nojo, Masaki Iijima, Ryuji Yoshiyama, and Hiroshi Tanaka. Recent developments in flue gas CO₂ recovery technology. In J. Gale and Y. Kaya, editors, Greenhouse Gas Control Technologies: Proceedings of the 6th International Conference on Greenhouse Gas Control Technologies, volume 2, pages 1057–1062. Elsevier Science Ltd., October 2002. 46

- [43] Tomio Mimura, S. Shimojo, T. Suda, M. Iijima, and S. Mitsuoka. Research and development on energy saving technology for flue gas carbon dioxide recovery and steam system in power plant. Energy Conversion and Management, 36(6–9):397–400, 1995. 46, 73, 78, 98
- [44] Tomio Mimura, Hidenobu Simayoshi, Taichiro Suda, Masaki Iijima, and Sigeaki Mitsuoka. Development of energy saving technology for flue gas carbon dioxide recovery in power plant by chemical absorption method and steam system. Energy Conversion and Management, 38:S57–S62, 1997. 47, 78, 98
- [45] Shinichirou Morimoto, Kotarou Taki, and Tadashi Maruyama. Current review of CO₂ separation and recovery technologies. In 4th Workshop of International Test Network for CO₂ capture, Kyoto, Japan, October 2002. IEA Greenhouse Gas R&D Programme. 92, 93
- [46] Eriko Muramatsu and Masaki Iijima. Life cycle assessment for CO₂ capture technology from exhaust gas of coal power plant. In J. Gale and Y. Kaya, editors, Greenhouse Gas Control Technologies: Proceedings of the 6th International Conference on Greenhouse Gas Control Technologies, volume 1, pages 57–62. Elsevier Science Ltd., October 2002. 46
- [47] Ken Olsen, Pascale Collas, Pierre Boileau, Dominique Blain, Chia Ha, Lori Henderson, Chang Liang, Scott McKibbin, and Laurent Moreal-à-l’Huissier. Canada’s greenhouse gas inventory: 1990–2000. Technical report, Environment Canada, June 2002. 2
- [48] Alfred Ong’iro, V. Ismet Ugursal, A. M. Al Taweel, and G. Lajeunesse. Thermodynamic simulation and evaluation of a steam CHP plant using aspen plus. Applied Thermal Engineering, 16(3):263–271, 1996. 11, 26, 31
- [49] Edward S. Rubin and Anand B. Rao. Uncertainties in CO₂ capture and sequestration costs. In J. Gale and Y. Kaya, editors, Greenhouse Gas Control Technologies: Proceedings of the 6th International Conference on Greenhouse Gas Control Technologies, volume 2, pages 1119–1124. Elsevier Science Ltd., October 2002. 98
- [50] Blair Seckington, May 2003. Personal communication. 4, 5
- [51] Blair Seckington, April 2004. Personal communication. 20
- [52] Ahmed Shafeen. Assessment of geological CO₂ sequestration in Ontario. Master’s thesis, University of Waterloo, 2003. 10

- [53] M. Simmonds, P. Hurst, M. B. Wilkinson, C. Watt, and C. A. Roberts. A study of very large scale post combustion CO₂ capture at a refining & petrochemical complex. In J. Gale and Y. Kaya, editors, Greenhouse Gas Control Technologies: Proceedings of the 6th International Conference on Greenhouse Gas Control Technologies, volume 1, pages 39–44. Elsevier Science Ltd., October 2002. 57, 83
- [54] David Singh, Eric Croiset, Peter L. Douglas, and Mark A. Douglas. Techno-economic study of CO₂ capture from an existing coal-fired power plant: Mea scrubbing vs. O₂/CO₂ recycle combustion. Energy Conversion and Management, 44(19):3073–3091, November 2002. 8, 11, 42, 45, 49, 93
- [55] David J. Singh. Simulation of CO₂ capture strategies for an existing coal fired power plant - MEA scrubbing versus O₂/CO₂ recycle combustion. Master's thesis, University of Waterloo, 2001. 8, 10, 11, 42, 45, 49, 54, 57, 92, 93
- [56] M. Slater, E. West, and C. L. Mariz. Carbon dioxide capture from multiple flue gas sources. In J. Gale and Y. Kaya, editors, Greenhouse Gas Control Technologies: Proceedings of the 6th International Conference on Greenhouse Gas Control Technologies, volume 1, pages 103–107. Elsevier Science Ltd., October 2002. 57
- [57] J. M. Smith, H. C. Van Ness, and M. M. Abbott. Introduction to Chemical Engineering Thermodynamics. McGraw-Hill Companies, Inc., sixth edition, 2001. 31
- [58] Giorgio Soave and Josep A. Feliu. Saving energy in distillation towers by feed splitting. Applied Thermal Engineering, 22:889–896, 2002. 44
- [59] R. C. Spencer, K. C. Cotton, and C. N. Cannon. A method for predicting the performance of steam turbine-generators. . . 16,500 kW and larger. Journal of Engineering for Power, 85:249–252, October 1963. 29, 30
- [60] Paitoon Tontiwachwuthikul, Christine Chan, Weerapong Kritpiphat, David De-Montigny, David Skoropad, Don Gelowitz, Adisorm Aroonwilas, Frank Mourits, Malcolm Wilson, and Larry Ward. Large scale carbon dioxide production from coal-fired power stations for enhanced oil recovery: a new economic feasibility study. Journal of Canadian Petroleum Technology, 37(11):48–55, November 1998. 47, 92
- [61] A. Veawab. Corrosion in CO₂ capture unit for coal-fired power plant flue gas. In J. Gale and Y. Kaya, editors, Greenhouse Gas Control Technologies: Proceedings

- of the 6th International Conference on Greenhouse Gas Control Technologies, volume 2, pages 1595–1598. Elsevier Science Ltd., October 2002. 78
- [62] James O. Wilkes. Fluid Mechanics for Chemical Engineers. Prentice-Hall PTR, Upper Saddle River, New Jersey, 1999. 105
- [63] M. Wilson, P. Tontiwachwuthikul, A. Chakma, R. Idem, A. Veawab, A. Aroonwilas, D. Gelowitz, J. Barrie, and C. Mariz. Test results from a CO₂ extraction pilot plant at Boundary Dam coal-fired power station. In J. Gale and Y. Kaya, editors, Greenhouse Gas Control Technologies: Proceedings of the 6th International Conference on Greenhouse Gas Control Technologies, volume 1, pages 31–36. Elsevier Science Ltd., October 2002. 83
- [64] M. A. Wilson, R. M. Wrubleski, and L. Yarborough. Recovery of CO₂ from power plant flue gases using amines. Energy Conversion and Management, 33(5–8):325–331, 1992. 83
- [65] Takahisa Yokoyama. Japanese R&D on CO₂ capture. In J. Gale and Y. Kaya, editors, Greenhouse Gas Control Technologies: Proceedings of the 6th International Conference on Greenhouse Gas Control Technologies, volume 1, pages 13–17. Elsevier Science Ltd., October 2002. 44